ANTICAKING METHODS FOR PHARMACEUTICAL GRADE SALT

A thesis presented in partial fulfilment of the requirements for the degree of Master of Technology in BioProcess Engineering at Massey University

Kellie J. Anthony

2005

ABSTRACT

This is an investigation into the causes of caking in the pharmaceutical grade salt produced by Dominion Salt Limited. It was found that the caking mechanism that occurs in sodium chloride is humidity caking. A moisture audit of the Dominion Salt plant showed that the primary factors causing caking are the initial water activity of the salt and the temperature gradient that the salt is exposed to during packing and storage.

Experiments were conducted to determine the physical properties of the salt: the bulk density, the thermal conductivity, the particle size distribution and the moisture sorption isotherm. Using these properties, a mathematical model was modified to predict whether caking would occur in a salt bed subjected to specific temperature and moisture conditions.

Model validation experiments were performed, where caking was produced by exposure to a temperature gradient. The mathematical model was compared to experimental data and altered until it accurately simulated observed results. The model was then used to predict the circumstances that will induce significant caking in a salt bed and a chart of the results collated to show when caking will occur. Given the salt temperature, the ambient temperature and the initial water activity, the chart can be used to determine whether caking will occur in the bagged salt.

ACKNOWLEDGEMENTS

During the course of this investigation I have received an incredible amount of support from a variety of sources.

Firstly, my principal academic supervisor, Tony Paterson. I've been extraordinarily lucky to have a supervisor that was so dedicated. We've had our differences, but (mostly) he's been fantastic. John Bronlund, my other academic supervisor, without whom I would still be puzzling over the mathematical model. My thanks also to the various members of the Institute of Technology and Engineering, I think I know almost everyone by name now, and most have helped me at some point during this project!

Dominion Salt Ltd of Mount Maunganui, thank you for providing me with a project and for your assistance in completing it. In particular my industrial supervisor Brent Cunliffe, you're a very patient man and I appreciate that you managed to make so much time in your hectic schedule to help me solve my problems.

I would like to thank my parents for their support, Mum for her constant ..... encouragement....and Pop for his ability to see the logical solution to any problem. I'm sorry I didn't manage to finish this thesis as your birthday present Mum, but please accept it as a very late gift.

The other postgraduate students in general, Mossop, Craig and Rachel in particular, many thanks for the hours of fun and laughter in the postgrad office. We probably should have been working, but I think I may have gone mad without some distractions. And yes, I'm aware that I was easily distracted!

TABLE OF CONTENTS

LIST OF FIGURES

LIST OF TABLES

CHAPTER ONE INTRODUCTION

Dominion Salt Limited has a processing plant at Mount Maunganui. At this plant raw solar salt is dissolved into brine, purified and dried to salt crystals. Several grades of salt are produced, the grade of interest for this project is the Pharmaceutical salt or BP salt.

In most of the salt grades produced by Dominion Salt, potassium ferrocyanide is added in minute amounts to the crystals after the centrifugal separation and before the drying process. This introduces an impurity on the surface that alters the crystal structure formed by the salt when it recrystallises. The addition of potassium ferrocyanide to the salt causes it to form a dendritic structure which is friable, and forms very weak intercrystalline bridging, preventing caking in bulk salt. Because pharmaceutical raw materials or products must be totally pure, this excludes the use of anticaking agents, such as potassium ferrocyanide, in the pharmaceutical grade salt.

This investigation began with a thorough review of the available literature on salt. Literature on caking in other powders was also reviewed, producing information regarding the effect of temperature, pressure and moisture content on the formation of liquid and solid bridging. This work indicated that the main mechanism for caking in salt is the formation of liquid and subsequently solid bridges between salt crystals caused by moisture movement within the salt bed. With an understanding of the humidity caking mechanism, the amount of caking caused in salt samples exposed to different humidity conditions needed to be established. This information was used to adapt (for salt) the mathematical model created by Bronlund (1997) to predict caking in lactose powders caused by temperature gradient induced moisture movement.

1.1 PROBLEM IDENTIFICATION

This project was commissioned by Dominion Salt to investigate the caking mechanism in salt, and to determine the causes of caking. The project aim was to create a mathematical model that would predict caking in salt for a given set of conditions. It was reasoned that if the source of the caking problem could be identified, steps could be taken in the drying processes to reduce, or possibly eliminate, caking in the salt.

Dominion Salt wishes to be able to produce free flowing salt without using anticaking agents. The primary reason for this is that anticaking agents are not permitted in pharmaceutical grade salt and thus the salt is difficult to transport and to use. The other main reason for producing salt that does not contain anticaking agent is that it would most probably be much more attractive to consumers. This is particularly true for the Japanese market. Japan recently put a trade embargo on any salt that had been treated with ferrocyanide, and any product containing salt treated with ferrocyanide. Because salt is an ingredient in so many food products, Japan's refusal to accept ferrocyanide containing goods caused a large disruption of international trade. Japan was forced to withdraw the ban, but remain dissatisfied with the presence of anticaking agents in their salt. It is expected that the Japanese market would react very favourably to a salt that was free of anticaking agents.

The staff at Dominion Salt have observed that caking occurs to varying degrees in the pharmaceutical salt product. On some occasions the salt will be free flowing, on some occasions there will be a small degree of caking present in the salt products, and on other occasions the salt will be totally caked throughout the salt bag. The caking causes difficulties in the packing, transportation and storage of the salt.

1.2 PROJECT AIMS

The aims of this investigation were to;

- Develop an understanding of the relationships between moisture and caking in bulk salt, and the effect of moisture adsorption on individual salt crystals.
- Identify the mechanism responsible for the caking of salt.
- Mathematically model and experimentally validate the effect of a temperature gradient on heat and moisture transfer within a packed bed of salt.

CHAPTER TWO LITERATURE REPORT

2.1 CAKING

Caking, in pharmaceutical grade salt, is when the individual salt particles become connected to the adjacent particles by solid crystalline bridges. This has been known to happen in bags that have been packed and stored for some time, or during transport. This section looks at the caking mechanisms described in the literature.

2.1.1 Mechanisms

The two primary mechanisms of caking in crystalline powders are humidity caking and amorphous recrystallisation. [Bronlund (1997)] As amorphous salt is only formed under very specific conditions, and does not exist in pure salt at all, [Gal (1975a)] the only mechanism of caking that will be considered is humidity caking.

Humidity caking has been summarised by Nelson (1949)

> "Powders, when exposed to conditions of high relative humidity, will adsorb moisture. A powder will, at equilibrium, give an equilibrium relative humidity, dependent on its moisture content. There exists what has been termed the critical relative humidity for adsorption to take place. This is the relative humidity at which pure sugar crystals change from a theoretically moisture free condition to a dissolved or liquid condition."

[Bronlund (1997)]

When salt is exposed to a high relative humidity environment, it adsorbs moisture. A liquid film forms on the surface of the crystals and allows bridges to form between particles, when it evaporates, crystalline salt bridges remain between the particles and caking occurs. [Moss *et al.* (1933)]

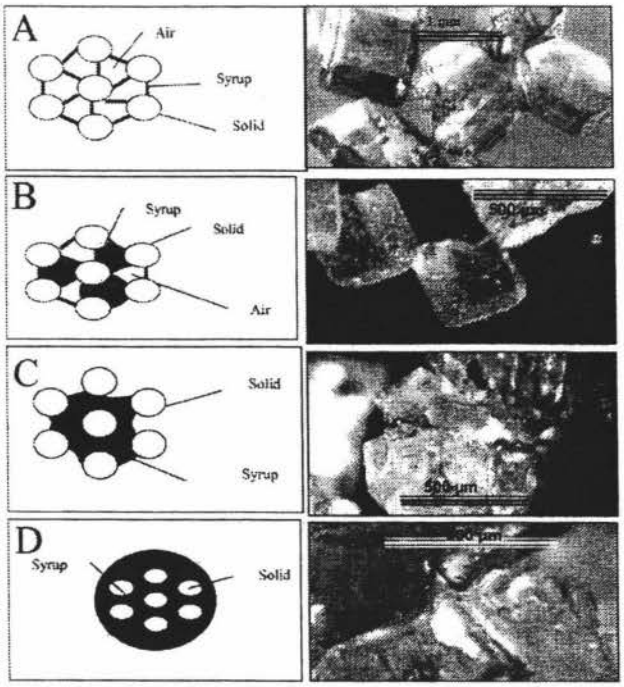

Figure 2. 1 Stages of wetting of crystals (A pendular, B funicular, C capillary, D drop).
[Mathlouthi and Roge (2003)]

There are four stages of humidity caking: [Mathlouthi and Roge (2003)]

A. Pendular stage of free flowing powders.
B. Funicular stage corresponds to establishing of contact between particles.
C. Capillary stage is reached when moisture is high enough to provoke liquid bridges between particles.
D. Drop stage when dissolution of particles is predominant.

In the pendular phase of humidity caking, the salt has adsorbed only a very small amount of moisture and appears dry. During the funicular stage of caking, the amount of moisture adsorbed by the salt increases and saturated salt solution begins to form on the surface of the particles. In the capillary phase, liquid bridges form between adjacent particles and in the drop phase, the salt particles are surrounded by a saturated salt solution. If drying occurs after wetting, caking is observed at a characteristic equilibrium Relative Humidity (ERH) at which water is released from powder particles which form solid bridges and agglomerate.
[Mathlouthi and Roge (2003)]

2.1.2 Important Variables in Caking

All finely ground materials exhibit a tendency to cake, the extent varies depending on the properties of the material, the temperature and the humidity of the material, the length of storage time and the method of storage, and the pressure exerted on the particles.

[Moss *et al*(1933)][Whynes and Dee (1957)]

2.1.2.1 Effect of Pressure on Caking

The effect of pressure (for example that caused by stacked bags) on a salt bed is that a larger number of contact points will form and hence more interparticle adhesion will occur. High pressures locally raise solubility so that when the resulting saturated solution flows into regions of lower pressure it is supersaturated and binds masses of particles together when it crystallises.

[Irani *et al* (1959)]

Variation of volume ($-\Delta V/V_0$) with pressure

Pressure (kPa)	**20°C**	**-78.8°C**
5	0.0192	0.0177
10	0.0365	0.0341
15	0.0523	0.0494
20	0.0664	0.0634
25	0.0798	0.0763
30	0.0919	0.0880
35	0.1029	0.0987
40	0.1130	0.1084
45	0.1223	0.1172
50	0.1309	0.1250

Table 2. 1 Variation of volume of solid NaCl with pressure

[Kaufman (1960)]

Number of compactions by hammer	Compression strength
	kg/cm^2
2	25.9
4	27.2
6	38.3
8	39.6
10	44.3
12	44.2
14	

Table 2. 2 Effect of pressure on caking of salt with an initial moisture content of 3.70%
[Bhatt and Datar (1968)]

The pressure due to stacked bags of salt is difficult to reproduce in the laboratory. However, the effect of such a scenario on the bags is to increase compaction, bulk density and points of contact between particles. Bhatt and Datar (1968) simulated the effect of pressure in the laboratory by compacting the salt by dropping a hammer onto the bags from a height of 27cm. The resulting bricks of salt were dried and the compression strength of the salt was measured with a texture analyser, by pressing continuously on the salt sample until it broke and measuring the amount of force required. This shows that the compression strength of bulk salt increases with compaction. [Bhatt and Datar (1968)]

2.1.2.2 Effect of Temperature and Moisture Content on Caking

Caking increases with the initial moisture content of the salt. Moisture remains in the voids between particles and produces saturated brine which dries and results in microcrystalline growth. These bridges bind adjoining particles causing agglomeration. There is a limit to the increase; above the saturation point additional moisture has no effect.
[Irani *et al* (1959)]

The effect of the initial moisture content of the salt was investigated by Bhatt and Datar (1968) by drying salt at 120°C and then placing the salt blocks into either a dry or humid atmosphere to cool. They found that salt with a higher initial moisture content formed a harder cake, and that salt cooled in a non-humid atmosphere caked harder than salt cooled in a humid atmosphere.

Non-Humid Atmosphere		Humid Atmosphere	
Initial moisture content	**Compression Strength**	**Initial moisture content**	**Compression Strength**
%	kg/cm^2	%	kg/cm^2
2.36	21.9	2.19	7.1
2.74	27.3	2.20	11.2
3.15	30.8	3.59	16.6
3.45	32.9	4.60	22.1
3.79	38.3	5.88	26.7
4.30	44.2	7.33	33.0
5.32	50.3		
6.44	60.3		

Table 2. 3 Effect of initial moisture content on caking of salt

[Bhatt and Datar (1968)]

Graphing the non-humid atmosphere data gave a straight line which passes through the origin. This means that if the other factors are constant (particle size, pressure, temperature), then caking is directly proportional to the initial moisture content.

A comparison of non-humid and humid atmospheres shows more caking for the non-humid drying conditions. Salt blocks are porous and the porosity increases as the moisture dries out. This leaves gaps or channels where moisture absorption can take place while cooling in humid conditions. This leads to some of the microcrystalline bridges dissolving and the compression strength decreasing. This is shown by the effect of relative humidity on the resulting strength of the solid bridges formed on drying.

The effect of relative humidity on caking strength was shown by Bhatt and Datar (1968). Salt samples with the same initial moisture content were placed into different relative humidity environments and the caking strength measured. The initial moisture content of the salt is 3.79%, which is quite high. The water activity of this salt would be approximately 0.8. [Chinachoti and Steinberg (1985)] When the sample is exposed to a low relative humidity environment the moisture evaporates leaving crystalline bridges between the particles.

Relative Humidity	Caking Strength
%	kg/cm^2
5	30.6
30	17.1
50	6.86
60	6.79
70	5.09

Table 2. 4 Effect of relative humidity on caking of salt with an initial moisture content of 3.79%

[Bhatt and Datar (1968)]

All soluble salts show a tendency to cake. To avoid caking, drying should be carried out at low temperatures or, if the start of the drying process is at high temperature, the finishing process should be at atmospheric temperature. Substances should not be packed hot unless all traces of moisture have been removed. A dry packing atmosphere should be maintained and packing the salt into a dry packing vessel will reduce caking.

[Lowry and Hemmings (1920)]

Temperature	Drying period	Caking strength
°C		kg/cm^2
29 ± 3	3 weeks	17.2
45	3 days	16.9
110	overnight	34.4
140	overnight	38.5

Table 2. 5 Effect of drying temperature on salt with an initial moisture content of 3.79%

[Bhatt and Datar (1968)]

When the salt is dried at high temperature the moisture evaporates causing crystalline bridges to form between particles. Temperature can have a considerable effect on the caking of salt, in particular the difference in the temperature of the salt and the temperature of the surroundings. If the difference is large there will be a greater tendency for the salt to cake. [Billings(2002)] [Bronlund(1997)]

Humidity caking occurs when a sample of salt is placed in an environment that has a higher relative humidity than the salt. The inequality causes moisture to be adsorbed onto the salt sample. This can also be caused by a temperature change in a salt sample, as described below.

When bulk salt is exposed to a temperature change, a temperature gradient occurs. An example of a situation where the salt is exposed to a temperature gradient is when salt is bagged. The salt is generally around 55°C when bagged, and the bag is then left in ambient conditions, approximately 25°C. When a temperature gradient is applied, the heat is not conducted instantly through the salt; the centre of the bag will remain at the original temperature, while the salt at the outside of the bag will equilibrate to the new temperature.

In a crystalline salt sample there are air pockets between the salt particles. The relative humidity of air is a function of its absolute humidity, or moisture content, and its temperature. Relative humidity is a ratio that compares the amount of water vapour in the air against the amount of water vapour that can be held by the air. As temperature decreases, the air is less able to hold water vapour, so if the absolute humidity remains the same the relative humidity will increase. There is a driving force to maintain equilibrium between the relative humidity of the air and the water activity of the salt. To maintain equilibrium, some of the water vapour in the air will be adsorbed onto the salt. Conversely, when the temperature of air is increased its capacity to hold water vapour is also increased. Thus, if there is no change in the absolute humidity, the relative humidity will decrease.

Figure 2.2 shows the moisture migration in a salt bed when a temperature gradient is applied in the form of a hot plate at one end of the bulk salt and a cold plate at the other. Note that in a true sample the air is dispersed through the salt sample, filling the void spaces between the particles.

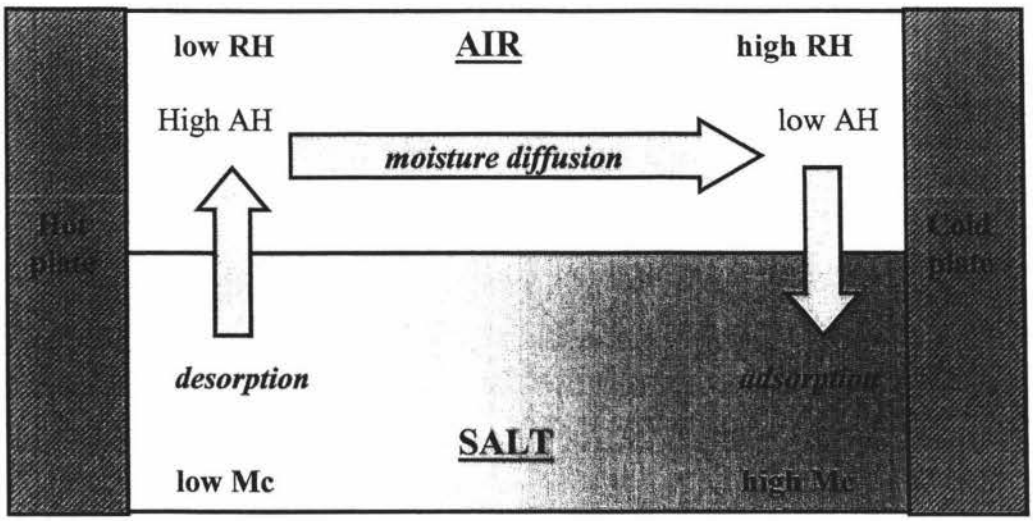

Figure 2. 2 Moisture migration in a salt bed

Locally, the air and the salt are in equilibrium. The salt closest to the cold plate has an increased moisture content and a saturated salt solution will form, creating liquid bridging. At the hot zone, moisture is desorbing from the salt into the air. However, the system is not at equilibrium because an absolute humidity gradient occurs in the air above the salt bed. To reach equilibrium, the moisture moves from the hot air to the cold air. It is assumed that moisture movement within the salt bed is negligible.

In the real system described, where a bag is filled with hot salt then subjected to ambient conditions, the hot zone represents the centre of the bag and the cold zone represents the ambient air outside the bag.

The centre of the bag will eventually cool as the heat is conducted to the edges of the bag and dispersed into the ambient environment. As the salt cools to ambient temperature, the moisture movement described above is reversed. At the edges of the bag the moisture begins to desorb back into the air and at the centre the moisture is readsorbed. Caking will occur at the bag edges as the liquid bridges crystallise into solid bridges.

The length of time taken to achieve uniform temperature throughout the bag depends on the size of the sample and the size of the temperature gradient.

2.1.2.3 Effect of Impurities on caking

Initial moisture content	Impurity concentration	Caking strength
%	mg/100g salt	kg/cm2
2.62	0.39	26.5
3.24	0.42	27.3
3.87	0.46	34.5
4.43	0.49	37.4
4.90	0.52	38.8
6.27	0.56	48.2

Table 2. 6 Effect of impurity concentration on caking

Impurities in the salt affect the initial moisture content as well as the caking strength of the salt. [Bhatt and Datar (1968)] The most common impurities in sodium chloride are calcium and magnesium salts. [Iyengar and Sen (1970)]

In impure salt, less microcrystalline bridges are formed. Caking is reduced in the presence of hygroscopic impurities.

Initial moisture content	Caking Strength Without impurity	Caking Strength With impurity	Caking Strength Difference	Decrease in caking strength
%	kg/cm^2	kg/cm^2	kg/cm^2	%
3.0	29.2	28.2	1.0	3.4
3.5	33.8	31.0	2.8	8.3
4.0	38.8	34.2	4.6	11.8
4.5	43.6	37.2	6.4	14.7
5.0	48.5	40.2	8.3	17.2
5.5	53.2	43.0	10.2	19.2
6.0	58.4	47.0	11.4	19.5

Table 2. 7 Effect of impurities on compression strength

[Bhatt and Datar (1968)]

2.1.2.4 Effect of Particle Size on caking

As particle size decreases, surface area, points of contact and bulk density increase. With coarser particles, points of contact are fewer and distances are larger; hence bridges are more easily broken.

Particle size	**Average particle size**	**Initial moisture**	**Compression strength**	**Decrease in size**	**Decrease in size**	**Increase in compression strength**	**Increase in compression strength**
BS mesh	mm	%	kg/cm^2	mm	%	kg/cm^2	%
-5 + 6	3.07	3.75± 0.25	0.93	-	-	-	-
-6 + 8	2.43	3.75± 0.25	1.21	0.64	20.8	0.28	30.1
-8 + 10	1.86	3.75± 0.25	1.39	1.21	39.4	0.46	49.5
-12 + 14	1.30	3.75± 0.25	3.89	1.77	57.7	2.96	318.3
-14 + 18	1.02	3.75± 0.25	5.48	2.05	66.8	4.55	489.3
-18 + 30	0.67	3.75± 0.25	6.05	2.40	78.2	6.12	658.0
-30 + 60	0.38	3.75± 0.25	17.66	2.69	87.6	16.73	1800.0
-5 + 60*	-	3.75± 0.25	11.63	-	-	-	-

*composite sample prepared by mixing all particle size range in equal proportions

Table 2. 8 Effect of particle size on caking

[Bhatt and Datar (1968)]

Van der Waals and electrostatic forces are the main binding forces in dry materials, these increase proportionally to particle diameter. As the particle size increases, the binding force increases, but the resistance force causing particle separation increases even more. As a result, cohesion should decrease linearly with increasing particle size. [Plink *et al* (1994)]

The salt produced by Dominion Salt Ltd is not of uniform size. The presence of fines in a salt sample will increase its cohesion, even without the effects of humidity caking occurring in the sample.

2.1.3 Anticaking Agents

Anticaking agents usually have low bulk densities and high surface areas. They improve the storage, handling flow property and hygroscopic behaviour of bulk materials. Anticaking agents are usually insoluble in water and act as a barrier during moisture sorption. [Bhatt and Datar (1968)] The chemicals listed in Table 2.9 below are all common anticaking agents used in sodium chloride.

Name	Proportion	Density	Initial moisture	Caking strength With anticake	Caking strength Without anticake	Caking strength Difference	Caking strength Difference
		g/cc	%	kg/cm^2	kg/cm^2	kg/cm^2	%
Tricalcium phosphate	0.75 %	0.65	2.73	23.7	26.7	3.0	11
Calcium carbonate	0.75 %	0.52	2.78	19.3	27.1	7.8	23
Magnesium carbonate	0.75 %	0.13	3.05	21.0	29.5	8.5	29
Calcium silicate	0.75 %	0.11	3.02	20.6	29.5	8.9	31
Sodium ferrocyanide	5ppm	-	3.58	13.8	34.9	21.1	59
Sodium ferrocyanide	10ppm	-	4.20	11.7	40.8	29.1	71

Table 2. 9 Effect of anti-caking agents on caking

[Bhatt and Datar (1968)]

Sodium ferrocyanide is the preferred anticaking agent for salt. When a film of solution containing sodium ferrocyanide evaporates, instead of the usual cubical crystals, skeletal or dendritic crystals form. These crystals have low mechanical strength, therefore caking is reduced. [Bhatt and Datar (1968)]

The caking of salt is attributed to the formation of solid intercrystalline bridges. These form by a recrystallisation process occurring on the surfaces of salt crystals. The addition of ferrocyanides to brines from which NaCl is crystallising causes the cubic crystal habit of NaCl to change. Ferrocyanides cause the intercrystalline caking bridges to become dendritic and therefore friable. When ferrocyanide is present on the surface of NaCl, the surface recrystallisation is hindered. [Bhatt and Datar (1968)]

Anticaking agent	Chemical Formula	Effect on crystal structure
Potassium ferrocyanide	$(K_4Fe(CN)_6)$	dendrites formed at 1ppm, excellent anticaking agent
Potassium ferricyanide	$(K_3Fe(CN)_6)$	dendrites form, very good anticaking agent
Sodium carbonyl ferrocyanide	$(NaFe(CN)_5CO)$	dendrites form, good anticaking agent
Sodium penta-cyano-amino-ferrate	$(NaFe(CN)_5NH_3)$	dendrites form, good anticaking agent
Potassium ruthenocyanide	$(K_4Ru(CN)_6)$	dendrites form, good anticaking agent
Potassium cobalticyanice	$(K_3Co(CN)_6)$	dendrites form, good anticaking agent
Potassium nickelocyanide	$(K_2Ni(CN)_4)$	slight inhibition, cubic crystals, poor anticake
Ammonia triacetamide	$N(CH_2CoNH_2)_3$	very good anticaking agent
Victamide	$(P_2O_5NH_3)$	dendrites form octahedral, very good anticaking agent

Table 2. 10 Effect of anti-caking agents on crystal structure

[Phoenix (1966)]

2.1.4 Binding Forces

The forces that bind particles together can be mechanical forces that arise due to the meshing of surface asperities, solid bridges due to recrystallisation of dissolved substances after drying, capillary forces due to adsorbed liquid layer, Van der Waals forces or electrostatic forces. The magnitude of the forces depends on environmental conditions, including humidity and the extent to which the material is, or has been pressed. [Plink *et al* (1994)]

In dry powders, such as salt, electrostatic effects are significant but Van der Waals forces generally dominate. Cohesive forces have a significant influence on powder characteristics. Cohesion is defined as the minimum strength required to separate particles when no normal stress is applied. It depends on interparticle binding forces and the method used to separate the particles. Dry materials comprised of small particles have higher cohesion values than coarse fractions.

[Plink *et al* (1994)]

Capillary forces have a role in flow behaviour, agglomeration of granular material and in moisture retention of a powder. A liquid at low viscosity forms a bridge between two particles, the capillary binding force F_H acts between the particles.

$$F_H = F_R + F_P \qquad \textbf{Equation 2. 1}$$

Liquid bridges are stable if the vapour pressure equals the partial pressure of the vapour in the surrounding air.

$$\frac{p}{p_0} = \exp\left[\frac{M_w p_k}{\rho R T}\right] \qquad \textbf{Equation 2. 2}$$

Where capillary pressure p_k is given by:

$$p_k = \sigma_{lg}\left(1/R_1 + 1/R_2\right) \qquad \textbf{Equation 2. 3}$$

[Schubert (1984)]

2.1.5 Moisture Relationships

Water contributes to the texture or structure of foodstuffs. Its interaction with chemical components present determines the storage stability. The degree of interaction depends on the amount of moisture present (g H_2O/100g solid) and its thermodynamic state (defined by chemical potential), or water activity.
[Labuza (1975)]

The form of water retention in a powder is a function of the nature of the solid, the ambient humidity, temperature and pressure.
[Coelho and Harnby (1978a)]

2.1.5.1 Types of Moisture

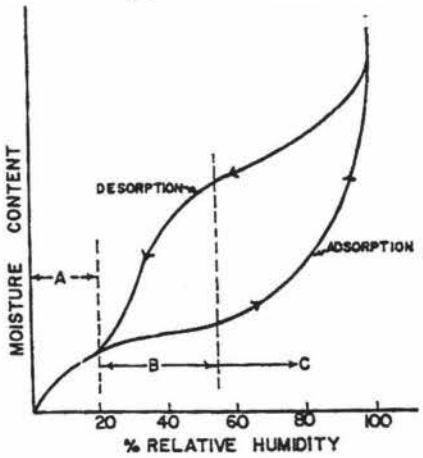

Figure 2. 3 General sorption isotherm

[Labuza (1968)], [Labuza (1975)]

The moisture sorption isotherm can be divided into three regions (A, B and C)

Region A Water is tightly bound or unavailable for reaction

Region B Water is loosely bound

Region C Water is present in capillaries, relatively free for reaction

[Labuza (1975)], [Labuza *et al* (1985)]

2.1.5.1.1 Free Moisture

Free moisture is found on the surface of the salt crystals in the form of adsorbed vapour. It is only present at very low relative humidities and can be easily removed by drying the salt. Free moisture is only present in Region C of Figure 2.3, it will either evaporate into the ambient surroundings or become bound moisture.

[Billings (2002)], [Labuza (1975)]

The amount of free moisture available in a salt sample is negligible, at low water activities (i.e. below 0.2), the moisture content is approximately 0.0001 ($g_{water}/g_{dry\ salt}$).

2.1.5.1.2 Bound Moisture

At low RH the adsorbed vapour forms a monomolecular layer of saturated salt solution known as the BET monolayer. As the RH increases, the thickness of the adsorbed layer increases from monomolecular to polymolecular. Graphically this is

Region B. In this point the water exerts solution and solvent properties and is still partially bound to the surface.
[Coelho and Harnby (1978a,b)] [Labuza (1975)] [Kuprianoff (1958)]

2.1.5.1.3 Interstitial Moisture

Interstitial water is water vapour present in the air that fills the voids or capillaries in the bulk salt. The amount of moisture present is directly related to the relative humidity of the surrounding air.
[Billings (2002)]

2.1.5.2 Water Activity

The water activity characterises the state of water in foods or the availability for physical, chemical and biological changes. Moisture content indicates the quantitative composition.
[Gal (1975a)]

The water activity of a material is the *relative* chemical activity of the water in that material. The water activity of water is 1.0 by definition. The water activity of the water in any material will be less than 1.0. This is a ratio and a dimensionless value. Because of the relative nature of water activity, small differences in a_w may be associated with large differences in moisture content and in the chemical properties of a system.

Micro-organism growth	Moisture equilibria
Hydration	Reaction equilibria
Reaction kinetics	Adsorption
Texture	Flavour

Table 2. 11 Factors associated with water activity

2.1.5.2.1 Measurement of Water Activity

The water activity of hygroscopic food materials may be determined using a dew point method. When water is absorbed by hygroscopic material, its vapour pressure (P) as a fraction of the vapour pressure of pure water (P_0) is a measure of its availability for biological processes.

$$a_w = \frac{P}{P_0}$$ **Equation 2. 4**

The relative humidity of the airspace above the salt is the same characteristic as the water activity of the salt, except that relative humidity (RH) is expressed as a percentage, and is a measure of the water available in the air space in contact with the salt rather than the salt itself. However, the two characteristics are interdependent so are considered the same measurement.

$$RH = 100 * \frac{P}{P_0}$$ **Equation 2. 5**

The factors affecting the choice of methods for measuring the water activity are:

Accuracy	Precision/reproducibility	Time required to achieve a result
Availability of equipment	Degree of skill/training required	Suitability for large numbers of samples
Man hours per sample	Moisture range of interest	Adaptability for automatic pressure control
Destructive/non-destructive	Sample size in relation to sampling problem	

Table 2. 12 Factors involved with selecting water activity measurement methods

[Stitt (1958)]

2.1.6 Moisture Migration

There are a variety of mechanisms of moisture migration through a packed bed of salt. When the salt bed is exposed to a temperature or relative humidity gradient, moisture movement will occur via all methods simultaneously.

2.1.6.1 Liquid Movement Caused by Capillary Forces

$$W_w = -AkX.\frac{dX}{ds}$$ **Equation 2. 6**

A relationship exists between the capillary tension and the moisture content in a salt bed. The liquid conductivity, kX, depends on capillary distribution and varies greatly with moisture content.

[Gorling (1958)]

2.1.6.2 Liquid Movement Caused by Surface Diffusion

Surface diffusion occurs in liquid layers adsorbed at the boundary of solid substances.

$$W_w = -U.\delta_b.\frac{dc_b}{ds}$$ **Equation 2. 7**

[Gorling (1958)]

2.1.6.3 Liquid Movement Caused by Water Vapour Diffusion

In air filled pores caused by differential partial pressures (where pore diameters are larger than the mean free path of water vapour molecules) moisture diffuses through the air spaces.

$$W_w = -\frac{A}{\mu}.\frac{\delta}{R_v T}.\frac{P}{P-P_v}.\frac{dP_v}{ds}$$ **Equation 2. 8**

[Gorling (1958)]

2.1.6.4 Liquid Movement Caused by Vapour Flow

Vapour flow causes differences in the pressure of dehydration processes where the heat transfer occurs in a special way. When the pore diameters exceed the mean free path of the vapour molecules, the flow obeys Poiseuilles equation. [Gorling (1958)]

2.2 MODELLING OF MOISTURE MIGRATION

2.2.1 Lactose Model Adaptation

The model formulated by Bronlund (1997), describes the caking of bulk lactose based on the principle of moisture migration due to temperature gradients within bulk powders in storage.

Bronlund (1997) describes how one dimensional moisture transport occurs due to a temperature gradient and uses it to predict moisture movement in cooling bags when exposed to a temperature gradient. The model was then used to predict when critical moisture values would occur under a described set of conditions and whether they would cause caking. This model was adapted to predict the moisture movement in salt beds caused by a temperature gradient.

It was assumed that the moisture movement between the salt particles is negligible.
The physical basis of the model was summarised as:

- One dimensional heat and moisture transport through a packed bed.
- Initially the salt has a constant moisture content throughout the bed.
- A temperature gradient is applied across the bed.
- The solid and gaseous phases are considered as continua with interaction over adjacent surfaces.
- Moisture diffusivity and thermal conductivity are treated as effective properties of the porous matrix.

One of the assumptions made in the formulation of the model was that the adsorption/desorption process was instantaneous.

The following sections have been directly adapted from Bronlund (1997) for the salt situation.

2.2.1.1 Local Thermal Equilibrium

Heat balance in the gas phase:

$$\varepsilon \cdot V \cdot \rho_a \frac{\partial h_g}{\partial t} = (1-\varepsilon) V \cdot A_s \cdot h_c \cdot [T_s - T] \qquad \textbf{Equation 2. 9}$$

By making the approximation:

$$\frac{dh_g}{dt} = c_{pa} \cdot \frac{dT}{dt} \qquad \textbf{Equation 2. 10}$$

Assume c_{pa}, ρ_a and h_c are constant, take LaPlace transform of above equation:

$$T(s) = \frac{T_s(s) + \tau T(0)}{\tau \cdot s + 1} \qquad \textbf{Equation 2. 11}$$

Where time constant τ

$$\tau = \frac{\varepsilon \rho_a c_{pa}}{(1-\varepsilon) A_s h_c} \qquad \textbf{Equation 2. 12}$$

If standard salt properties are used and a surface heat transfer coefficient h_c=3W/m^{2}K (stagnant air) then the first order time constant τ is less than a second. Therefore the assumption of local thermal equilibrium is valid.

2.2.1.2 Local Moisture Equilibrium

Mass balance for solid phase:

$$(1-\varepsilon) \cdot V \cdot \rho_s \frac{\partial M}{\partial t} = k_g \cdot A_s \cdot (1-\varepsilon) \cdot (P_v - P_s) \qquad \textbf{Equation 2. 13}$$

Assume the isotherm is linear (true for a_w 0.1-0.6). Use the value for saturated salt vapour pressure then:

$$P_s = P_w \cdot A_w = 2.2x10^6 M \qquad \textbf{Equation 2. 14}$$

Substitute 2.14 into 2.13. Assume k_g and ρ_s are independent of temperature. Take the LaPlace transform

$$M(s) = \frac{P_v(s) + \tau \cdot M(0)}{\tau \cdot s + 1} \qquad \textbf{Equation 2. 15}$$

The first order time constant:

$$\tau = \frac{\rho_s}{2.2x10^6 \cdot k_g \cdot A_s}$$ **Equation 2. 16**

Using standard salt properties and an estimated surface mass transfer coefficient k_g of $1.8x10^6 s.m^{-1}$, then τ is less than a second. Sorption occurs quickly, hence the assumption of local moisture equilibrium is valid.

2.2.1.3 Negligible Convection

If the Rayleigh number (N_{Ra}) is less than $4\pi^2$ then negligible convection can be assumed.

$$N_{Ra} = \frac{\rho_a \cdot g \cdot \alpha \cdot K \cdot L \cdot \Delta T}{\lambda \mu}$$ **Equation 2. 17**

Worst case scenario salt properties:

$\alpha = 1/298K$

$L = 1m$

$\mu = 1.8 \times 10^{-5}$ Pa.s

$K = 1.98 \times 10^{-7} s^{-3}$

$\Delta T = 20°C$

$N_{Ra} = 0.05$. Considerably less than the critical value of $4\pi^2$. It can be concluded that natural convection is not significant.

2.2.1.4 Negligible Heat and Moisture Transport Due to Changes in Air Density

Upon heating, air density decreases. The effect of thermal expansion and contraction provides extra moisture movement in the direction of the temperature gradient. Air movement out of a fixed volume carries heat and moisture with it. It is assumed that the amount of heat and moisture movement from this mechanism is negligible in a time step. This means that the only way the total amount of moisture in a node could change is by diffusion and condensation, and those processes are being modelled. This way all moisture is accounted for.

2.2.1.5 Mode of Moisture Movement

Other modes of moisture transfer are surface diffusion, capillary action and diffusion through particles, as discussed in section 2.1.6. These modes of moisture transfer are not significant because crystals are structured, there is no room for free moisture. Surface diffusion is also insignificant because the amount of moisture present at less than 75% RH is very small (only a few monolayers thick).

2.2.1.6 Mathematical Formulation

The model is summarised as transport equations 2.18 and 2.19.

$$\frac{\partial Q}{\partial t} = D \cdot \varepsilon \cdot V \cdot \frac{\partial^2 [H \cdot \rho_a h_v]}{\partial x^2} + \lambda \cdot V \cdot \frac{\partial^2 T}{\partial x^2} \qquad \text{for } t > 0, \quad 0 < x < L \qquad \textbf{Equation 2. 18}$$

$$\frac{\partial W}{\partial t} = D \cdot \varepsilon \cdot V \cdot \frac{\partial^2 [H \cdot \rho_a]}{\partial x^2} \qquad \text{for } t > 0, \quad 0 < x < L \qquad \textbf{Equation 2. 19}$$

2.2.1.6.1 Initial Conditions

$$T = f(T_{initial}) \qquad \text{for all x @ t=0} \qquad \textbf{Equation 2. 20}$$

$$W = f(RH_{initial}) \qquad \text{for all x @ t=0} \qquad \textbf{Equation 2. 21}$$

2.2.1.6.2 Boundary Conditions

Boundary conditions are used to describe the heat transfer over boundaries. This is more consistent than assuming a constant boundary temperature.

$$h_c(T - T_a) = 0 \qquad \text{for } t \geq 0, \quad x=0, L \qquad \textbf{Equation 2. 22}$$

No moisture diffusion occurs over the top and bottom boundaries so a symmetry boundary is used to describe the moisture transport boundaries.

$$\frac{\partial (H \rho_a)}{\partial x} = 0 \qquad \text{for } t \geq 0, \quad x=0, L \qquad \textbf{Equation 2. 23}$$

2.2.1.7 Model Precision Accuracy Using Lactose Properties

The model was evaluated in terms of its ability to predict experimental results.

2.2.1.7.1 Temperature Prediction

The surface heat transfer coefficient must be high because there is good heat transfer between the metal plate and the lactose.

Parameters used in the model for prediction with lactose

Thermal conductivity	0.175 $W.m^{-1}K^{-1}$
Porosity	0.4
Effective Diffusivity	ϵD_{air}
Slab thickness	0.078m
Initial water activity	0.68
Initial temperature	19.5°C
Fitted isotherm	Tss isotherm*

Table 2. 13 Model parameters for temperature prediction in lactose

*refer to section 2.4.3 Isotherm models.

Excellent temperature predictions were obtained. Sensitivity analysis showed that the range of thermal conductivity values (from the infinite cylinder experiments) resulted in differences up to 3°C. The average value gave the best predictions.

2.2.1.7.2 Surface Relative Humidity Prediction

Predicted profiles were similar in nature to the experimental trends. Several parameters influence the accuracy of the model; porosity, initial water activity, initial temperature, moisture diffusivity, slab thickness and the shape of the isotherm.

Sensitivity analysis of the lactose results showed that increasing porosity increases the rate of moisture migration. Adjustment of diffusivity allowed good cold surface predictions. And changing the initial water activity values gave predictions which were shifted up or down without significantly altering the profile shape. The slab thickness had very little effect on the outcome of the model (which proves the validity

of the assumption of one-dimensional heat transfer) and the shape of the isotherm had the largest effect on surface RH predictions.

δ/τ_2	0.7
Slab thickness	0.078m
Initial water activity	0.68
Initial temperature	19°C

Table 2. 14 Model parameters for RH prediction in lactose

2.2.2 Sucrose Model

Billings (2002) successfully applied Bronlund's (1997) model to bulk sucrose to show the moisture movement in sucrose and to predict the amount of caking likely to result from the moisture movement.

Five input parameters were found to have an impact on the model results:

- Thickness of the slab.
- Initial water activity of the sample.
- Porosity of the sample bed.
- Heat transfer coefficient of the material between the sugar and the cooling plates.
- Temperature difference between plates.

It was assumed that the porosity and heat transfer coefficient were constants, with the porosity determined experimentally. There are five parameters for describing the state of the sugar: initial sugar temperature and water activity, the percentage that is amorphous sucrose, the initial crystallinity of that amorphous fraction and the porosity of the bed.

2.2.3 Conclusion

In order to create a mathematical model to predict caking in salt, the physical values for the model parameters must be found. Some were available in literature while others were measured experimentally.

2.3 PROPERTIES OF SALT

2.3.1 Physical Properties

To understand salt and its caking mechanism, the properties of salt were examined.

Property	Salt	Sodium	Chloride
Chemical symbol	NaCl	Na	Cl
% Composition	100	39.3358	60.6642
Atomic Number		11	17
Molecular weight	55.448	22.991	35.457

Table 2. 15 Properties of NaCl

Calcium and Magnesium salts are the most common impurities in sodium chloride. [Iyengar and Sen (1970)]

2.3.1.1 Phases of Sodium Chloride

There are four phases of sodium chloride, crystalline, dissolved, bound and amorphous.

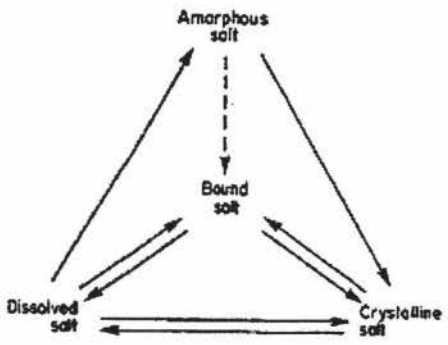

Figure 2. 4 Phases and phase changes of sodium chloride

[Gal (1975)a]

The phase that is stable or dominant is determined primarily by the water activity of the salt. However, in the case of amorphous phase, the mixing ratio of casein-NaCl is crucial. Amorphous sodium chloride only forms under very specific conditions (only one example could be found in literature). When mixed with casein, the salt becomes

amorphous if there is a small excess of salt relative to the binding capacity of casein, and the mixture is exposed to rapid freezing and dehydration.

[Gal (1975)b]

2.3.1.2 Density of Solid Sodium Chloride

Temperature (°C)	Density (g/cm^3)
-184	2.208
-79	2.186
0	2.168
10	2.165
20	2.163
20.8	2.162
25	2.161
30	2.160
40	2.158
50	2.155

Table 2. 16 Density of solid NaCl

[Kaufmann (1960)]

2.3.2 Thermal Properties

Property	Symbol	Value	Units
Melting point		800.8 ± 0.5	°C
Boiling point (NaCl)		1465	°C
Boiling point (sat. aqueous soln)		108.7	°C
Heat of formation (0°K)	$\Delta H_f°$	-97.755	kcal/mole
Heat of formation (298.16°K)	$\Delta H_f°$	-98.232	kcal/mole
Entropy (298.16°K)	S°	17.30	cal/mol
Heat capacity (298.16°K)	Cp°	11.88	cal/mol
Specific Heat Capacity (25°C) (0-20°C)		0.204 0.2027	cal/g°C cal/g°C

Table 2. 17 Thermal properties of NaCl

[Kaufmann (1960)]

The thermal conductivity of salt varies from sample to sample, depending on other physical properties, such as the bulk density of the sample. As the thermal conductivity is particularly important for the mathematical model, it was measured experimentally.

2.4 MOISTURE SORPTION ISOTHERMS

2.4.1 Objective

Sorption isotherms show the dependence of water activity on the water content at definite temperatures and pressures. A sorption isotherm relates the energy level of the water in a system to its distribution between solid and gaseous phases. It characterises the degree of water binding for different relative humidities.
[Audu *et al.* (1978)] [Smith *et al.* (1981)]

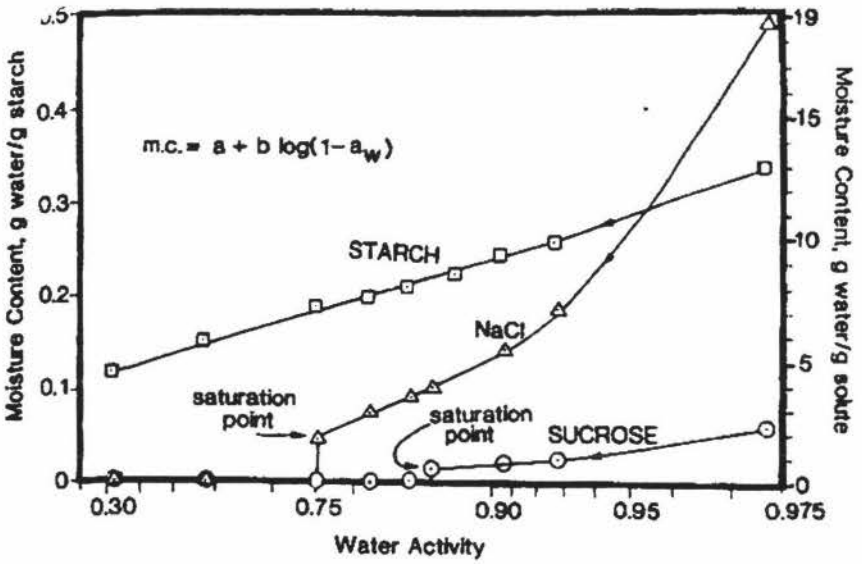

Figure 2. 5 Desorption isotherm data at 25°C for NaCl, sucrose and starch
[Chinachoti and Steinberg (1986)]

A sorption isotherm is a plot of the amount of water absorbed as a function of the relative humidity of the vapour space surrounding the material. Moisture sorption data is useful in determination of techniques for processing and packaging of dehydrated foods and the prediction of undesirable chemical, physical and microbiological changes that might occur during storage.
[Gur-Arieh *et al.* (1965)] [Labuza *et al.* 1985)]

Adsorption of water onto a surface may have physical or chemical origins. A particular shaped isotherm results with crystals like NaCl because anhydrous crystals like NaCl contain only traces of water at low/medium RH. Thus the adsorption corresponds to saturation equilibrium (vertical line on adsorption curve, for salt this is

at 75.3%). On a sorption isotherm graph this appears as a horizontal equilibrium of hydration followed by vertical saturation equilibrium. During the establishment of adsorption or desorption isotherm, a polymorphic rearrangement (anhydrous to hydrate) occurs, followed by a change in the saturation equilibrium.
[Mathlouthi and Roge (2003)]

As a general rule, the water activity decreases when the temperature is increased and the amount of adsorbed water remains constant. This can be explained using the equation of free energy

$$\Delta G = \Delta H - T\Delta S \qquad \textbf{Equation 2. 24}$$

Adsorption is spontaneous so ΔG is negative. Water is less free to escape to the atmosphere, so ΔS is less than 0, and then ΔH is less than 0. An increase in temperature is not favourable to the adsorption of water.
[Mathlouthi and Roge (2003)]

2.4.2 Measurement Methods for Sorption Isotherms

2.4.2.1 Constant Relative Humidity Desiccator Method

The sample is allowed to equilibrate in a closed desiccator at atmospheric pressure with a saturated salt solution. Equilibration of the moisture content requires a relatively long time period, at least three weeks.
[Gur-Arieh *et al.* (1965)] [Bell and Labuza (2000)] [Laaksonen *et al.* (2001)]

Because isotherm data is based on the moisture content at equilibrium with a known water activity, it is critical to allow sufficient time for complete equilibration. This can be accomplished by removing the sample at specified time intervals, weighing and replacing it in the chamber. When the sample shows no weight gain after three consecutive weighings it can be considered to be at its equilibrium moisture content. At each weighing time, the atmosphere in the desiccator will be mixed with room air. Thereafter, some time will be required for the air to re-equilibrate with the saturated solution. During this time the sample will be adjusting to a "false" water activity. If this disturbance could be reduced or eliminated, this would reduce the equilibration time. When a dry sample is placed in a desiccator, it will absorb vapour molecules from the vapour space. To maintain the relative humidity, the salt solution must

compensate by replacing vapour molecules. Reducing the number of samples (and therefore the volume of desiccator required) would reduce the equilibration time.
[Lang *et al.* (1981)]

2.4.2.2 Gravimetric Methods

1. Methods with Continuous Registration of Weight Change

If the balance is a fixed part of the apparatus, weight changes can be determined continuously, without interrupting the sorption process. Using an evacuated system accelerates the diffusion of water molecules from the reservoir to the sample.
[Gal (1975a)]

One example of this type of equipment is the Thermal Gravimetric Analyser owned by Massey University. The TGA consists of a furnace through which gases can be passed over a sample. The sample is suspended on a beam in the centre of the furnace, which also acts as a balance, sensitive to weight changes as small as 0.001mg.

2. Dynamic Systems

Circulated air is used to maintain RH. The primary problem with these systems is accurately maintaining the RH of the air. Precise measurements of weight without loss of accuracy are possible if the air flow is constant. The limitations of dynamic systems are that only one sample can be processed at a time and that the weight/time curves of many swelling substances go through a maximum (adsorption) or a minimum (desorption) which prevents, or complicates using this system.
[Gal (1975a)]

2.4.2.3 Manometric and Hygrometric Methods

Manometric and hygrometric methods are used for rapid and convenient determination of the water activity in process or quality control. Direct hygrometric methods use dew point sensor or hygrosensors.

The problems with using these systems are the evaluation of exact time to reach equilibrium states between the sample and the sensing element, the temperature

control to prevent fluctuations in the reading and the instability of instruments (recalibrate as often as possible).

[Gal (1975a)]

2.4.3 Isotherm Models

The usefulness of any one model for describing the whole isotherm is limited. [Labuza *et al.* (1985)]

The Langmuir Isotherm, or kinetic model, describes the adsorption of the monolayer by porous solids.

$$V = V_m \frac{(ba_w)}{(k + ba_w)}$$ **Equation 2. 25**

Where $k = 1/P_0$ **Equation 2. 26**

$$b = k_0 \exp\frac{(Q_s/RT)}{RT}$$ **Equation 2. 27**

The Langmuir equation fails to describe the complete isotherm because it assumes that Q_s is constant and that the maximum adsorption is a monolayer.

[Labuza (1968)]

The BET (Brunauer, Emmet, Teller) isotherm model assumes that the heat of adsorption of the first layer is larger than that of subsequent layers, which are equal to the latent heat of vapourisation.

$$\frac{V}{V_m} = \frac{c \cdot a_w}{(1 - a_w)[1 + (c-1) \cdot a_w]}$$ **Equation 2. 28**

Where $c = k \exp(Q_s / R \cdot T)$ **Equation 2. 29**

$$k = \frac{accommdationcoefficient}{frequencyfactor} \approx 1$$ **Equation 2. 30**

[Labuza (1968)]

The GAB (Guggenheim, Anderson, de Boer) model equation is as follows:

$$m = \frac{m_0 c_G k a_w}{(1 - k a_w)(1 - k a_w + c_g k a_w)}$$ **Equation 2. 31**

[Peleg (1993)]

The Clausius Clapeyron Equation is used to predict sorption isotherm values at temperatures other than experimental temperatures.

$$\frac{d(\ln a_w)}{d\left(\frac{1}{T}\right)} = \frac{Q_s}{R}$$ **Equation 2. 32**

Isotherms should show a decrease in the amount of water adsorbed with an increase in temperature at a constant water activity. To find Q_s, isotherms must be measured at a minimum of two temperatures. This equation only applies when the moisture content of the system remains constant.
[Gal (1975a)] [Labuza (1968)] [Labuza *et al.* (1985)]

The Peleg model is not derived theoretically and is an empirical moisture sorption model.

$$m = k_1 a_w^{n1} + k_2 a_w^{n2}$$ **Equation 2. 33**

Where k_1, k_2, n_1, n_2 are all constants. ($n_1<1$, $n_2>1$)
[Peleg (1993)]

The Smith isotherm describes two fractions of water adsorbed onto a dry surface. The first fraction has a higher than normal heat of condensation and follows the Langmuir isotherm. The second fraction consists of multiple layers of condensed water molecules which block the evaporation of the first layer.

$$M = a + b\log(1 - a_w)$$ **Equation 2. 34**

The values for salt at the saturation relative humidity are a_w=0.753, a=-5.1118, b=-12.5857. [Lang and Steinberg (1981)]

The Smith isotherm only applies above the saturation relative humidity and so is of limited value to this study.

The Tss isotherm equation was used by Bronlund (1997) in the mathematical model created for lactose. It is based on the GAB model, but assumes that after a certain number of moisture layers have been adsorbed the moisture behaves as liquid water.

$$M = \frac{M_0 \cdot c \cdot H \cdot f \cdot a_w H'}{(1 - f \cdot a_w)[1 + (c \cdot H - 1) f \cdot a_w]}$$ **Equation 2. 35**

$$H' = 1 + \frac{H - 1}{H} \cdot \frac{1 - f \cdot a_w}{1 - a_w} \cdot [h + (1 - h) \cdot a_w]$$ **Equation 2. 36**

$$H = 1 + \frac{1 - f}{f} \cdot \frac{(f \cdot a_w)^h}{1 - a_w}$$ **Equation 2. 37**

[Bronlund (1997)], [Timmerman (1989)], [Timmerman and Chirife (1991)]

2.4.4 Literature Sorption Isotherms for Sodium Chloride

Relative Humidity	Moisture content
%	%
10	0.10
20	0.11
30	0.11
40	0.11
50	0.11
60	0.13
70	0.14
75.3	Saturated solution

Table 2. 18 Equilibrium moisture content of NaCl at different relative humidities

[Iyengar and Sen (1970)]

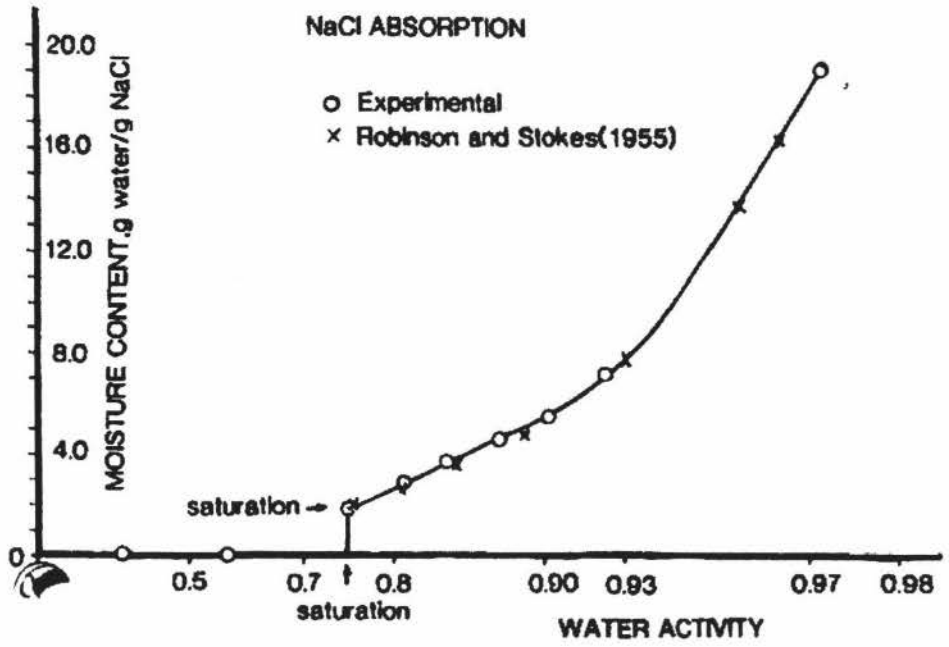

Figure 2. 6 Sorption isotherm at 25°C for NaCl
[Chinachoti and Steinberg (1985)]

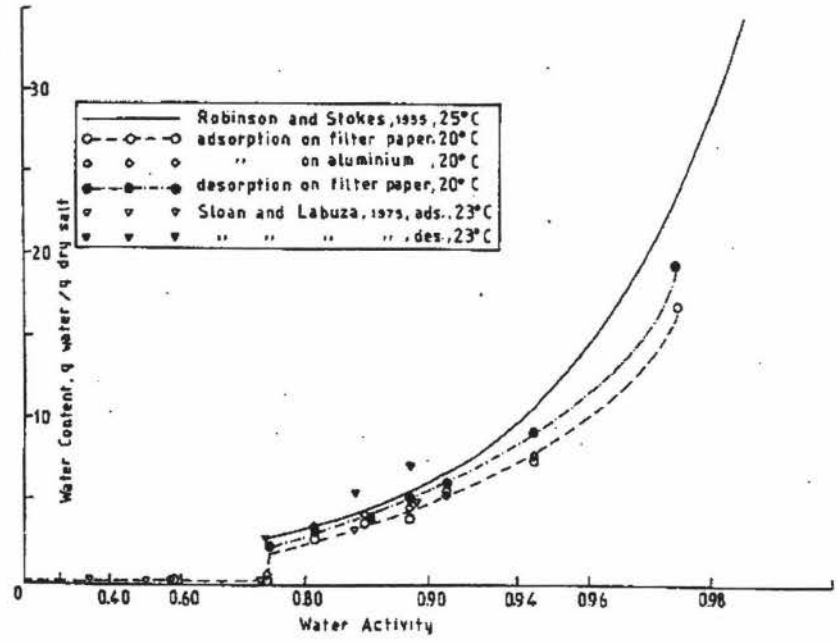

Figure 2. 7 Smith plots for adsorption and desorption of water by sodium chloride
[Hardy and Steinberg (1984)]

It can be seen from Figures 2.6 and 2.7 that the amount of water held by the salt below the saturation water activity (0.753) is very small compared to above this point.

The shape of the salt isotherm is unique in that a large degree of moisture adsorption takes place at the saturation point.

2.4.5 Summary

The isotherm models researched are all general models. Sodium chloride does not follow the standard isotherm shape, the saturation relative humidity covers a large range of moisture content values. The unusual shape of the isotherm eliminates the use of any of the standard equations to describe moisture sorption in salt. Smith's isotherm fits for relative humidities above saturation, but this project is focussed on crystalline salt and drying. The literature data for the NaCl isotherm below the saturation point is scarce, so there is a need to confirm the low water activity data, and to find a suitable isotherm equation for use in the mathematical model.

2.5 CONCLUSION

Salt often cakes during storage and transportation. The caking mechanism for salt is humidity caking, as salt has no amorphous content under normal processing conditions.

Bronlund's (1997) mathematical model will be adapted to create a mathematical model for the caking of bulk salt. Experiments will be performed to determine the thermal and physical properties of the salt (e.g. the thermal conductivity and the bulk density) and the adsorption isotherm of the salt. These need to be done to provide the parameters for the salt caking model. The model will be validated against controlled experimental temperature gradients applied to salt samples with known moisture contents and water activities.

If the water activity of the sample and the temperature gradient that the sample will be exposed to are known, the mathematical model can be used to predict the likelihood of caking occurring in the salt, which is the aim of the investigation.

CHAPTER THREE PHYSICAL PROPERTIES

3.1 INTRODUCTION

The aim of this investigation is to model the effect of temperature gradients and the resulting moisture movement on the caking of bulk salt.

In order to create the mathematical model, certain characteristics of the salt must be known. Some of these were available in the literature (see Chapter Two), but many needed to be determined experimentally. Some characteristics of the salt depend on the salt history; these will vary between salt samples.

Experiments were conducted to determine the moisture sorption properties of the salt, the thermal conductivity, the particle size distribution, the bulk density and the porosity of the salt.

The results from each set of experiments were used to define the physical properties of the salt for use in the mathematical model.

3.2 BULK DENSITY OF SALT

3.2.1 Introduction

The bulk density of the salt is critical for this investigation because it affects the thermal conductivity and the porosity of the salt. The bulk density of the salt varies with the amount of compaction. Pressure or movement will cause the salt to shift and settle into a more packed formation.

The density of the salt at Dominion Salt Ltd varies depending on which stage of the process it is at. The salt leaving the Dominion Salt plant in bags has been subjected to sufficient movement and compaction to ensure that the salt has all settled into a packed formation.

To determine the range of densities occurring in the salt, a series of density experiments were conducted. Tapping the side of the container causes the salt to settle to the level of compaction created during the bagging and stacking processes. The density will change according to the particle size distribution. A range of particle sizes can mesh together more tightly than uniform particles.

3.2.2 Experiments

3.2.2.1 Aims

To determine the range of salt bulk densities likely to occur in the plant.

To determine a typical salt bulk density value for use in the model.

3.2.2.2 Experimental Apparatus

320 mL plastic sample container

Mettler Balance

3.2.2.3 Experimental Method

The plastic sample container was weighed. The container was then filled with water and the weight of water measured. This weight was then used to calculate the volume of the container. The container was dried by standing upside down overnight.

Poured bulk density:

Salt was poured gently into the sample container. A ruler was used to gently scrape the excess salt from the top of the container, ensuring that the salt was level with the top. The weight was then recorded. This was repeated until three measurements agreed.

Tapped bulk density:

Salt was poured into the sample container until it was approximately one third full. The sides of the container were then tapped until the salt had finished settling. This was repeated until the container was full. At this point the salt was physically compacted with the surface level with the top of the container. The weight of the salt in the container was then measured. This procedure was repeated until three measurements agreed.

3.2.3 Results

The mass of salt in each density experiment was recorded and then the density of the sample was calculated using equation 3.1.

$$\rho = \frac{m}{V} \qquad \textbf{Equation 3. 1}$$

The lowest value recorded for the mass of salt in the poured density experiments was 243g. The bulk density was calculated:

$$\rho = \frac{243g}{231cm^3} \qquad \textbf{Equation 3. 2}$$

Minimum density value $\rho_{min} = 1.052$ g/cm^3 or 1052 kg/m^3.

The average value for the mass of salt in the tapped density experiments was found to be 301 ± 0.1 g. The volume of the plastic sample container was 231 mL or 231 cm^3. The bulk density was then calculated.

$$\rho = \frac{301g}{231cm^3} \qquad \textbf{Equation 3. 3}$$

The typical bulk density of the salt was calculated to be $\rho = 1300 \pm 5$ kg/m^3.

3.2.4 Porosity

The porosity of the salt bed is closely related to its bulk density. The porosity is a measure of the void or air spaces in the salt sample, so the more densely packed the salt, the lower the porosity. In any salt sample, the salt crystals and the air spaces are in equilibrium. Air has different thermal properties to salt. To accurately model the effect of a temperature change on a salt sample, the porosity must be known.

The porosity can be found from the bulk density using Equation 3.4.

$$\rho_{bulk} = (1-\varepsilon)\rho_{particle} \qquad \textbf{Equation 3. 4}$$

From the bulk density experiments, the typical value for the bulk density was found to be 1,300 kg/m^3 and from Kaufmann (1960) the particle density of salt is 2161 kg/m^3, the porosity of the packed salt was calculated to be 0.398 ± 0.005.

3.3 PARTICLE SIZE DISTRIBUTION

3.3.1 Introduction

The particle size distribution of the salt is not directly involved in the mathematical model, but it has a large effect on salt properties and the propensity to cake.

The particle size distribution affects the bulk density of the salt because if a range of particle sizes is present the salt can compact much more than uniformly sized particles. A range of particle sizes also increases the number of contact points between salt crystals, affecting the thermal conductivity. The amount of heat conduction is increased because contact between particles allows conduction of heat from one particle to the next, rather than convection through the air spaces. Both increased bulk density and thermal conductivity will increase the tendency of the salt to cake. The presence of fines has also been shown to increase the amount of caking because smaller particles dissolve in a smaller amount of water. Thus, fines begin forming liquid bridges at a lower moisture content, increasing the level of caking. [Bhatt and Datar (1968)] [Bagster (1970)]

The plant is cleaned thoroughly before pharmaceutical salt is produced, to ensure that no anti-cake is still present in the process. When the plant is started up again the initial particle size of the salt is significantly smaller than the particle size of salt taken later in the day. To determine the difference in particle sizes, samples were taken hourly from start up and measured. The salt is considered to have reached a typical particle size profile within four hours of start up. Because the initial salt makes up only a small portion of the salt, the fourth hour sample is regarded as typical.

3.3.2 Experiments

3.3.2.1 Aims

To determine the typical particle size distribution.

To determine the average particle size.

3.3.2.2 Experimental Apparatus

Mettler PE 160 Balance

Endecotts Laboratory Test Sieves

Sizes: 710, 600, 500, 455, 425, 355, 250, 212, 180 μm

Retsch AS200 Mechanical shaker

3.3.2.3 Experimental Method

The sieves were stacked with the largest sieve (710μm) at the top and the smallest sieve (180μm) at the bottom. A weighed sample of approximately 100g was poured into the top sieve. The stack of sieves was then placed on the mechanical shaker for ten minutes. At the end of this time the weight of salt in each sieve was measured and the distribution calculated. Experiments were conducted weekly at start up over a period of several months, thus data was obtained for all ambient conditions.

3.3.3 Results

It was found that the results for the hourly particle size distributions had very little variation from day to day. The figure below shows the average percentage of salt passing through each sieve for the one, two and three hourly average distributions.

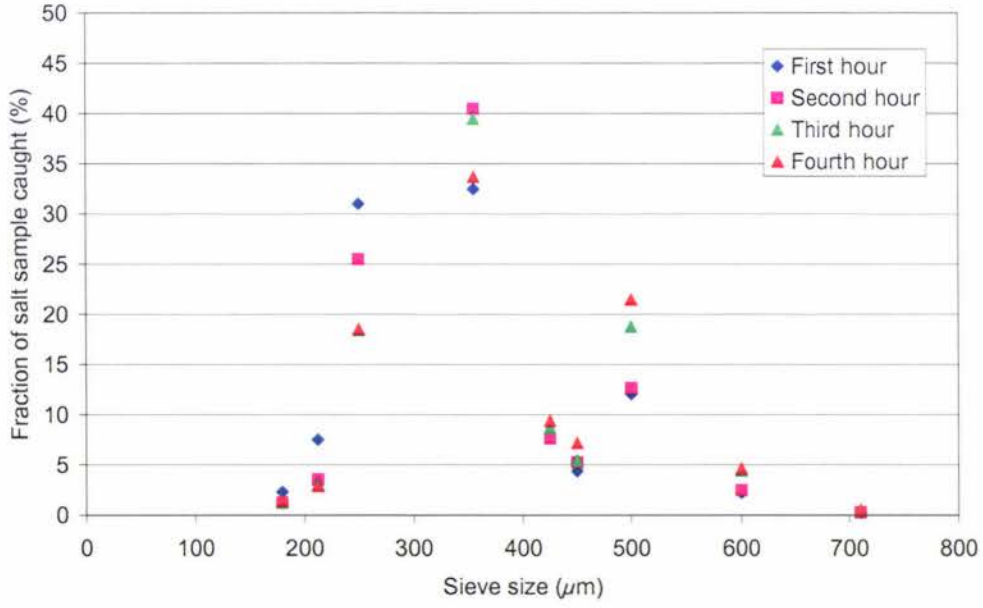

Figure 3. 1 Raw data example from particle size distribution experiments

To calculate the fraction of salt passing through each sieve the fractions caught in all of the sieves below were added. These were then plotted against the particle size to obtain the distribution. The particle size distributions of the salt at various times from start up are shown in figure 3.2:

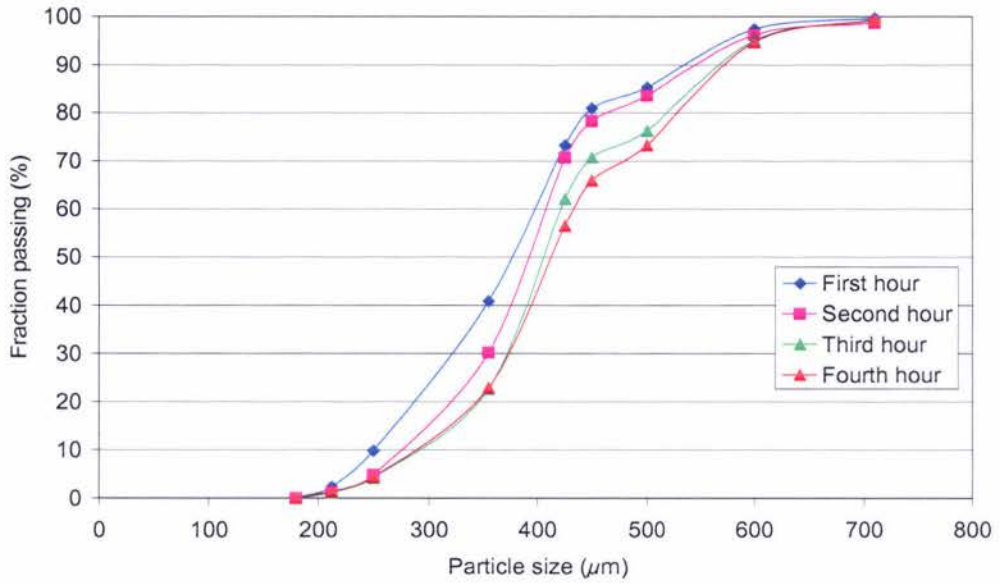

Figure 3. 2 Typical hourly particle size distribution profiles

The salt was considered to have reached its typical particle size by the fourth hour after start up. The results from the fourth hour samples particle size distributions of salt were averaged to obtain a typical value for the salt, shown in Figure 3.

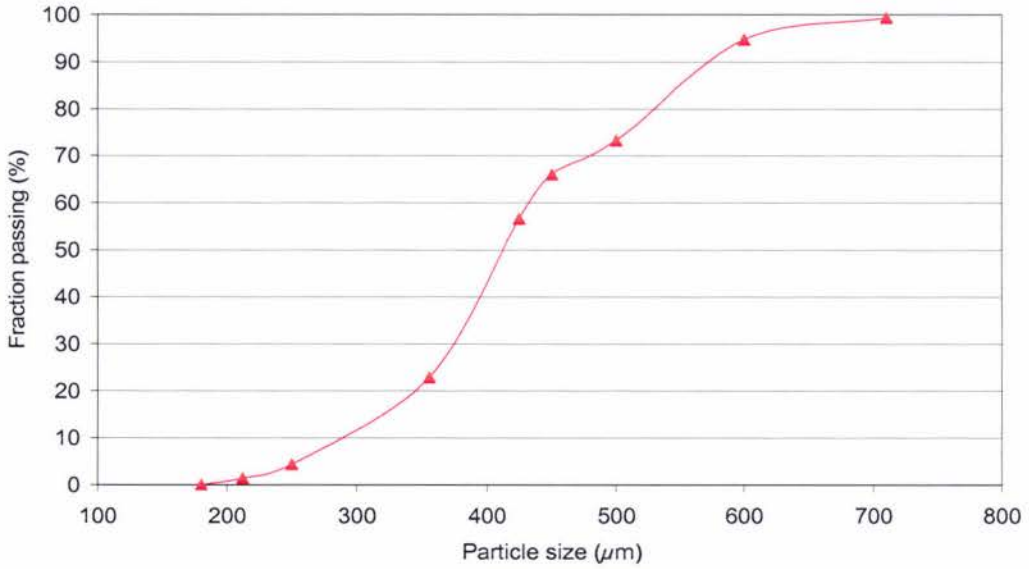

Figure 3. 3 Typical particle size distribution

The typical average particle size for pharmaceutical grade salt is 410μm.

3.4 THERMAL CONDUCTIVITY

3.4.1 Introduction

When bulk salt is subjected to a temperature gradient, moisture migration occurs. To predict the temperature profile of the salt through the sample the effective thermal conductivity of the salt bed must be known.

Carslaw and Jaeger (1959) solved the differential equations for the heat conduction in an infinitely long cylinder.

$$Y = 1 - 2\sum_{n=1}^{\infty} \frac{\exp(-\beta_n^2 \times \alpha \cdot t / r^2)}{\beta_n J_1(\beta_n)} \qquad \textbf{Equation 3. 5}$$

For $\alpha t/r > 0.15$ only the first two terms of the series are significant and the solution can be evaluated by noting $ß_1 = 2.405$, $ß_2 = 5.520$, $J_1(ß_1) = 0.519$ and $J_2(ß_2) = -0.340$.

Using the infinite cylinder model (Equation 3.5), the fraction of accomplished change (1-Y), at differing values of Fourier number ($\alpha.t/r^2$), was calculated by Bronlund (1997).

1-Y	$\alpha.t/r^2$
0.15205	0.1
0.498494	0.2
0.717524	0.3
0.841531	0.4
0.911129	0.5

Table 3. 1 Accomplished temperature change in an infinitely long cylinder

Because thermal conductivity will vary for different salt samples, experiments were performed on a large number of samples and a typical value calculated.

3.4.2 Experiment

3.4.2.1 Aims

To determine the range of possible thermal conductivity values for salt.

To find the typical thermal conductivity for salt.

3.4.2.2 Experimental Apparatus

An infinite cylinder was approximated by using a copper tube 300mm long by 80mm in diameter. The temperature at the centre of the cylinder was measured at different depths by placing a piece of string inside the cylinder that has two thermocouples attached at one-third and two-thirds of the length of the cylinder. Polystyrene blocks at each end of the cylinder ensured that all heat transfer was one dimensional. Attaching one end of the string to the bottom polystyrene block ensured that the thermocouples were in the same place for each experiment. Thermocouples were also taped to the outside of the cylinder using aluminium tape, so the temperature at the outside could be measured and compared with the centre temperature.

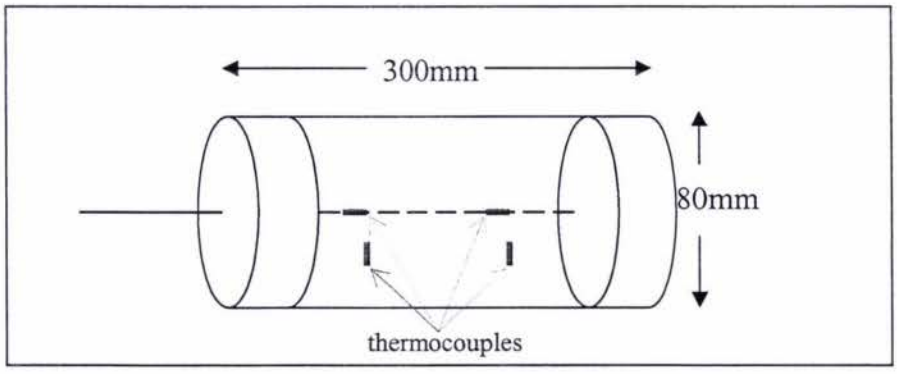

Figure 3. 4 Infinite cylinder

A Grant W38 Waterbath thermostat and pump unit was placed in a large bucket to create a high temperature environment.

3.4.2.3 Experimental Method

The cylinder was filled with salt while the string was held taut. The cylinder was tapped during filling in order to achieve maximum density, simulating the salt after bagging and storage. With the cylinder full, the top polystyrene plug was put in place and the cylinder sealed at the top and bottom with silicon-coated fibre gaskets, which were then clamped down to ensure the cylinder was watertight. Once the salt in the cylinder had equilibrated to room temperature, the cylinder was immersed in the water filled bucket, and the resulting temperature measurements recorded using a Pico TC08 data logger.

3.4.3 Results

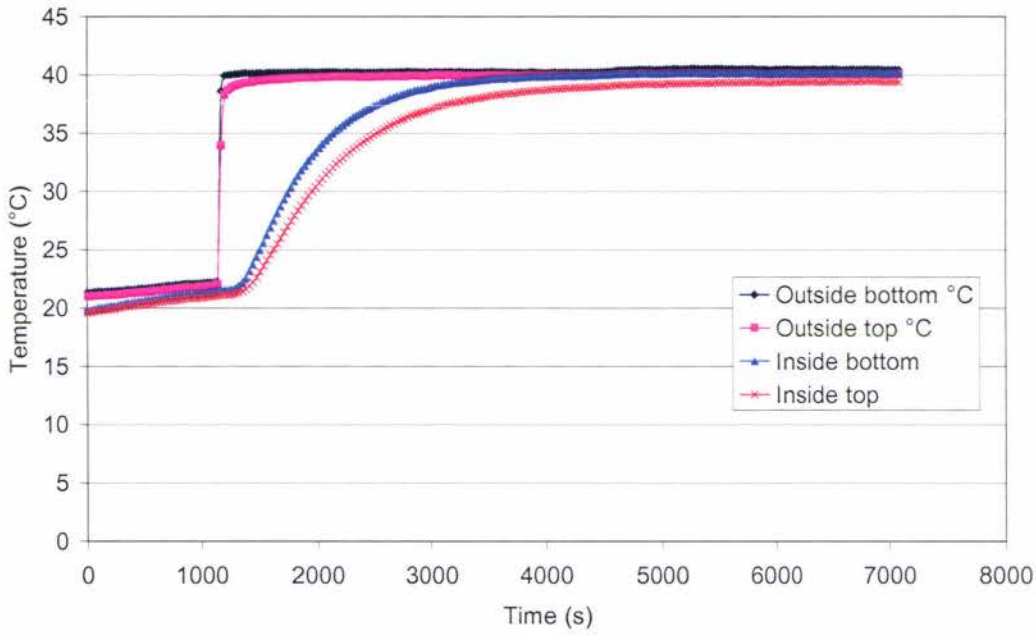

Figure 3. 5 Infinite cylinder raw data example

Infinite cylinder experiments were conducted on each of the hourly samples taken from start up. Very little variation was found between samples and the fourth hourly sample was considered to be typical of the salt in general.

Bronlund (1997) and Billings (2002) used the same infinite cylinder in their work on lactose and sucrose respectively. They proved that under ideal circumstances, the inside top and the inside bottom readings would be the same at all times. This was not

the case in these experiments as the water bath available was not deep enough. In the calculations it was decided to use only the Inside bottom measurement.

The fraction of unaccomplished temperature change was calculated and plotted against time. The linear section of the graph was plotted on a semi-log scale and the equation of the line found.

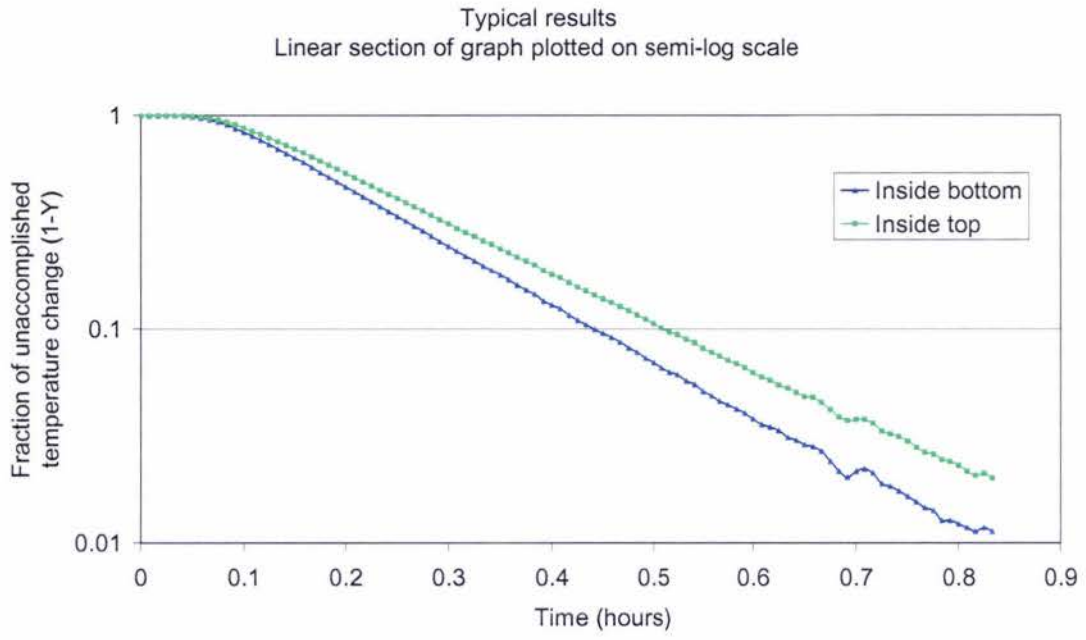

Figure 3. 6 Typical results for infinite cylinder experiments

3.4.4 Calculations

The equation for the straight line section of the graph was used to find the time for a given value of Y, corresponding to the 1-Y column in Table 3.2. By substituting into the appropriate $\alpha t/r^2$ term, and since r was known to be 0.04m, the thermal diffusivity α was calculated. Equation 3.6 was then used to calculate the thermal conductivity λ. These calculations were programmed into a spreadsheet and 5 estimates of t calculated to give an average estimate of the equipment.

$$\lambda = \alpha \cdot \rho \cdot C_p \qquad \textbf{Equation 3. 6}$$

1-y	$\alpha.t/r^2$	Y	t	alpha	λ	
	(m^{-1})		(s)	(m/s)	(W/mK)	
0.15205	0.1	0.848	296	5.40E-07	0.877	
0.49849	0.2	0.502	611	5.23E-07	0.851	
0.71752	0.3	0.282	810	5.92E-07	0.962	
0.84153	0.4	0.158	923	6.93E-07	1.13	
0.91113	0.5	0.089	986	8.11E-07	1.32	
				6.32E-07	1.03	Average
				1.20E-07	0.195	Std.

Table 3. 2 Thermal conductivity calculations

The average or typical value for the thermal diffusivity α was found to be:

6.319×10^{-7}m/s

$$\lambda = 6.319e-07 \times 1300 \times 850$$ **Equation 3. 7**

The typical value for thermal conductivity of salt was calculated to be:
$\lambda = 1.027 \pm 0.24$ W/mK error

3.5 MOISTURE SORPTION ISOTHERMS

3.5.1 Introduction

A moisture sorption isotherm is a plot of the moisture content against relative humidity (%) or water activity (fraction). A small amount of water adsorption causes a large change in the water activity of salt below the saturation point of a_w= 0.753 (25°C). The maximum moisture content recorded in literature below the saturation humidity of the salt was 0.14%.
[Iyengar and Sen (1970)]

Because the moisture content is so small, it is very difficult to measure. A much more practical and reliable measurement is the water activity of the salt. The moisture sorption characteristics of the salt must be known to calculate the amount of water that will be adsorbed by the salt under different relative humidity conditions. The amount of moisture adsorbed by the salt is determined by the relative humidity of the surrounding air. The relative humidity (RH) of the air is a function of the absolute humidity (mass of water vapour) and the temperature.

Three methods were used to measure salt isotherms, the evacuated or vacuum desiccator method, the Thermal Gravimetric Analyser (TGA) method and a long term (non-evacuated) desiccator method. The salt samples were placed into the constant relative humidity environment, and the moisture content measured, until they were considered to have reached equilibrium.

3.5.2 Experimental Aims

The aim of each of these experiments was to determine the moisture content of the salt at a range of relative humidities below the saturation RH and to measure a moisture sorption isotherm. The three methods were compared to each other and to literature values.

3.5.3 Vacuum Desiccator Method

Placing dry samples over saturated salt solutions is a traditional method of determining moisture sorption properties. [Gal (1975a)][Bell and Labuza (2000)] An evacuated desiccator environment will reach equilibrium more rapidly.
[Gal (1975a)][Gur-Arieh *et al.* (1965)][Laaksonen *et al.* (2001)]

If the system was placed under a vacuum the saturated salt solution would be able to create a constant RH environment much more quickly, as less water molecules are required to evaporate to achieve the equilibrium conditions. It follows therefore, that a salt sample in an evacuated desiccator would reach the equilibrium RH and the corresponding moisture content more rapidly than a sample in a non-evacuated desiccator.

3.5.3.1 Experimental Apparatus

Vacuum desiccators (x7)

Moisture dishes and lids (x35)

Constant temperature incubator

Mettler 160 Balance

3.5.3.2 Materials

Sodium chloride (NaCl)

Saturated salt solutions

Lithium chloride (LiCl)	11.3% RH
Potassium acetate (CH_2COOK)	22.5% RH
Magnesium chloride ($MgCl_2$)	32.8% RH
Potassium carbonate (K_2CO_3)	43.2% RH
Magnesium nitrate ($Mg(NO_3)_2$)	52.9% RH
Potassium iodide (KI)	68.9% RH

Phosphorous pentoxide powder (P_2O_5)

[Greenspan (1977)]

3.5.3.3 Experimental Method

A saturated solution was placed in each desiccator, with the exception of the desiccator which contained phosphorous pentoxide powder. The moisture dishes were dried overnight in a 130°C oven, cooled in a desiccator over P_2O_5 and weighed. Salt samples of approximately 5g were weighed into each of the moisture dishes and the weight recorded. Five moisture dishes and lids were placed into each of the desiccators and a vacuum applied to -70kPa (gauge). The desiccators were then placed into a constant temperature incubator at 25°C. After 24 hours the desiccators were removed, the lids were replaced on the moisture dishes and the samples weighed. Laaksonen *et al.* (2001) suggested that 72 hours in an evacuated desiccator would be sufficient to attain equilibrium. It can be seen from Figure 3.7 that the samples had not reached equilibrium after 72 hours, the moisture contents were still increasing.

3.5.3.4 Results

The average moisture content of the five samples was calculated for each desiccator at each sample time.

Salt	**a_w**	**24 hours**	**48 hours**	**72 hours**
		(% dry basis)	(% dry basis)	(% dry basis)
P_2O_5	0	0.00082	0.00032	0.00163
LiCl	0.113	0.00125	0.00197	0.00343
CH_2COOK	0.216	0.00070	0.00188	0.00398
$MgCl_2$	0.316	0.00078	0.00216	0.00279
K_2CO_3	0.432	0.00049	0.00063	0.00224
$Mg(NO_3)_2$	0.484	0.00207	0.00276	0.00390
KI	0.661	0.00125	0.00425	0.00630

Table 3. 3 Vacuum desiccator results

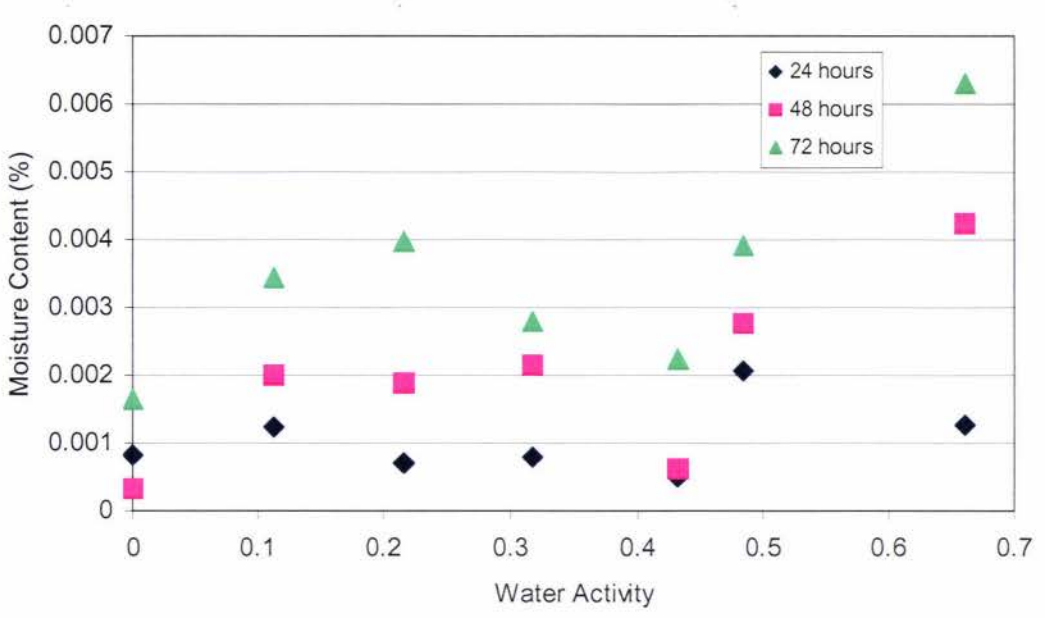

Figure 3. 7 Vacuum desiccator results

3.5.3.5 Analysis

The samples were meant to be at equilibrium after a 72-hour period, but it can be seen that the moisture content was still increasing. With the sample weights still increasing and the experimental problems in maintaining a vacuum in the desiccators, it was decided to concentrate on the non-evacuated method, giving sufficient time for the samples to come to equilibrium.

3.5.4 Non-Evacuated Desiccator Method

This method involves samples placed in a non-evacuated airtight desiccator and left undisturbed for a considerable length of time. In this experiment the samples were left for approximately twelve weeks to equilibrate. Sorption equilibration generally requires one to ten weeks, depending on the material being tested [Lang *et al.* (1981)]. It was decided that a twelve week period would be sufficient to ensure that equilibrium was reached.

The non-evacuated method and the evacuated method are considered to be equally accurate but the non-evacuated method requires a much longer time period to achieve equilibrium. The disadvantage to this method compared to the other two methods is that it was not easy to repeat if errors were made. The advantage to this experiment is that all desiccators are known to be airtight and that because the desiccators are left undisturbed for the entire period, the relative humidity of the environment remains at equilibrium rather than being exposed to ambient conditions and then equilibrating again.

The aims of this experiment were to provide a comparison for the other two experimental methods and to provide samples for use in the caking strength experiments.

3.5.4.1 Experimental Apparatus

Airtight plastic "lunchbox" desiccators

Mettler AE200 Balance

Aluminium moisture dishes

Incubator

3.5.4.2 Materials

Lithium chloride

Potassium acetate

Magnesium chloride

Magnesium nitrate

Potassium iodide

Sodium nitrate

Sodium chloride

3.5.4.3 Experimental Method

Plastic desiccators containing a range of saturated salt solutions (given in Table 3.4) were set up for the caking strength experiments. The salt samples used in the experiment were dried overnight in a 100°C oven and cooled in a desiccator containing phosphorous pentoxide. Each desiccator held four salt samples for a period of approximately twelve weeks. The desiccators were sealed and left undisturbed in an air-conditioned room at 21°C. Before the caking strength was measured the wet weight was recorded. Half of the samples were then dried and reweighed. Thus the moisture content was obtained for each sample. The following salt solutions and their saturation relative humidities were used in the desiccators.

3.5.4.4 Results

Salt Solution	Formula	Saturation RH	Average Moisture Content
		(%)	(% dry basis)
Lithium chloride	LiCl	11.3	0.002918
Potassium acetate	CH_3COOK	22.5	0.003778
Magnesium chloride	$MgCl_2$	32.8	0.002255
Magnesium nitrate	$Mg(NO_3)_2$	52.9	0.006589
Potassium iodide	KI	68.9	0.020555
Sodium nitrate	$Na(NO_3)$	75	0.716447

Table 3. 4 Saturated salt solutions

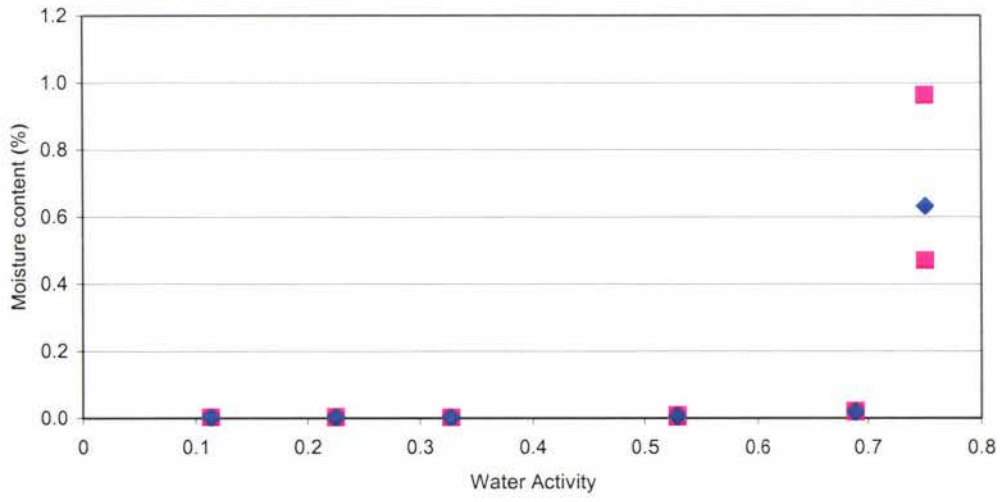

Figure 3. 8 Desiccator isotherm for NaCl

Expanding the scale shows the shape of the isotherm for the lower values of moisture content.

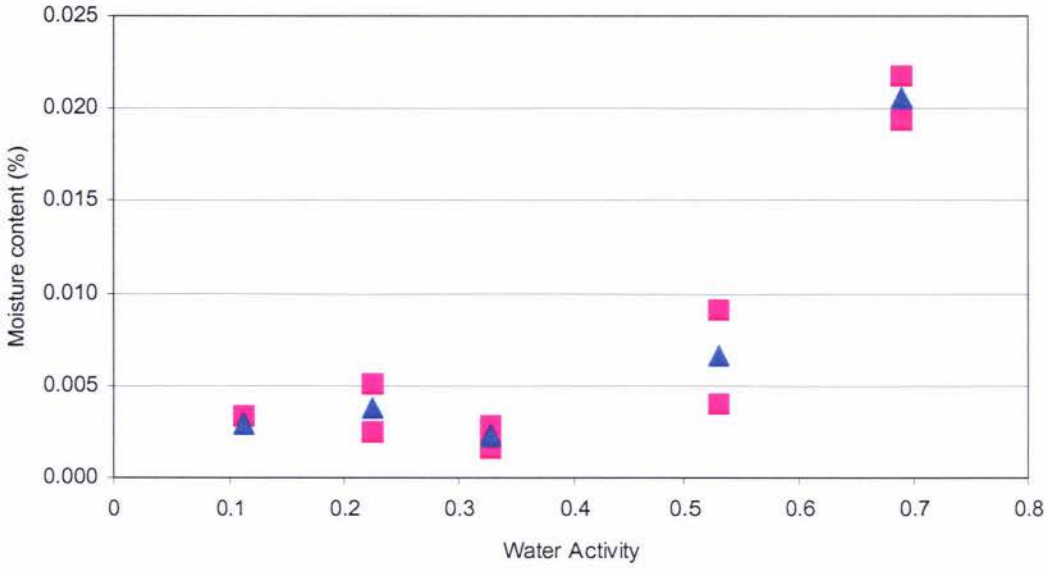

Figure 3. 9 Moisture sorption isotherm for low RH

3.5.5 Thermal Gravimetric Method

The Thermal Gravimetric Analyser is a sophisticated piece of equipment purchased by the university just prior to this project to perform differential scanning calorimetry (DSC) on soil samples. It was thought to be suitable for the purpose of determining the moisture sorption characteristics of salt, but because it was new equipment there were unforeseen difficulties with data generation and analysis. The data was difficult to interpret and as a consequence much data analysis was performed.

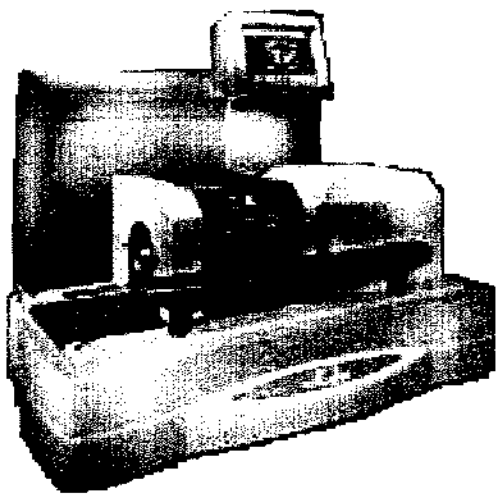

Figure 3. 10 TGA isotherm equipment

The advantage of using the TGA is that it is able to record very small changes in weight and temperature, and thus should be able to produce very accurate moisture sorption information.

3.5.5.1 Experimental Apparatus

Q600 Series Thermal Gravimetric Analyser (TGA)

Humidity generator, Massey University designed rig. [O'Donnell *et al.* (2002)]

CT-840 HyCal Dew Point and Temperature Transmitter (RH probe)

Sample cups were placed onto the balance within the furnace of the TGA. Weight and temperature readings were taken by the TGA at approximately 1 second intervals. The humidity generator was used to create a humid atmosphere within the TGA.

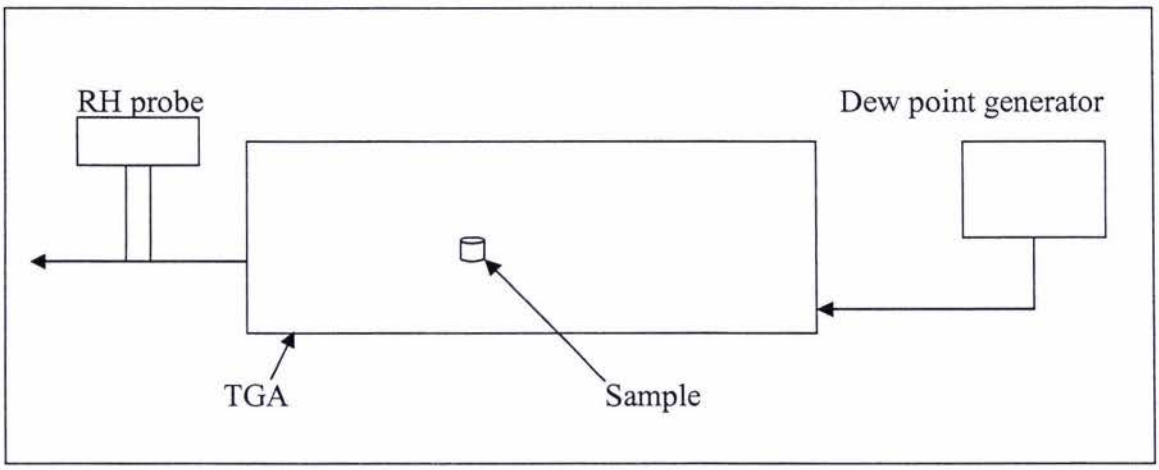

Figure 3. 11 TGA equipment

3.5.5.2 Experimental Method

A salt sample was placed inside the TGA and the TGA furnace heated to 130°C for a minimum period of 3 hours to dry the salt sample. The temperature was lowered to 40°C. When the samples had reached a constant weight the temperature of the dew point generator was increased to begin producing humid air. The relative humidity inside the furnace was measured by the RH probe (placed in the outlet air stream). When the sample had reached constant weight the temperature on the dew point generator was altered to create a different RH inside the furnace.

3.5.5.3 Results

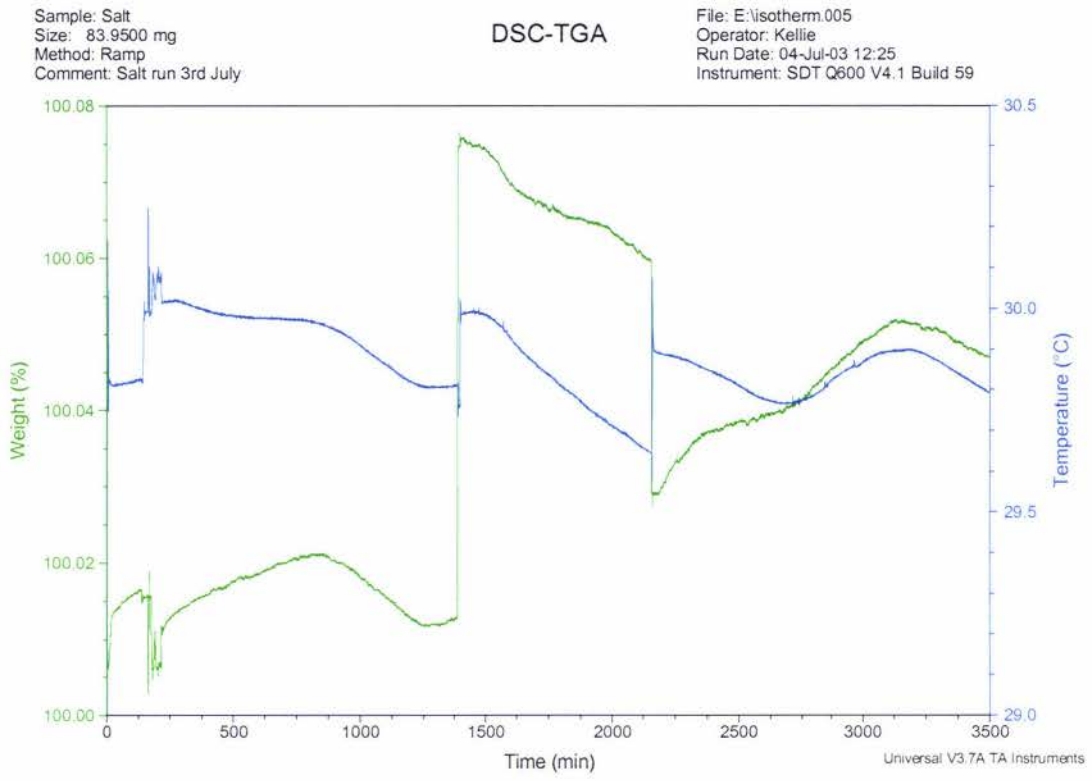

Figure 3. 12 TGA raw data

Figure 3.12 shows the data of weight percentage plotted against temperature. Two straight line sections are shown with different slopes. The first is at the lower total gas flow rate, and the second is at the higher gas flow rate. The top part also shows some dependence of weight versus temperature (1390 to 2157 min), but it is not quite linear. The deviation was thought to be because of the changing gas flow rate over this time.

Initial experiments performed with the TGA showed that the temperature variations inside the furnace due to ambient temperature changes led to unacceptable weight measurement variations. There was no constant temperature room available for the instrument, so insulation was provided by a Perspex box wrapped in insulating material with a heat lamp to maintain temperature.

3.5.5.4 Analysis

A calibration was performed with the aim of removing this temperature effect, but it was unsuccessful. To remove the temperature effect, a separate run was performed where the temperature was increased without altering the humidity of the furnace (Shown in Figure 3.13). From this experiment a correlation equation was obtained that was applied to the data.

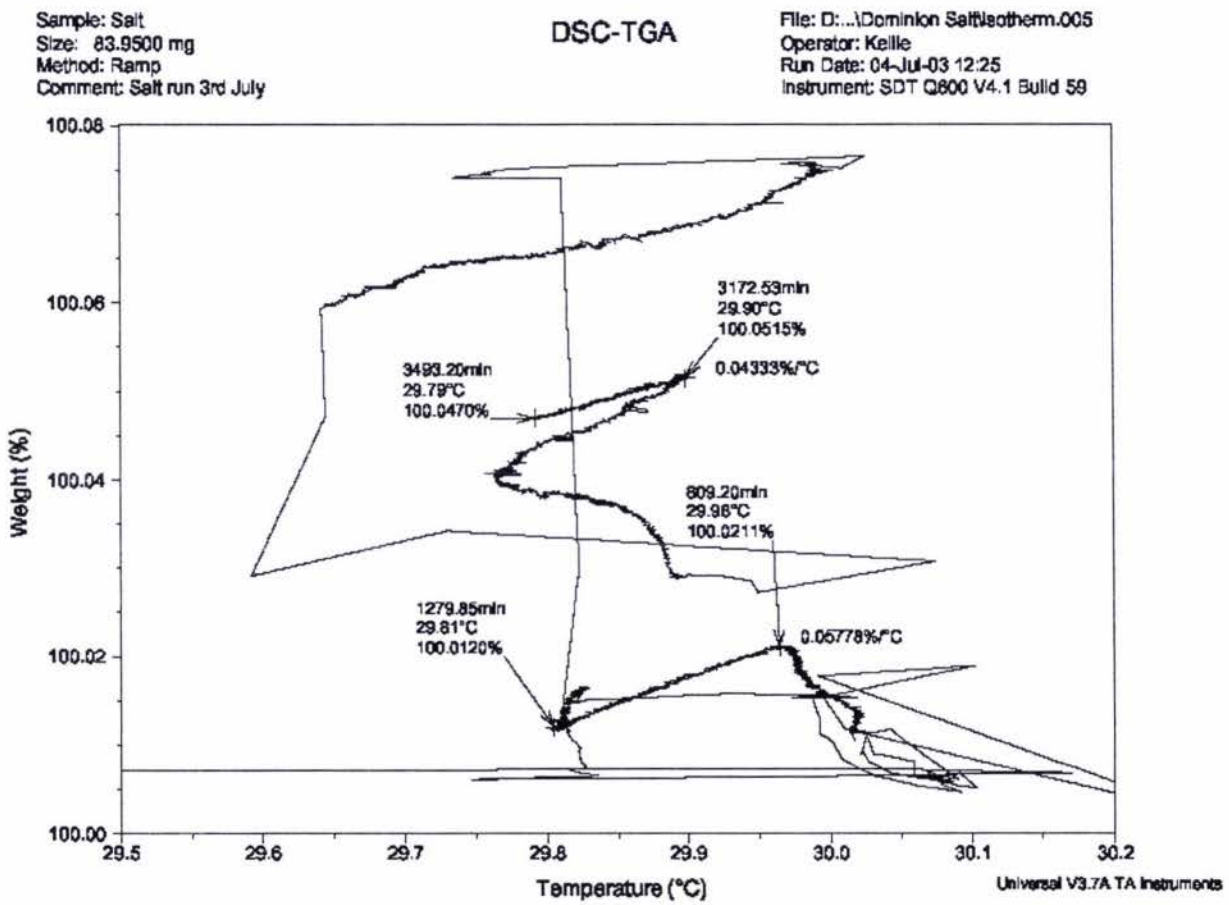

Figure 3. 13 Correlation of TGA data

Figure 3.14 shows the weight data corrected for the temperature effect by calculating the difference between the actual temperature and the set point temperature of 30 °C and multiplying this by the slope worked out in Figure 3.13 for the particular flow rate in use at the time the measurement was taken.

The RH profile with time was:

At zero time the RH was changed and it took about 20 minutes to stabilise at 36.5% and 23.9°C. At 1390 min the gas was changed to dry gas and the RH settled to 5.5% at 22°C. At 2157 min the saturated air was turned on. In the morning, the box temperature had dropped to 19.8°C from the desired 23°C with the heating light being on continuously. The air temperature in the room was 11.6°C. RH was 38.0% at a temperature of 20.5°C At the end of the run the RH was reading 38.1% at a temperature of 20.9°C. Figure 3.14 shows that there was some adsorption each time the RH was increased from a low value to a higher value. The amount of adsorption is only 0.018 mg in 84 mg of salt, or 0.021%. This small amount is still clearly shown in the graph.

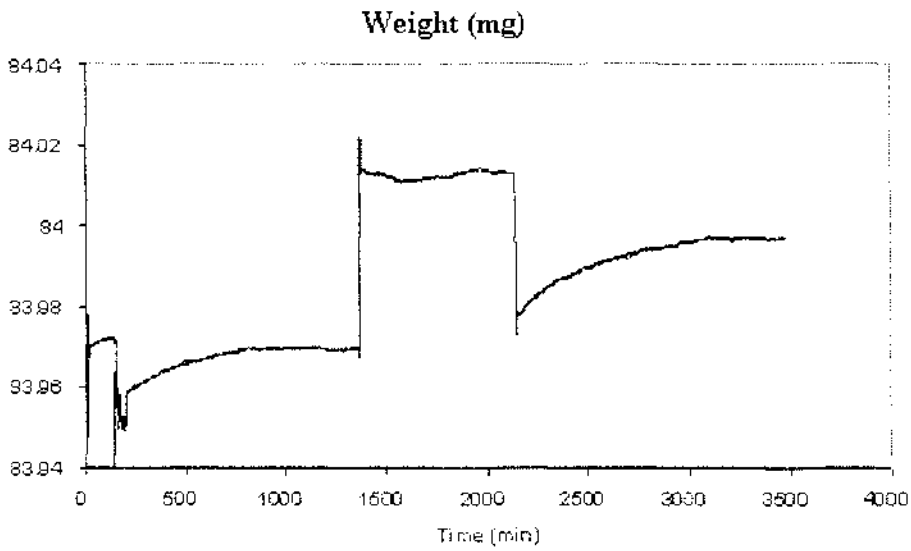

Figure 3. 14 TGA results

3.5.5.5 Conclusion

It was decided that persisting with this method would not be an effective use of time. Obtaining weight measurements was exceedingly difficult due to the sensitivity of the balance. Any change in air flow rate or ambient temperature caused a large shift in the weight measurement recorded.

3.5.6 Literature Results

See Figure 2. 8 Desorption isotherm data at 25°C for NaCl, sucrose and starch.

Chinachoti and Steinberg (1985) did not find any adsorption data for salt below the saturation relative humidity. Iyengar and Sen (1970) generated some approximate data for moisture adsorption onto salt at low RH values. See Table 3.5 below. This data is all much higher than the data generated in these experiments, but is of similar scale.

Relative Humidity	Moisture content
%	%
10	0.10
20	0.11
30	0.11
40	0.11
50	0.11
60	0.13
70	0.14
75.3	Saturated solution

Table 3. 5 Equilibrium moisture content of NaCl at different relative humidities

[Iyengar and Sen (1970)]

3.5.7 Isotherm Prediction

The traditional isotherm equations (Langmuir, BET, GAB, Tss) were applied to the isotherm data below the saturation point (75.3% RH) but none fit the data satisfactorily. In order to obtain a better fit, two equations of the forms shown below (Equation 3.8 and 3.9) were applied, by adjusting the constants in each equation to minimise the sum of squares in the error.

The isotherm equation that will be used in the model is derived from the moisture sorption isotherm for NaCl.

$$Mc = \frac{a_w + b \cdot a_w}{(0.75305 - a_w) \cdot c}$$ **Equation 3. 8**

$$Mc = \frac{a_w (a + b \cdot a_w)}{(c - a_w)}$$ **Equation 3. 9**

Parameter	Equation 3.8	Equation 3.9
a	0.001655	0.00309888
b	-0.0002	-0.00119408
c	0.752403	0.75302664

Table 3. 6 Isotherm equation parameters for salt

Equation 3.9 was created after plotting Equation 3.8 against the data. Equation 3.8 fits the higher relative humidity values well, but for this project the low relative humidity curve is much more relevant to caking. Equation 3.9 was created to pass through the origin, which is critical as at a 0%RH, the moisture content is 0kg/kg dry salt.

The predicted data for both equations is plotted against the actual data using the non-evacuated desiccator results. The vertical scale of the graph has been expanded to check the fit of the equation for low relative humidity values. The data point at 75% RH, 0.63g/100$g_{dry\ salt}$ is off the scale.

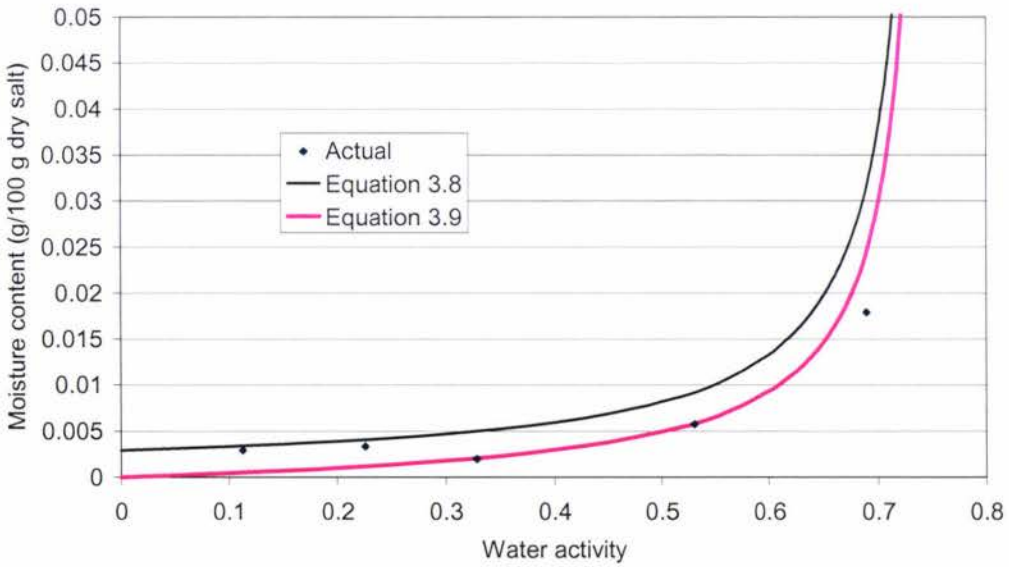

Figure 3. 15 Predicted vs. actual isotherm data

3.6 MOISTURE AUDIT OF DOMINION SALT

3.6.1 Introduction

To understand the conditions that the salt is exposed to, a moisture audit was conducted at the Dominion Salt plant. The audit was performed to measure the conditions in and around the fluidised bed drier and the bagging room.

The fluidised bed drier is the last stage of water removal from the salt. Thus the moisture audit was mostly concerned with the salt emerging from the drier.

3.6.2 Experiments

3.6.2.1 Aim

To determine the typical water activity or relative humidity of the salt.

3.6.2.2 Experimental Apparatus

CT-840 HyCal Dew Point and Temperature Trasmitter (Large RH probe)

IH-3602-A HyCal Relative Humidity probe, El Monte, USA

Thermo-hygro probe

Retort stand

Plastic sample containers

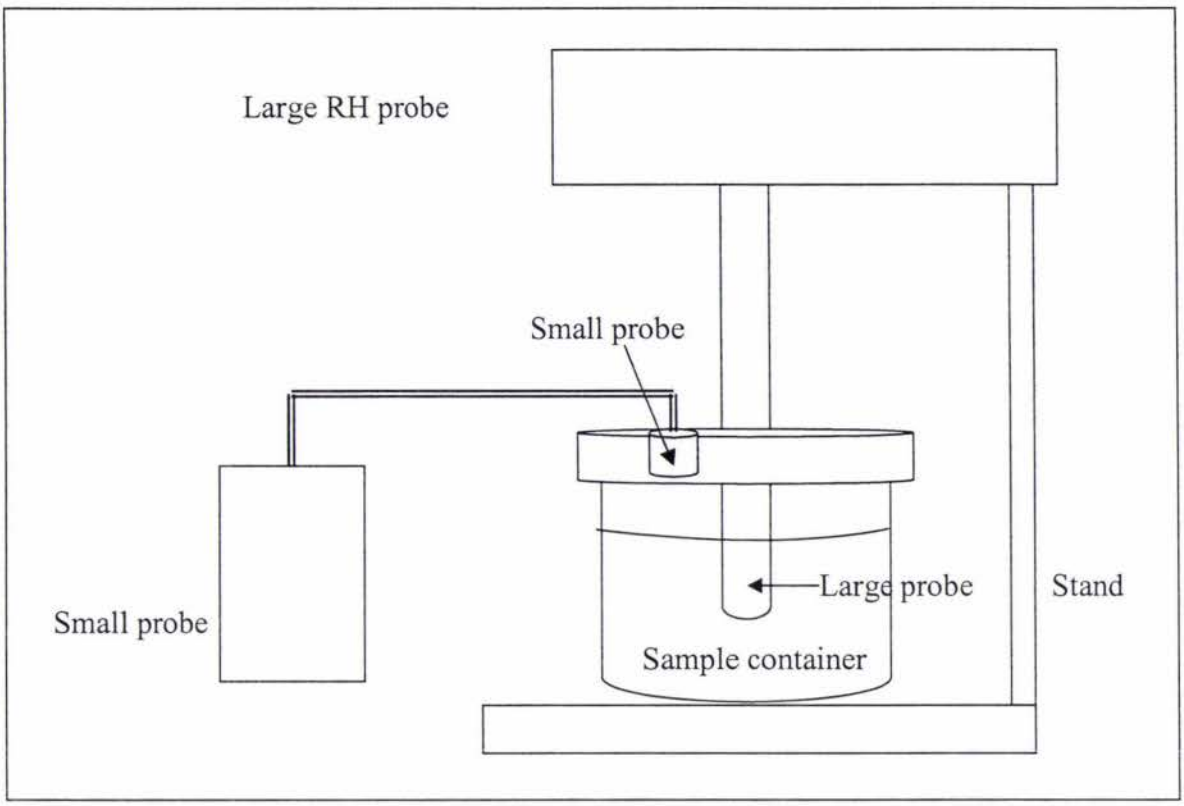

Figure 3. 16 Moisture audit experimental set-up

3.6.2.3 Experimental Method

Weekly experiments were performed at plant start-up over a period of several months. Samples were taken hourly from the start of pharmaceutical grade salt runs. At this time samples were taken for other experiments, specifically the Infinite Cylinder and particle size distribution experiments. 0Samples were taken from the conveyor belt exiting the fluidised bed drier and clarifier and placed in plastic sample bags. The salt was then transported as quickly as possible, poured into an airtight plastic sample container and tested with the relative humidity probes. The large humidity probe was inserted into approximately the centre of the salt sample to measure the relative humidity and the temperature of the salt. The small humidity probe was set into the container lid and measured the humidity of the air space above the salt. In addition to these two probes, the thermo-hygro sensor was placed on top of the large relative humidity display box to measure the temperature and relative humidity of the ambient conditions surrounding the experiment. Measurements were recorded for an hour until the next sample was taken. This was generally long enough for the salt to approach the ambient temperature.

3.6.3 Results

It was found that the moisture audit results did not vary greatly between hourly samples. Figure 3.17 shows a set of results gained from one of the fourth hourly samples. This result is representative of the other experiments. This set of data was chosen because it covered a longer time period than most of the other experiments and the final humidities and temperatures can be seen. The moisture movement from the salt to the air and back again can clearly be seen. When the container is filled with salt and placed onto the probes ambient air is trapped in the headspace of the container. This air is at the ambient temperature and RH and it takes some time for equilibrium to form between the salt and the air. This can be seen initially as the hot salt disperses moisture and heat (not shown) into the air. The equilibrium takes 15 to 20 minutes and can be seen as a peak on the humidity plots. The equilibrium is not maintained for long, because the heat in the salt and the air is dispersed into the ambient environment. As the air cools the moisture diffuses back into the salt. The final result is a salt sample in equilibrium with the air around it at ambient temperature. The relative humidity of the sample was measured at 77.5% by the large RH probe that was embedded in the salt.

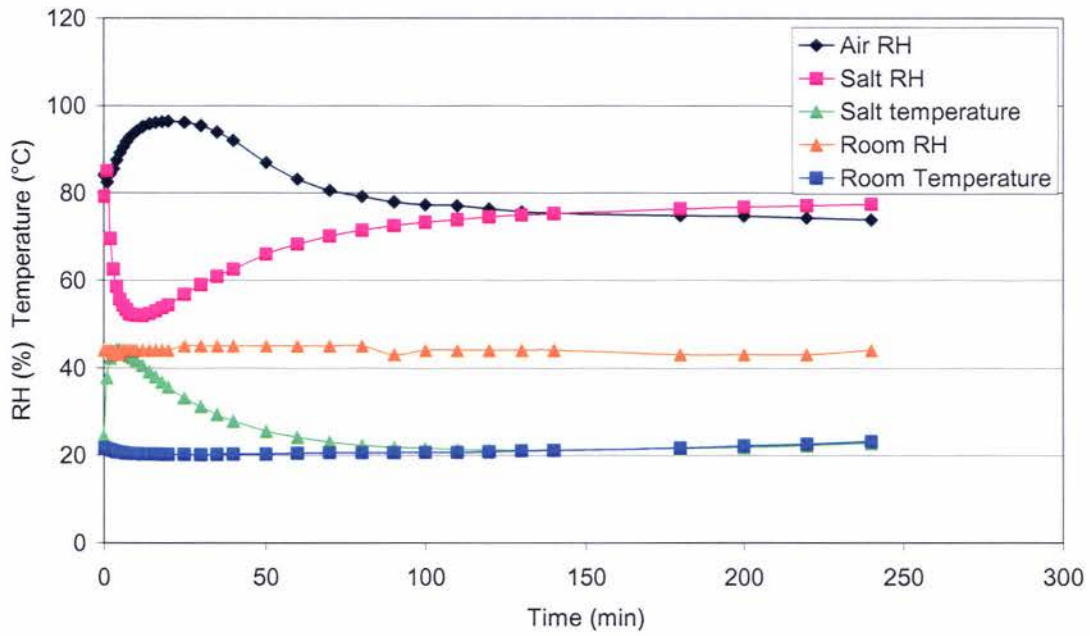

Figure 3. 17 Typical moisture audit results

3.6.4 Analysis

It was found in almost every experiment that the relative humidity of the salt at room temperature was above 75.3%, the saturation RH. It was also noted during these experiments that an accurate picture of the moisture migration from the hot salt could be observed. The moisture from the salt evaporated into the air space from the hot salt, and then as the salt cooled the moisture migrated back into the salt samples. Once at room temperature equilibrium was reached, the salt and the air above it generally had very similar relative humidities.

There was a small amount of error in the large RH probe. The final RH of the salt was often above 75.3%, although this should mean that it was an unsaturated solution, which was never the case. The salt always remained solid, which has a maximum RH of 75.3%.

3.7 CONCLUSION

The results from the experiments will be used in the mathematical model to predict caking in salt.

Characteristic	Symbol	Value	Error	Units
Bulk density –poured	ρ_{bulk}	1052	± 5	kg/m^3
Bulk density - tapped	ρ_{bulk}	1300	± 5	kg/m^3
Particle density	$\rho_{particle}$	2161	± 5	kg/m^3
Porosity	ϵ	0.398	± 0.002	
Thermal diffusivity	α	$6.319x10^{-7}$		m^2/s
Thermal conductivity	λ	1.027	± 0.24	W/mK
Typical RH	RH	75.3		%

Table 3. 7 Characteristics of NaCl

The adsorption isotherm results for salt are;

Salt solution	Water activity	Vacuum results	Non-vacuum results	Predicted values
		(% dry basis)	(% dry basis)	(% dry basis)
Phosphorous pentoxide	0	0.0016		0
Lithium chloride	0.113	0.0034	0.0029	0.002
Potassium acetate	0.220	0.0040	0.0038	0.007
Magnesium chloride	0.322	0.0028	0.0023	0.0015
Potassium acetate	0.432	0.0022		0.0032
Magnesium nitrate	0.529	0.0039	0.0066	0.0060
Potassium iodide	0.689	0.0063	0.0206	0.0125
Sodium nitrate	0.75		0.7164	

Table 3. 8 Sorption characteristics for NaCl

The isotherm values that will be used in the mathematical model are the non-evacuated desiccator values as they are considered to be more accurate. The vacuum desiccator data had not reached equilibrium, whereas the non-evacuated desiccators had been undisturbed for twelve weeks and definitely should have reached equilibrium.

CHAPTER FOUR CAKING

4.1 INTRODUCTION

Salt is a hygroscopic compound. Caking in a salt bed can be a result of a small moisture gain. At the saturation water activity (0.753 at 25°C) moisture is adsorbed onto the salt crystals and begins to form a saturated solution on the surface of the crystals. This liquid can collect between particles and is known as liquid bridging, as has been discussed in section 2.1. When the moisture content of the salt is lowered, through evaporation, through moisture migration induced by a temperature gradient, or through exposure to a lower RH environment, the liquid bridges recrystallise, forming solid bridges between the salt crystals.

4.2 MOISTURE ADSORPTION

Salt adsorbs moisture, forming a saturated solution on the surface of the crystals. The solution condenses first in the capillaries. The presence of capillaries is signified by hysteresis in the moisture sorption isotherm (between the adsorption and the desorption isotherms) observed by Hardy and Steinberg (1984).

Adsorption occurs initially as a monolayer on the crystal surface, including the capillaries. This monomolecular layer of water is known as the BET monolayer, after Brunauer *et al.* (1938), who created an isotherm model based on monomolecular adsorption. As adsorption continues the thickness of the adsorbed layer increases from monomolecular to polymolecular. [Coelho and Harnby (1978a, b)] [Labuza (1975)] [Kuprianoff (1958)]

The thickness of the polymolecular layer of saturated NaCl solution on the surface of the crystal increases in the capillary before elsewhere on the crystal surface. This is due to the pressure within the capillary being slightly lower than the surrounding atmosphere. [Billings (2002)], [Schubert (1984)]. When the solution eventually fills the entire capillary it begins to form bridges between adjacent particles. This is known as liquid bridging, and has a considerable effect on the flow behaviour of the salt. The formation of liquid bridges has been experimentally observed by Schubert (1984).

4.3 CAPILLARY CONDENSATION

Bulk material has a void space, existing as a branched polymorphic capillary system, depending on the particle size distribution, the shape distribution and the structure of packing. The capillary pressure contributes to the adhesion force between particles if it creates a pressure deficiency within the pore or capillary. The capillary pressure can be calculated from equation 4.1.

$$p_k = \sigma_{lg}\left(\frac{1}{R_1}+\frac{1}{R_2}\right) \qquad \textbf{Equation 4. 1}$$

The pressure within the capillary is dependent on the radius of the liquid surface, which in turn is a function of the capillary radius.

When the humidity approaches saturation, capillary condensation occurs and moisture will be present in the form of liquid bridges at the contact points between particles. In the pendular state (see figure 2.1), liquid bridges have the greatest contribution to moisture content, although adsorbed layers are present on the particle surfaces. As the amount of liquid increases, the salt moves into the funicular state, where liquid bridges and pores filled with liquid are present. When the pores are completely filled the salt is in the capillary state. The capillary pressure, and therefore the capillary radius, is decisive for liquid retention.

To calculate the capillary radius, the Kelvin equation is used.

$$A_w = e^{\left(\frac{-2\sigma\cdot\cos\theta\cdot V_0}{r_k\cdot RT}\right)} \qquad \textbf{Equation 4. 2}$$

The molecular volume of water is $6.13\text{x}10^{-5}$ m^3/mol. The surface tension of a saturated salt solution is $82.55\text{x}10^{-3}$ N/m. [Weast and Astle (1980)]

Using these values, the capillary radius was calculated over a range of water activity values.

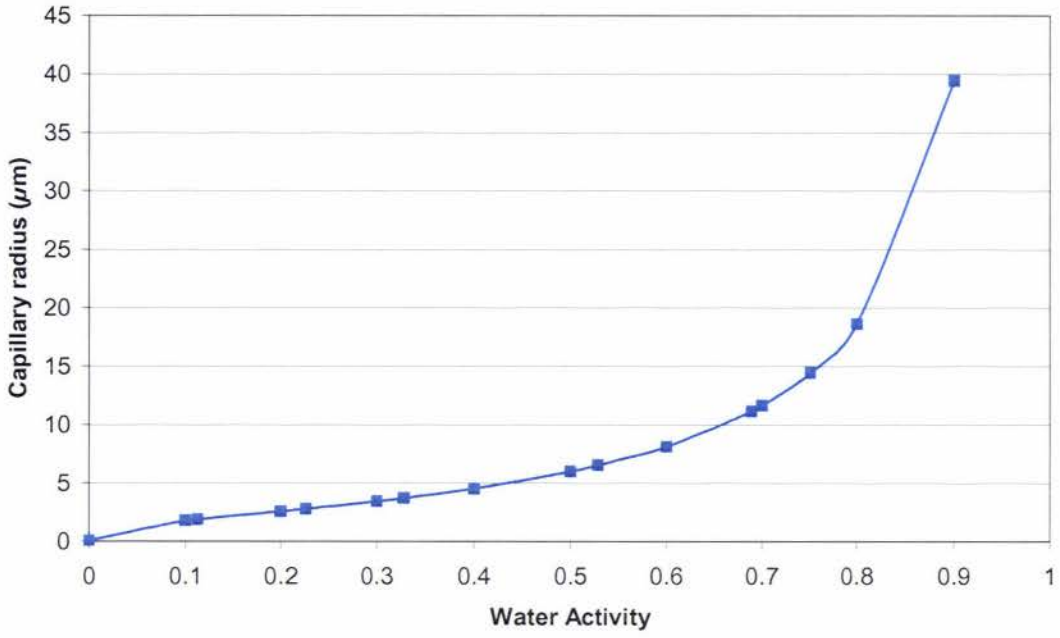

Figure 4. 1 Change in capillary radius with water activity for NaCl at 20°C

4.4 CAKING STRENGTH EXPERIMENTS

The strength of the cake formed under different relative humidity environments was tested in these experiments. It is known that liquid bridging will occur at the saturated water activity (0.753 at 25°C) but, as stated in Section 3.3, if fines are present in a salt sample, caking can occur at water activities below the saturation point. [Bhatt and Datar (1968)] [Bagster (1970)] This is shown in Figure 4.1.

Liquid bridges restrict the flowability of the salt by causing agglomerations to form. By testing the wet cake strength of samples subjected to a range of relative humidities, the extent and the effect of agglomeration can be determined. In this experiment the dry caked strength was also tested, giving a comparison between the strength of liquid and solid bridging.

4.4.1 Experiment One

Sorption equilibration generally requires one to ten weeks, depending on the material. [Lang *et al.* (1981)] It was decided that a twelve week period would be sufficient to ensure that equilibrium was reached.

4.4.1.1 Aim

To measure the wet cake strength and the dry cake strength of the salt at each relative humidity.

4.4.1.2 Experimental Apparatus

Airtight plastic "lunchbox" desiccators x6

Mettler AE200 Balance

Aluminium moisture dishes

Incubator

Penetrometer

Blowtester

The penetrometer and the blowtester were both made by Massey University technicians for the purpose of testing the cake strength of powders.

The penetrometer was designed using a multi-point penetrometry technique used by Baker and Mai (1982). Thirty two flat headed, 1mm diameter pins were pressed into a plastic dish. 1mm pins were used so that bending and disalignment of the pins did not occur. The probe was mounted in the arm of a stripped down beam balance which, through the counter weight system, allowed the probe to be suspended weightless above the salt sample.

The blowtester consists of a thin metal cylinder on a stand that can be placed upon the salt sample. The flowrate of nitrogen gas through the blowtester is controlled by a needle valve and measured using a rotameter. The amount of force required to create channelling in the salt sample is proportional to the flowrate of gas through the blowtester and the diameter of the blowtester aperture. Hence the volumetric flow through the blowtester is a direct indication of the relative size of force of cohesiveness of the powders being tested.

[Paterson *et al.* (2001)]

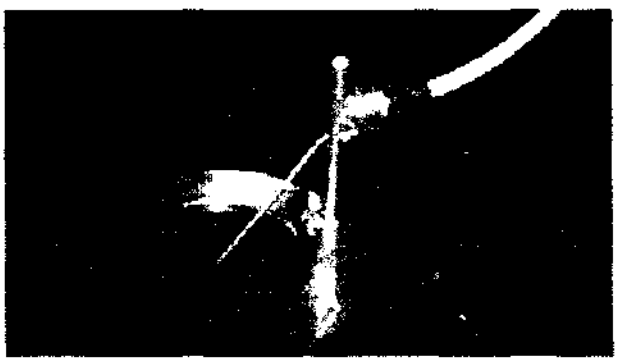

Figure 4. 2 Blowtester

4.4.1.3 Materials

Sodium chloride samples

Saturated salt solutions;

Salt Solution	Saturation Relative Humidity
Lithium chloride	11.3%
Potassium acetate	22.5%
Magnesium chloride	32.8%
Magnesium nitrate	52.9%
Potassium iodide	68.9%
Sodium nitrate	75%

Table 4. 1 Relative humidity of saturated salt solutions used in experiment one

4.4.1.4 Experimental Method

The desiccators were labelled and a saturated salt solution was poured into the bottom of each desiccator. A raised plastic tray was inserted into the bottom of each desiccator to ensure that the moisture dishes did not come into contact with the saturated solution. The moisture dishes were washed with detergent and rinsed with deionised water. They were then dried at 130°C overnight to ensure that they were cleaned of any substances that may affect the results of the experiment. The moisture dishes were labelled and weighed. They were then filled with salt that had been dried overnight at 130°C, until the surface of the salt was level with the top of the moisture dish.

Four samples were placed into each desiccator and the desiccators sealed. The desiccators were placed under a bench in an air conditioned room with a temperature of approximately 21°C. After the twelve week period all of the salt samples were removed and weighed. Two of the samples from each desiccator were dried overnight at 130°C and left to cool in the desiccator. The other two samples were tested immediately using the penetrometer and the blowtester to find the wet cake strength. When the remaining two samples from each desiccator had been dried and cooled they were weighed and then tested for the dry cake strength.

4.4.1.5 Results

For both the blowtester and the penetrometer experiments, it was found that the caking created in the highest relative humidity environment (Sodium nitrate 75%RH) was too strong to be measured with the equipment available (the upper limit for the blow tester was 60L/min). This in itself is a good indication of the strength of the cake formed, but was not quantifiable and therefore could not be plotted on a graph with the other data.

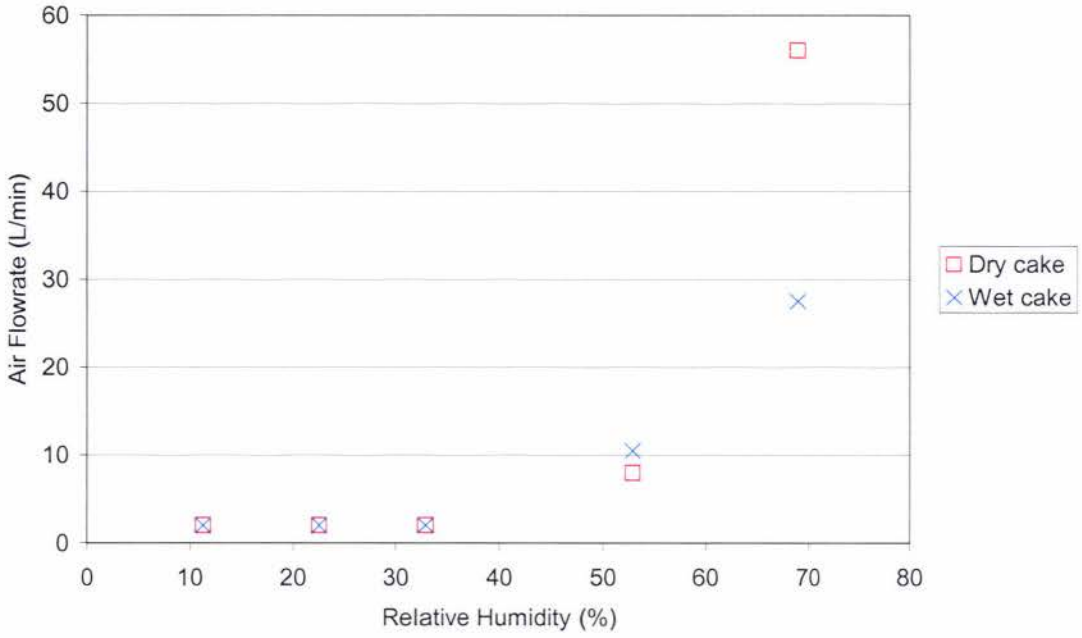

Figure 4. 3 Caking strength results, blowtester

In Figure 4.2, for the 53% RH sample the wet cake strength seems to be higher than the dry cake strength. The difference is not significant and is most probably attributable to experimental error.

It should be noted that at the breakthrough mass the penetrometer was forced through the hard layer on the salt surface. After breakthrough had occurred, the probe penetrated different distances into the salt bed.

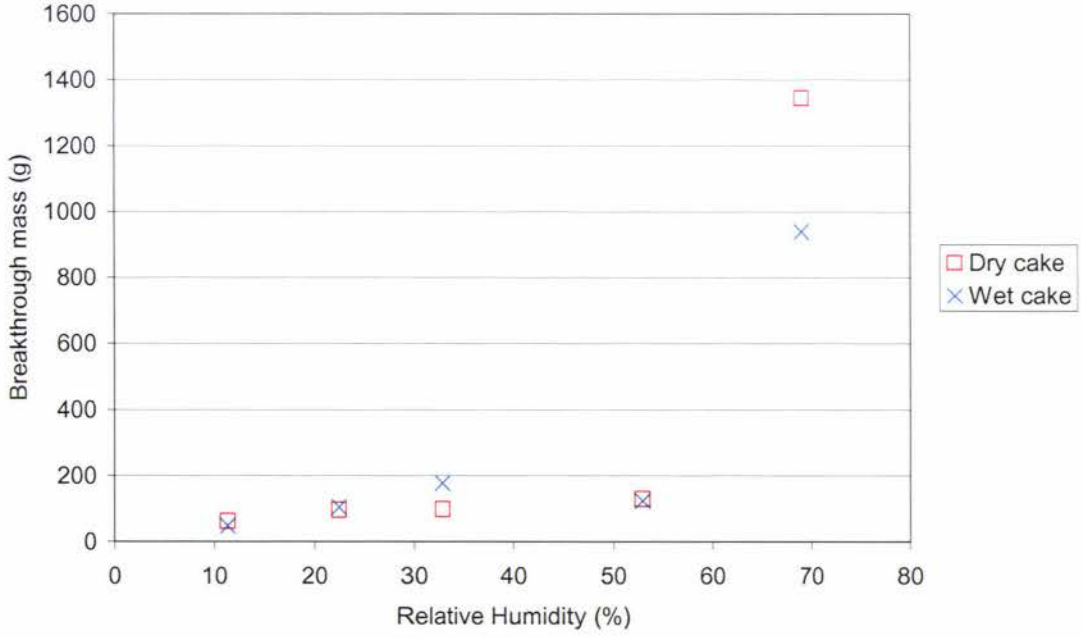

Figure 4. 4 Caking strength results, penetrometer

There is agreement in shape between the two cake strength methods tested. The data patterns are very similar, with the exception of the 53% results. The blowtester results showed a higher degree of caking at this humidity than the penetrometer results exhibited. Both methods showed an asymptotic increase in caking strength as the critical saturation relative humidity (75.3%) was approached.

If the breakthrough data is plotted against the capillary radius (calculated using the Kelvin equation), the data shows two straight lines. The section of the data gives a horizontal or very nearly horizontal line, indicating that the capillary radius has little effect on caking at low relative humidities. The intersection of the lines shows the point at which capillary condensation has an effect on caking strength. Above this point cake strength increases with capillary radius.

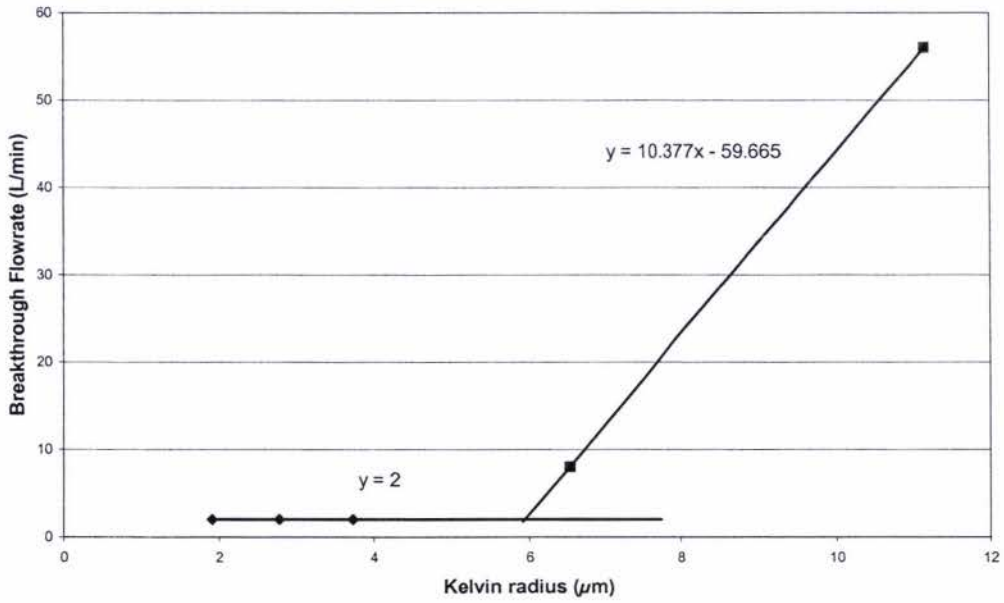

Figure 4. 5 Breakthrough flowrate versus Kelvin radius for blowtester caking strength experiment

The intersection of the lines was found by solving the two equations simultaneously. The critical Kelvin radius is 5.557 μm, which corresponds to a water activity of approximately 0.5.

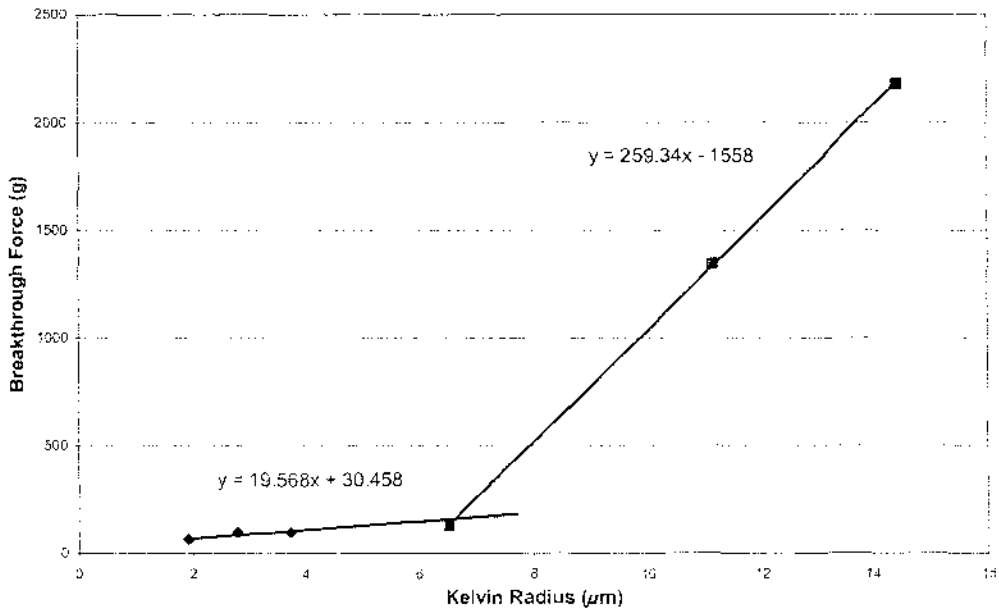

Figure 4. 6 Breakthrough force versus kelvin radius for penetrometer caking strength experiment

The critical Kelvin radius was found to be 6.6248μm, which equates to a water activity of 0.53.

Brookes (2000) and Foster (2002) considered the caking strength to be significant when the breakthrough flowrate exceeds 8L/min when tested with the blowtester. This agrees with observations made about the hardness of the caking in salt during the experiments. It can be seen from Figure 4.2 that significant caking begins to occur in salt at a water activity of 0.53. Thus, when the model is used to predict caking in salt samples, any sample that reaches a water activity of 0.53 will be considered to have a significant amount of caking present.

4.4.2 Experiment Two

The moisture content of salt at the saturation water activity of 0.753 (at 25°C) can vary to a considerable extent. At the saturation point the salt may have a moisture content as low as 0.02% [See Moisture Sorption Isotherm experiments, section 3.5]. At this water activity the salt may also be a saturated solution containing only a small amount of salt crystals and a moisture content of $2g_{H_2O}/g_{dry\ salt}$. As a consequence, the caking strength will vary greatly at this water activity also.

The second cake strength experiment was to determine the moisture content and cake strength of salt samples exposed to the saturation relative humidity for different periods of time. Theoretically, if a dry sample is exposed to the saturation RH for long enough, it will become a saturated solution, but it was not clear whether the amount of liquid solution will increase with time.

4.4.2.1 Aim

To investigate whether the amount of liquid bridging increases when samples are exposed to saturation relative humidity for longer time periods.

4.4.2.2 Experimental Apparatus

Large airtight plastic "lunchbox" desiccator

Vacuum desiccator

Mettler AE200 Balance

Plastic Petri dishes (moisture dishes)

Incubator

Penetrometer

Blowtester

4.4.2.3 Materials

Sodium chloride saturated solution

Sodium chloride samples

Phosphorous pentoxide

4.4.2.4 Experimental Method

A saturated solution of sodium chloride was placed in the bottom of the large plastic desiccator. A raised tray was placed in the bottom of the desiccator to ensure that the moisture dishes were not in contact with the saturated solution.

Salt was dried at 130°C overnight and cooled in the desiccator. The Petri dishes were dried in a 50°C oven overnight, labelled and weighed. The dry salt was then weighed into the dishes, ensuring that the surface of the salt was level with the top of the dish. Three samples (two salt samples and one empty Petri dish) for each day were placed into the plastic desiccator, which was placed in the air-conditioned room. Plastic will absorb moisture also, and it was imperative that the amount of moisture absorbed by the dishes was known so that it could be deducted from the salt moisture content. Metal moisture dishes would have been preferred for this experiment but were not available.

At each sample time the three Petri dishes were removed from the desiccator and weighed. One of the salt samples was tested using the blowtester for wet cake strength; the other sample and the empty Petri dish were dried overnight in a 50°C oven and cooled in the vacuum desiccator containing phosphorous pentoxide. The remaining sample and the empty Petri dish were reweighed to establish the moisture content. The moisture absorbed by the Petri dish was deducted from the amount of water adsorbed by the salt sample to obtain the true moisture content value. The sample was then tested using the blowtester for dry cake strength.

4.4.2.5 Results

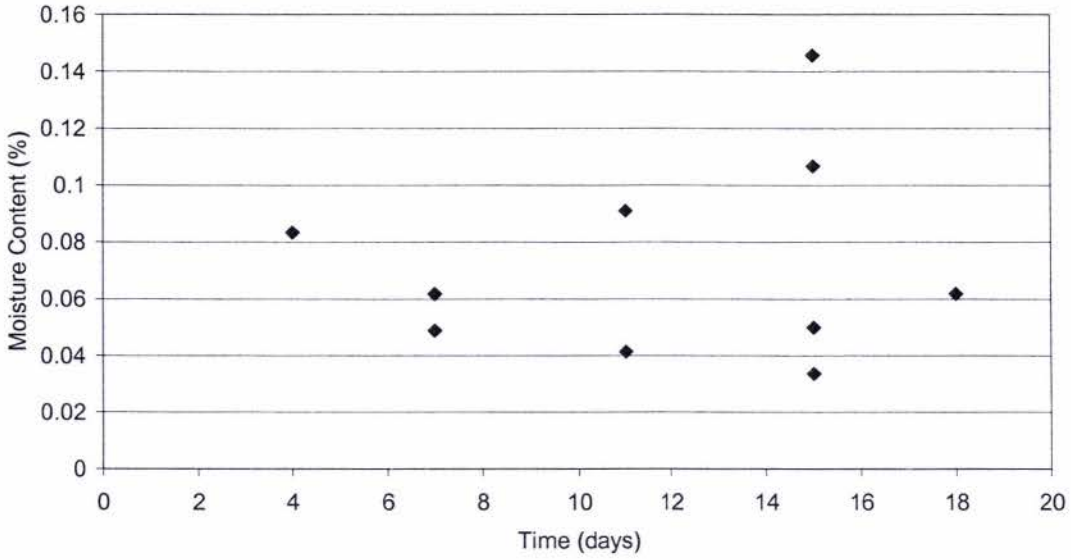

Figure 4. 7 Experiment two results

It can be seen from figure 4.6 that the moisture content of the salt is not a function of the amount of time it is exposed to the saturation relative humidity. Therefore caking strength will not increase as the time period of exposure increases, as demonstrated in figure 4.7.

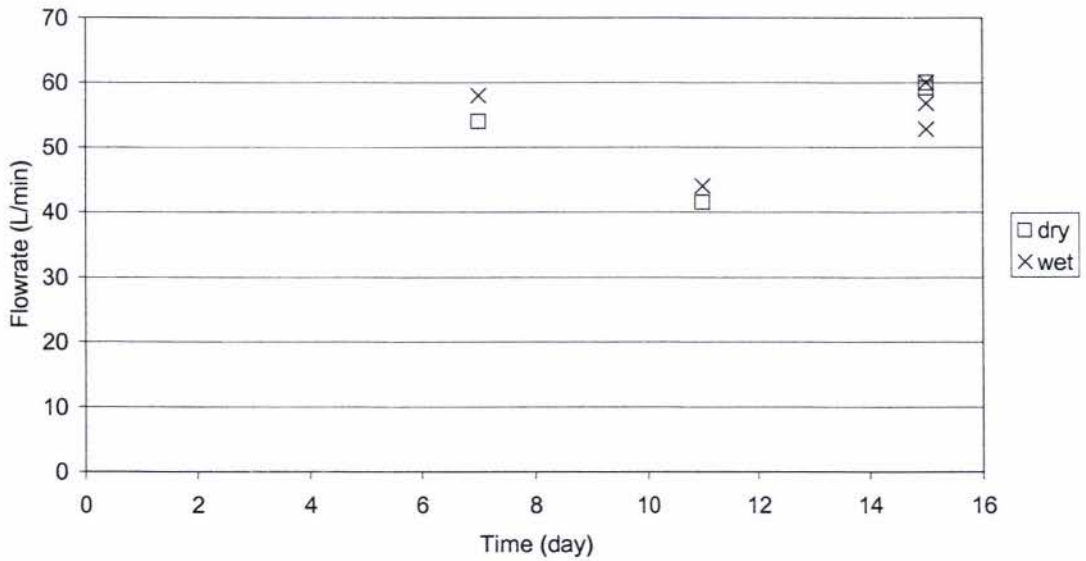

Figure 4. 8 Saturation results, daily cake strength

It can be seen in Figure 4.7, (and also in Experiment One, Figures 4.2 and 4.3) that the dry cake had similar strength to the wet cake. This means that the solid bridges are approximately the same strength as the liquid bridges they formed from.

The maximum flowrate measurable with the blowtester equipment was 60L/min. In many cases, from day 4 samples to day 21 samples, this flowrate was not sufficient to create channelling in the salt sample. The moisture content of the sample did not seem to have any bearing on the strength of cake formed.

4.5 CONCLUSION

Use of the Kelvin Equation has shown that significant caking occurs in salt as a result of the liquid bridges formed by capillary condensation when the salt is exposed to an ambient relative humidity greater than 53%. A temperature gradient causes moisture migration within the salt sample, creating areas of high relative humidity where water is adsorbed by the salt. When the temperature gradient is removed the water will desorb from the liquid bridging, leaving solid bridges between the particles. Experimental work has shown little difference between the liquid and solid bridge strengths.

A relative humidity of 53% or higher will cause sufficient water adsorption onto the salt bed to create a significant amount of caking. The maximum moisture content recorded was 0.8% when the salt was exposed to 75% RH. The cake strength created by this moisture adsorption exceeded the maximum breakthrough force available from the blowtester.

When salt is exposed to the saturation RH, the moisture content is not a function of the number of days exposed, therefore the caking strength does not increase with time exposed to high RH atmosphere.

CHAPTER FIVE MATHEMATICAL MODEL

5.1 INTRODUCTION

It has been determined that the primary caking mechanism that occurs in the salt is humidity caking. It is known that in the salt produced by Dominion Salt Limited the relative humidity is often at the saturation relative humidity or a little below. Hence it is deduced that the main cause of caking in a salt bed is not adsorption of more moisture from the ambient environment, but migration of existing moisture caused by temperature gradients within the salt bed.

The aim of this project was to use a mathematical model to predict the level of caking that will occur in a salt bed subjected to a temperature gradient. Permission was obtained from John Bronlund to use the model that he created for a similar project on lactose. The model was adapted for salt.
[Bronlund (1997).]

5.2 FORMULATION OF THE TRANSPORT MODEL

The mathematical model will be based on the conceptual caking model described in Chapter Two.

The physical basis of the model can be described as a packed bed of salt. Initially the salt bed and the air space have constant temperature and relative humidities. When a temperature gradient is applied across the bed one-dimensional heat and moisture transfer occur through the bed.

5.3 NUMERICAL SOLUTION OF THE TRANSPORT MODEL

5.3.1Selection of Numerical Solution Model

The model summarised in section 2.2, shows the solution of two coupled partial differential equations was required. One equation describes the transport of heat and the other the transport of moisture through the salt slab. Some algebraic equations

used in the model are non linear. The complexity of the model makes the analytical solution difficult and, with the advent of inexpensive computing facilities, the model was best solved numerically.

Bronlund (1997) compares the most common methods for the numerical solution of partial differential equations, Explicit finite difference schemes, Implicit finite difference schemes and Finite elements methods. He concludes that the explicit finite differences scheme was the most appropriate for use with this model.

5.3.2Numerical Solution

The equations representing the salt slab were solved using an explicit finite differences scheme. The salt slab was divided into several nodes where the content of each node was considered uniform. By discretising the continuous system in this way, a series of equations that describe transport of heat and moisture between adjacent nodes were derived.

The partial differential equations were approximated using the expanded Taylor series and these equations, together with the boundary conditions, initial conditions and algebraic equations that characterise the system, were solved using Borland's C++ programming language.

The formulation of the finite difference equations for the system can be found in greater detail in Appendix A4.

The program was written in Borland C++ by Bronlund (1997) using object orientated programming techniques. Object oriented programming offers many advantages over conventional "top down" programming. The first and most important of these advantages is that by treating each item in the real world as a separate subject, the program is more closely representing the actual system. By treating each node as a separate object that interacts with neighbouring nodes or boundaries, the salt slab is simulated more closely.

5.4 MODEL VALIDATION

5.4.1 Model Parameters

The physical properties used in the model were taken from literature or determined experimentally. These values can be found in Chapters Two and Three. Some of the parameters have been written in to the C++ code for the mathematical model. Others were entered manually each time and some of these changed with each run, for example the initial water activity and temperature. The following parameters remained the same for each run.

Parameter	Value
Time step	0.1 s
Total simulation time	10 000s
Number of nodes	10
Slab thickness	0.1m
Initial percentage amorphous	1e-18
Initial crystallinity of amorphous	1e-18
Porosity	0.4
Bottom heat transfer coefficient	25 W/m^2K
Top heat transfer coefficient	170 W/m^2K

Table 5. 1 Model parameters for salt

Generally speaking, the heat transfer coefficients should have been the same for the hot and the cold situations. Early model runs showed that the heat transfer coefficients had a large effect on the prediction accuracy of the model, and that the accuracy for each value was different for the hot and cold plates. Repeatedly running the model and comparing to experimental data to find the optimal values obtained the heat transfer coefficients used. As the moisture migration occurs rapidly when the salt is exposed to a temperature gradient, the heat transfer coefficients were chosen based on the prediction of the end point of the moisture transfer rather than the rate of transfer.

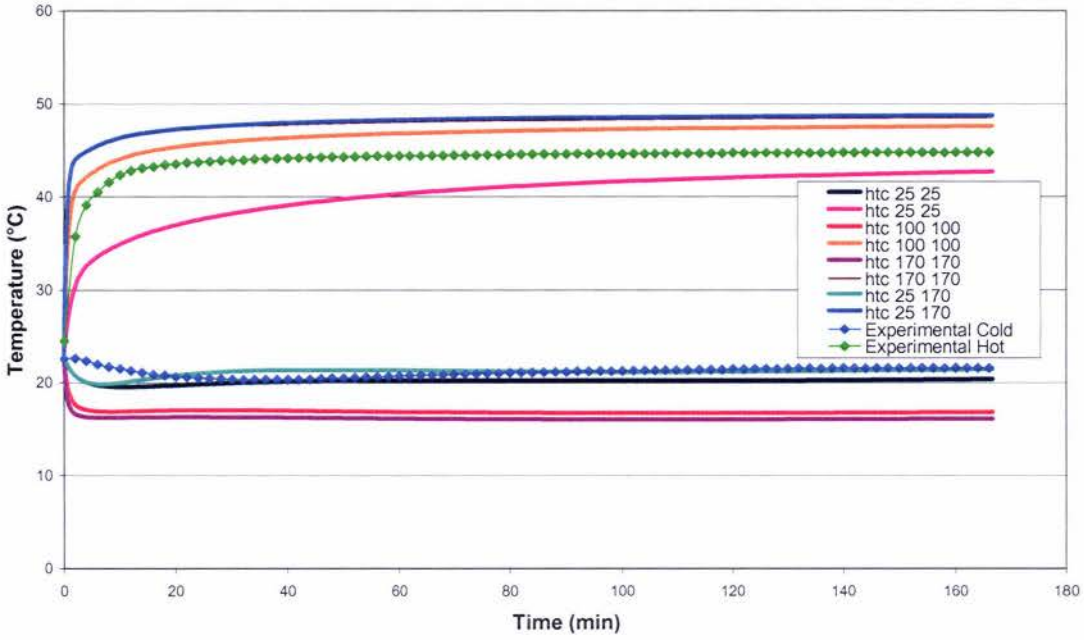

Figure 5. 1 Comparison of temperature prediction for different heat transfer coefficients

Figure 5.1 shows the temperature prediction for the different heat transfer coefficients, while Figure 5.2 shows the corresponding water activity predictions.

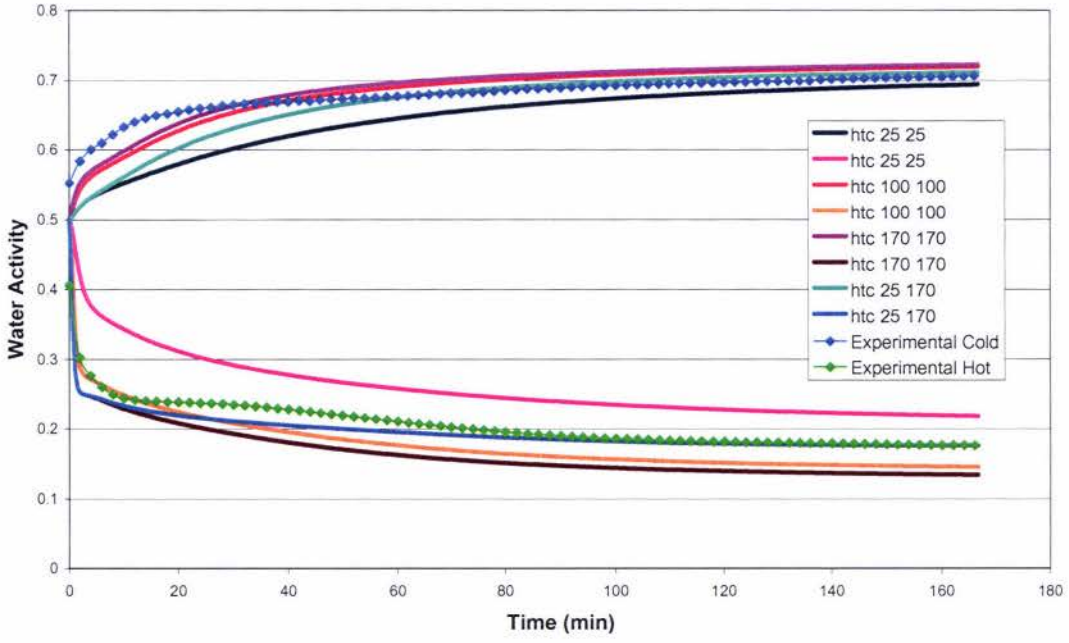

Figure 5. 2 Comparison of water activity predictions for different heat transfer coefficients

It can be seen that, for the cold situation, a very low heat transfer coefficient gives the best fit. A value of 25 W/m^2K was chosen for the cold side of the salt bed. For the hot situation a much larger heat transfer coefficient was required for accurate model prediction. A value of 170 W/m^2K was chosen for the hot side of the salt bed. No good explanation could be found for the difference in heat transfer, but using different values gives a very good fit to experimental data

5.4.2 Isotherm Equations

Three isotherm equations were used in the mathematical model to compare the different results achieved. Equations 3.8 and 3.9 were used, as well as a linear model.

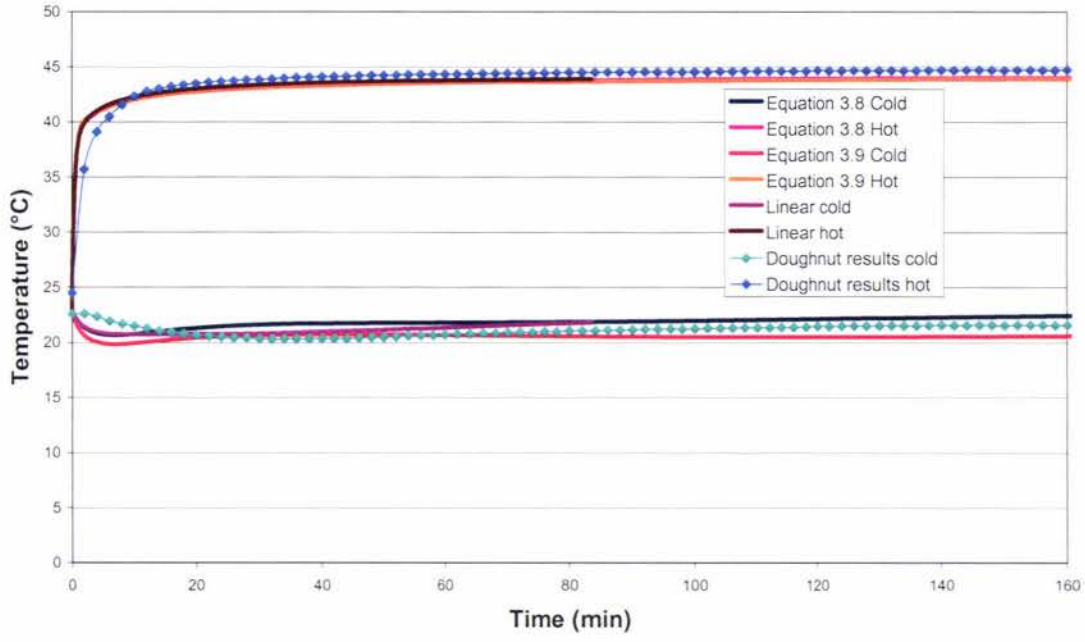

Figure 5. 3 Temperature comparison of isotherm equations in model

It can be seen from Figure 5.3 that all isotherm equations gave roughly the same temperature predictions.

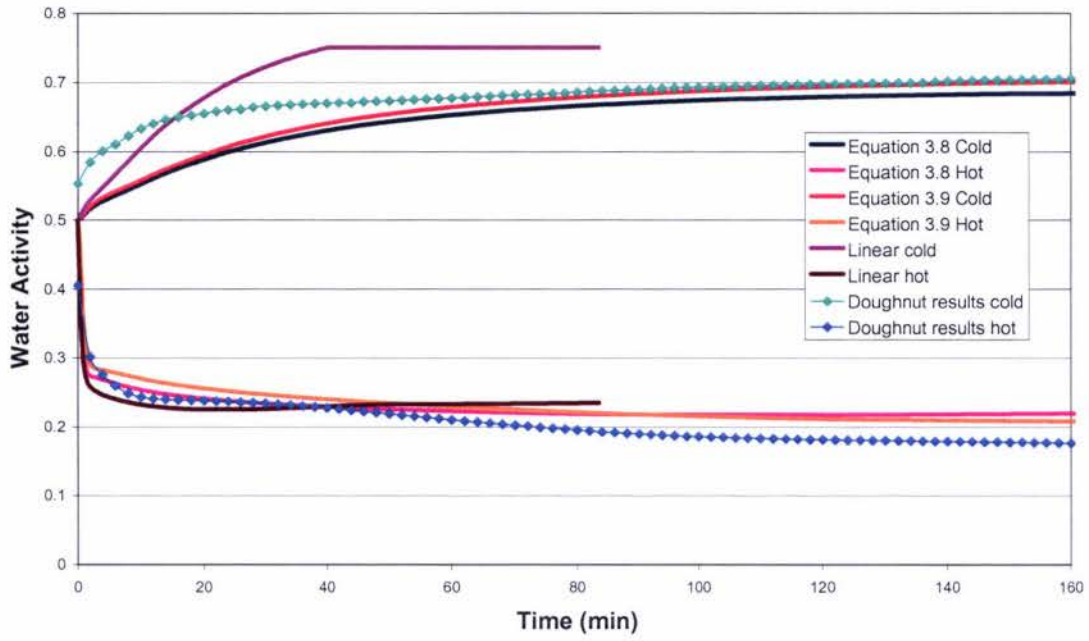

Figure 5. 4 Water activity comparison of isotherm equations in model

Figure 5.4 shows that the linear equation model reacts more quickly than the other two models, but does not give an accurate end point for the water activity. It was decided that the end point was the most important aspect of the model, as the salt bags would generally be exposed to any temperature gradient for a considerable length of time. It can be seen that Equation 3.9 gave the most accurate end point water activities for both the hot and cold ends of the salt bed, therefore this mathematical model was chosen to predict the data.

These results show that the amount of moisture that needs to move to alter the water activity of the salt is considerably less than that shown by the isotherms. This is consistent with the fact that it takes a long time for the salt to come to actual equilibrium with the air it is in contact with. This model assumes an instantaneous reaching of equilibrium and hence it calculates more water will be adsorbed at a given RH in a given time interval than will actually occur. Future work could look at building this dynamic into the model.

5.4.3 Model Validation Experiments

The purpose of model validation experiments is to compare the model predictions to actual physical data. The experiments involve creating a temperature gradient across a salt bed, then monitoring the thermal gradient and the resulting moisture migration through the salt bed.

The piece of equipment used for the model validation experiments was nicknamed the doughnut due to its appearance. The doughnut is comprised of three pieces of polystyrene. Two are flat circular pieces with a shallow depression in the inner side of each. The depressions were created to accommodate hollow metal plates, which are filled with water of a chosen temperature to create the desired temperature gradient across the salt. The centre piece of polystyrene is a flat ring or doughnut shape, with a hole in the centre. When the polystyrene pieces are stacked together the hole in the centre piece becomes a chamber with the metal plates on either side. The chamber is filled with salt and then the plates are filled with water of different temperatures to create a thermal gradient.

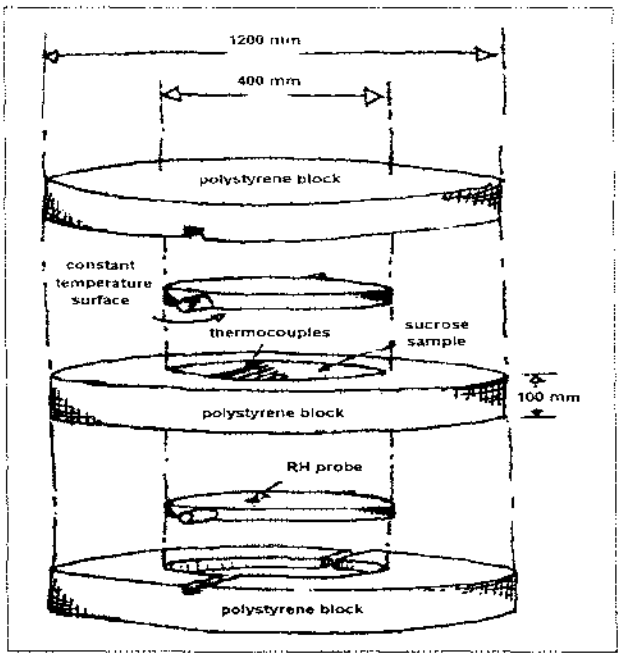

Figure 5. 5 Transport model validation experimental rig

[Bronlund (1997)]

The reason that the doughnut is manufactured from large slabs of polystyrene is to ensure that heat transfer is one-dimensional. Thermocouples were placed diagonally

across the central chamber to allow the measurement of the temperature profile across the bed. The thermocouples were placed in different axial positions across the bed to ensure that any others near by did not interfere with each thermocouple.

To observe the moisture migration within the salt bed, calibrated HyCal relative humidity probes were placed at each surface of the salt slab. The probes were mounted flush into the stainless steel plates as seen in figure 5.5. Surface relative humidity data allowed partial validation of the predicted moisture migration within the slab. If the boundary relative humidity measurements were accurately predicted then this was a good indication that the predicted moisture profile over the bed was also correct.

5.4.3.1 Experimental Aim

To compare predicted results with experimental data to ascertain the accuracy of the model.

If the model was found to be lacking accuracy the comparison with experimental data was used to alter aspects of the model, with the aim of improving the accuracy of predictions.

5.4.3.2 Experimental Apparatus

HyCal relative humidity probes x2

PicoTC08 data logger

Grant W8 water bath

Doughnut

5.4.3.3 Experimental Method

The designated cold plate was attached to mains water supply (approximately 17°C). The temperature of the water does not vary significantly so the cold plate was considered to be at constant temperature. The temperature in the hot plate was maintained by attaching it to a constant temperature water bath. The central piece of polystyrene was placed on top of the bottom piece and filled with salt. The salt was

levelled with a ruler to the height of the polystyrene and then the top plate was placed on the top of the apparatus. The water flow was turned on and the thermocouple and RH probe readings recorded by the TC08 data logger. The experiment was run until all temperatures and relative humidities were considered to be stable. When the moisture migration was considered to have ceased the top plate was taken away and the blowtester very carefully used to ascertain the strength of caking at several points in the salt bed.

5.4.3.4 Results

5.4.3.4.1 25°C Temperature Gradient

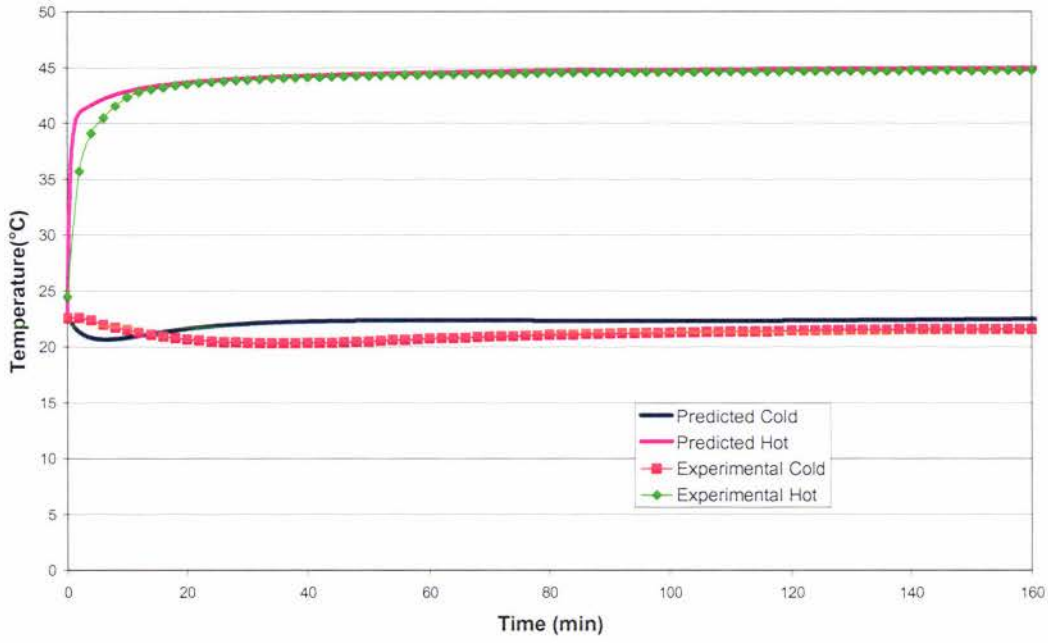

Figure 5. 6 25°C gradient temperature results

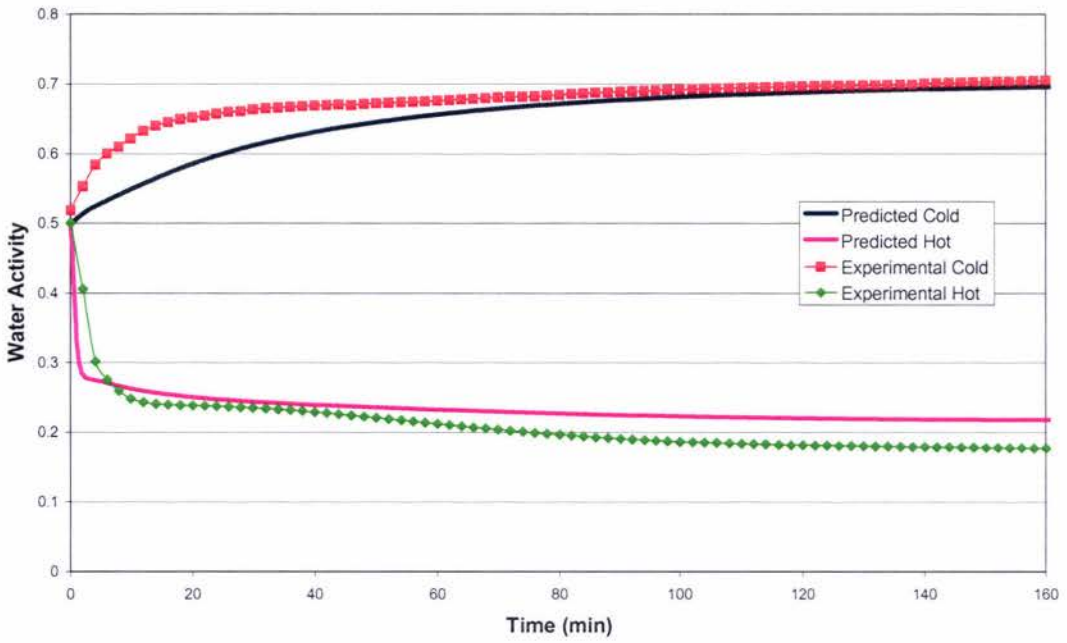

Figure 5. 7 25°C gradient water activity results

Figure 5.7 shows the effect of a temperature gradient on water activity. The humidity increases to a water activity of 0.7 at the cold plate. When the experiment was finished and the caking strength measurements recorded through the salt bed, it was observed that the salt that had been in contact with the cold plate had caked to the point where it could not be measured with the blowtester. The caking in the salt was strong enough that pieces could be picked up, and were difficult to break by crushing between the fingers.

Node	**Distance from hot plate (cm)**	**Channelling flow rate (blow tester) [L/min]**
Top	9	60 +
8	7	14
6	5	10
4	3	2
2	1	2
Bottom	0	2

Table 5. 2 Doughnut caking strength results 25° temperature gradient

It can be seen from Table 5.2 that the caking created by a 25°C temperature gradient is significant.

While 2 L/min indicates totally free flowing salt, caked salt with a channel flow rate of 8L/min or greater is caked to a degree that will change its flow characteristics.

5.4.3.4.2 40°C Temperature Gradient

This is a typical temperature gradient that salt is exposed to during bagging. The salt is bagged at up to 65°C and the ambient temperature in the bagging room is often 25°C.

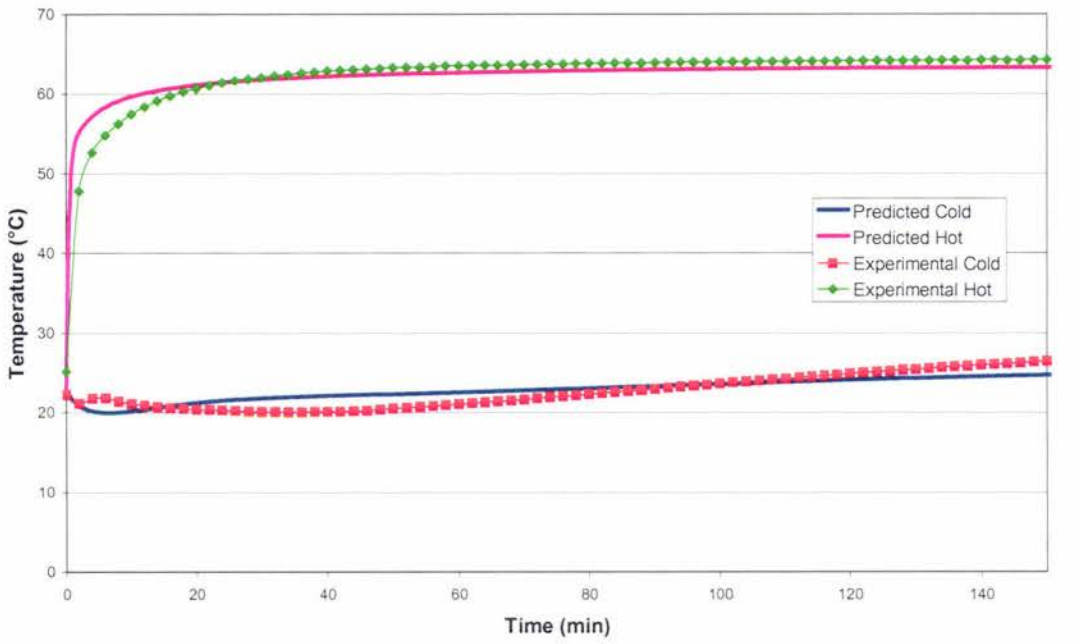

Figure 5. 8 40°C gradient temperature results

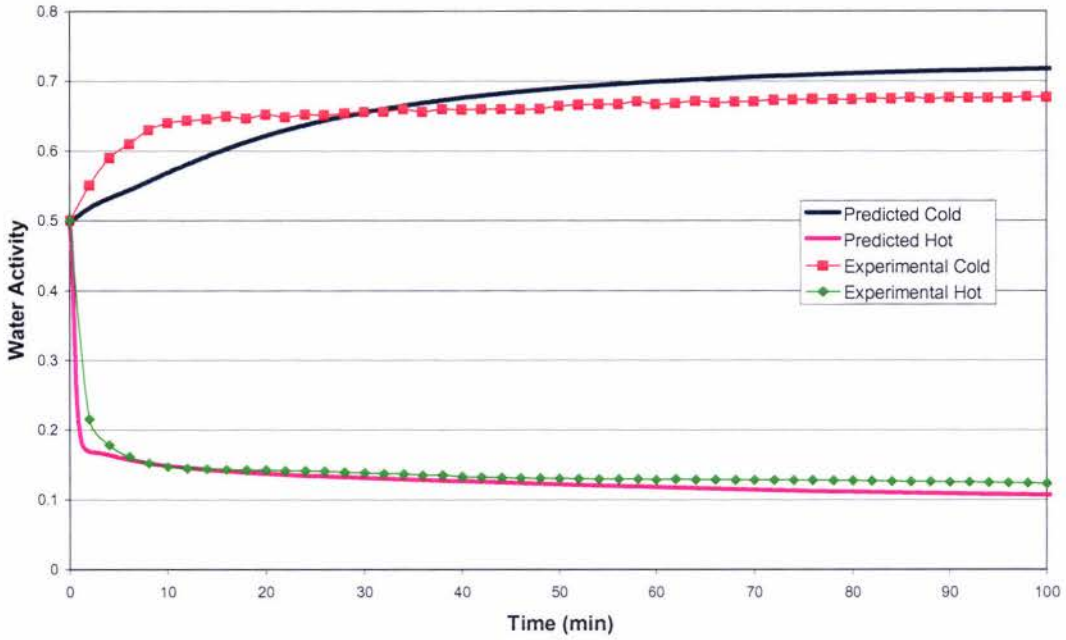

Figure 5. 9 40°C gradient water activity results

Node	Distance from hot plate (cm)	Channelling flow rate (blow tester) [L/min]
Top	0	2
8	1	5
6	3	14
4	5	18
2	7	24
Bottom	9	60 +

Table 5. 3 Doughnut caking strength results 40° temperature gradient

It can be seen from Table 5.2 and Table 5.3 that a 15°C increase in temperature gradient leads to a large increase in the caking throughout the salt bed. At both temperature gradients the salt at the cold plate was caked beyond measurement, but with a larger temperature gradient the strength of caking increases right through the salt, except at the hot plate where it remains free flowing.

5.4.3.4.3 50°C Temperature Gradient

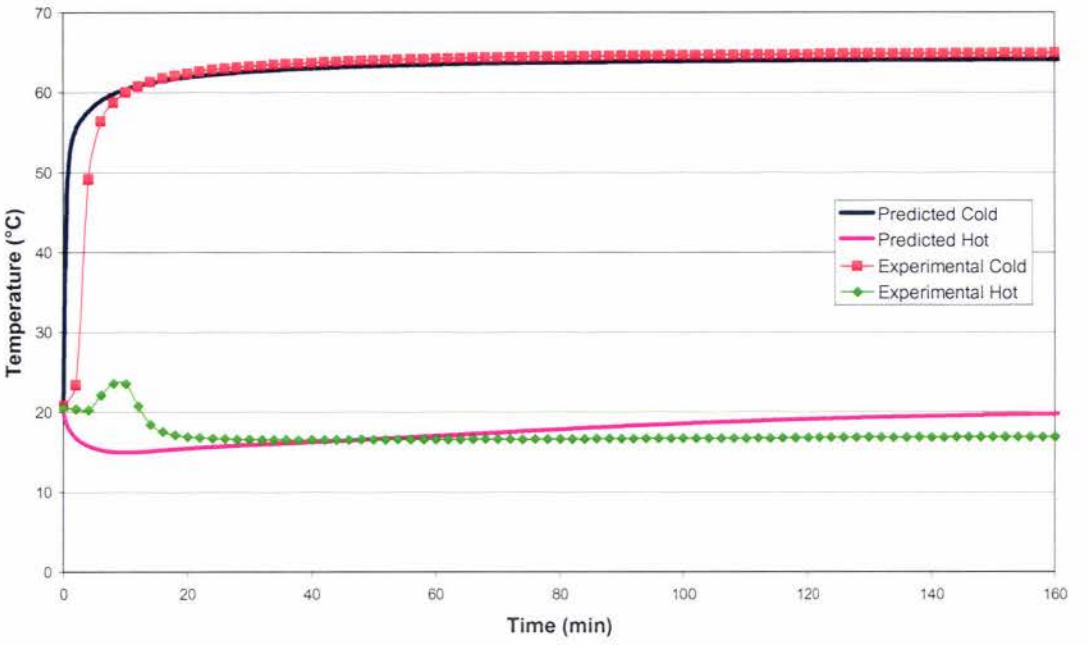

Figure 5. 10 50°C gradient temperature results

The 50°C gradient was chosen as an experiment because this is the maximum temperature gradient that the salt could be exposed to. Salt exits the Fluidised Bed Drier (FBD) at approximately 70°C and the ambient temperature in the drier room can be as low as 20°C. The temperature of this room is generally higher due to radiated heat from the drier, but during the start up phase it has been recorded as low as 20°C.

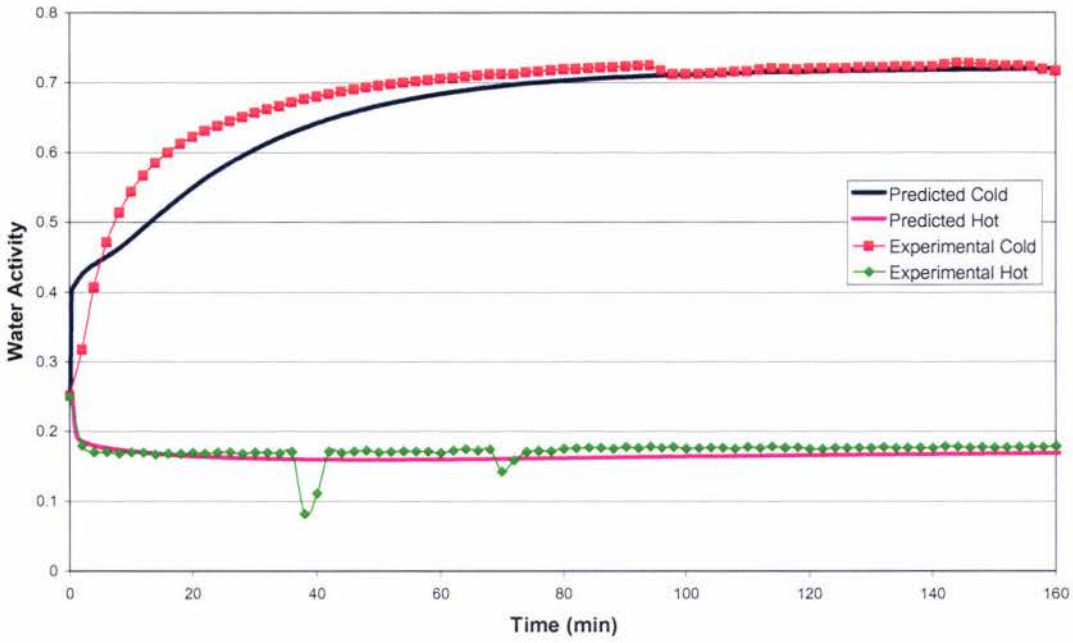

Figure 5. 11 50° gradient water activity results

Node	Distance from hot plate (cm)	Channelling flow rate (blow tester) [L/min]
Top	9	60 +
8	7	26
6	5	14
4	3	10
2	1	4
Bottom	0	2

Table 5. 4 Doughnut caking strength results 50° temperature gradient

Comparison of caking strength results from the 40°C gradient and the 50°C gradient show that the caking is not increased considerably by the increased gradient.

5.5 PREDICTED RESULTS

Once the mathematical model had been validated, it was used to create a prediction chart. The prediction chart encompasses all conditions that the salt may be exposed to. To create the chart, an ambient (cold) temperature and a salt bagging (hot) temperature were chosen and the model run with initial water activities until a minimum initial water activity that will cause caking in the salt was found. It should be noted that the final water activity used to create the chart was 0.53, the point at which significant caking begins to occur in the salt bed.

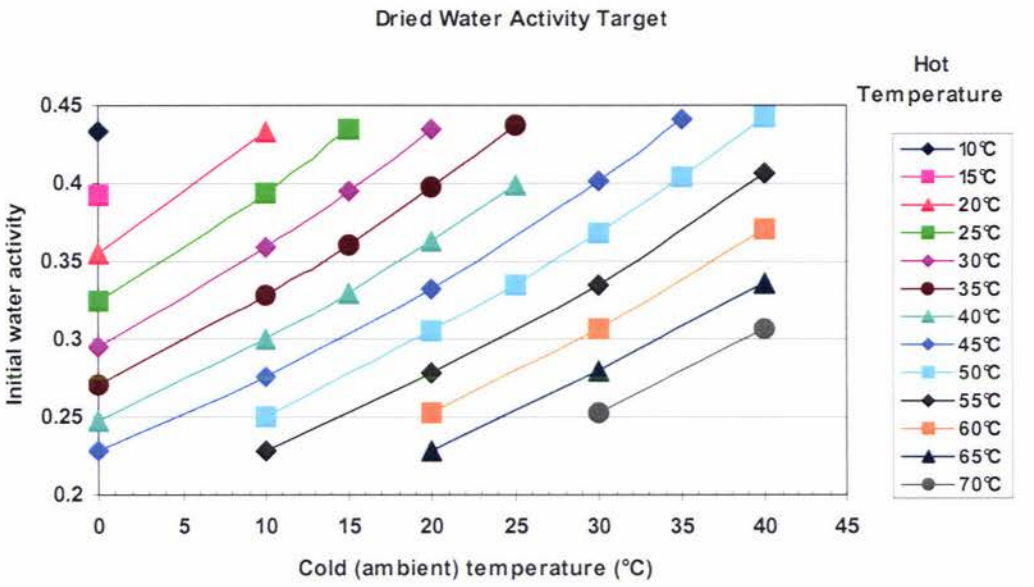

Figure 5. 12 Initial water activity required for each initial temperature and temperature gradient to cause a final water activity of 0.53

This chart can be used to determine the minimum initial water activity that will cause caking in a salt bed for given temperature gradients. For example, if the temperature of the salt that is being bagged is 55°C and the ambient temperature is 20°C, if the water activity is below 0.27 the salt will not cake. The degree of caking will increase with a larger temperature gradient or an increased initial water activity.

An alternative use of the chart is to see what temperature gradient needs to occur during transport to induce caking. For example, if salt has been bagged at a water

activity of 0.3 and successfully cooled to 20°C, then as long as the salt is not exposed to temperatures above 49°C, it should not cake.

5.6 CONCLUSION

The model can be used to accurately predict caking in a salt bed exposed to a given set of conditions. Figure 5.12 can be used to determine the minimum initial water activity that will cause caking in salt for each temperature condition. Figure 5.12 does not indicate the strength of cake formed; it shows only where significant caking begins to occur. It can be seen from Figure 5.12 that the larger the temperature gradient the salt is exposed to, the lower the water activity that will cause caking. It can also be seen that the higher the temperatures the lower the critical water activity to cause caking.

CHAPTER SIX CONCLUSION

The aims of this investigation were to:

- Develop an understanding of moisture relationships in bulk salt and the effect of moisture adsorption on individual salt crystals.
- Identify the mechanism responsible for caking in salt.
- Mathematically model and experimentally validate the effect of a temperature gradient on heat and moisture transfer within a packed bed of salt.

Dry salt adsorbs water from the air under humid conditions. If the ambient relative humidity is in excess of 53%, sufficient moisture will be adsorbed to cause caking in the salt. The primary mechanism that creates caking in salt is the humidity caking mechanism. The adsorption of water by salt causes a saturated salt solution to form on the surface of the salt crystals. The thickness of this layer increases as the moisture content increases until liquid bridges form between adjacent particles.

The moisture audit experiments showed that the water activity of the salt is generally well above 0.53, so it was concluded that caking is not caused by the adsorption of moisture from the atmosphere, but by the migration of moisture within a sealed system caused by a thermal gradient.

The information generated by the literature search and the experiments performed were used to create a mathematical model. The model predicts the heat and moisture transfer within a salt bed caused by a temperature gradient.

The amount of caking occurring in the salt bags produced by Dominion Salt Ltd is largely attributable to the temperature conditions the bags are exposed to and the level of moisture in the salt when bagged. The salt is generally free flowing throughout the drying process. Some caking occurs in the silos, where the salt comes into contact with the colder steel, but the main occurrence of caking is in the packed bags. The salt is generally packed at around 55°C. The average ambient temperature is 20°C, so the temperature gradient that the salt is exposed to at this point is 35°C. It can be seen

from the doughnut experiments (Section 5.4) that this temperature gradient causes a large water activity gradient across the salt bed.

As shown in the caking strength experiments, in Section 4.4, a water activity of 0.53 or greater will cause caking in the salt. The moisture audit experiments, Section 3.6, show that the water activity of the salt is often in excess of 0.53. This means that liquid bridges are present in the majority of the salt. At this water activity the bridges are easily disrupted, and transport of the salt along the conveyor belt, into the silos and then into the bags is sufficient to achieve free flowing salt. However, the degree of liquid bridges that occur increases with the water activity between 0.53 and 0.75. When the salt is exposed to a temperature gradient (i.e. when packed) the water activity at the edges of the bags increases and the liquid bridges form to a greater degree. As the bags cool to ambient temperature these bridges solidify, forming solid crystalline bridges between the particles. The salt in the bags remains largely undisturbed as it cools and so these bridges are not disrupted.

6.1 RECOMMENDATIONS

The amount of water required to induce caking in salt is very small. Therefore it will be extremely difficult to alter the drying process at the plant to remove this last amount of water.

It is recommended that instead of increasing the amount of drying of the salt, it would be more effective to concentrate on the cooling process after drying. Currently the salt is cooled by ambient air in the classifier, it is then transported by conveyor belt to the silos where it is left for a period of time before it is bagged. To decrease the temperature gradient that the salt it exposed to, it should be cooled before being bagged, preferably with dehumidified air. It is suggested that if the salt is left to cool in the silos, it is likely that the caking will still occur. Ideally, the salt should be cooled while moving, or in an insulated silo (made from material with a low thermal conductivity).

REFERENCES

Audu, T. O. K., M. Loncin, H. Weisser. (1978). "Sorption Isotherms of Sugars." Lebensm.-Wiss.u.Technol 11: 31-34.

Bagster, D. F. (1970). "Cause, Prevention and Measurement of the Caking of Refined Sugar - A Review." International Sugar Journal 72: 298-302.

Baker, C. J. and T. V. Mai (1982). "Physical Effects of Direct Drilling Equipment on Undisturbed Soils. IV. Techniques for Measuring Soil Compaction in the Vicinity of Drilled Grooves." NZ Journal of Agricultural Research 25: 43-49.

Bell, L. N. and T. P. Labuza (2000). Moisture Sorption: Practical Aspects of Isotherm Measurement and Use. Saint Paul, American Association of Cereal Chemists.

Bhatt, M. P. and D. S. Datar (1968). "Caking of Salt." Salt Research and Industry 5(3): 57-67.

Billings, S. (2002). The Mathematical Model of Caking in Bulk Sucrose. Palmerston North, New Zealand, Massey University.

Bronlund, J. (1997). Modelling of the caking of Bulk Lactose. Palmerston North, New Zealand, Massey University.

Brookes, G. F. (2000). The Sticking and Crystallisation of Amorphous Lactose. Palmerston North, New Zealand, Massey University.

Brunauer, S., P. H. Emmet, E. Teller. (1938). "Adsorption of Gases in Multimolecular Layers." Journal of the American Chemists Society 60: 309-319.

Carslaw, H. S. and J. C. Jaeger (1959). Conduction of Heat in Solids. Oxford, Clarendon Press.

Chinachoti, P. and M. P. Steinberg (1985). "Interaction of Sodium Chloride with Raw Starch in Freeze-Dried Mixtures as Shown by Water Sorption." Journal of Food Science 80: 825-828.

Chinachoti, P. and M. P. Steinberg (1986). "Interaction of Solutes with Raw Starch during Desorption as Shown by Water Retention." Journal of Food Science 51(2): 450-452.

Coelho, M. C. and N. Harnby (1978a). "Moisture Bonding in Powders." Powder Technology 20(1978): 201-205.

Coelho, M. C. and N. Harnby (1978b). "The Effect of Humidity on the Form of Water Retention in a Powder." Powder Technology 20: 197-200.

Foster, K. D. (2002). The Prediction of Sticking in Dairy Powders. Palmerston North, New Zealand, Massey University.

Gal, S. (1975a). Solvent versus Non-Solvent Water in Casein-Sodium Chloride-Water Systems. Water Relations in Foods. R. B. Duckworth. London, Academic Press: 183-191.

Gal, S. (1975b). Recent Advances in Techniques for the Determination of Sorption Isotherms. Water Relations of Foods. R. B. Duckworth. London, Academic Press: 139-154.

Gorling, P. (1958). Physical Phenomena During the Drying of Foodstuffs. Fundamental Aspects of the Drying of Foodstuffs. London, The Society of Chemical Industry: 42-53.

Greenspan, L. (1977). "Humidity Fixed Points of Binary Saturated Aqueous Solutions." Journal of Research of the National Bureau of Standards A. Physics and Chemistry 81(A): 89-96.

Gur-Arieh, C., A. I. Nelson, M. P. Steinberg, L. S. Wei. (1965). "A Method for Rapid Determination of Moisture-Adsorption Isotherms of Solid Particles." Journal of Food Science 30(1): 105-110.

Hardy, J. L. and M. P. Steinberg (1984). "Interaction Between Sodium Chloride and Paracasein as Determined by Water Sorption." Journal of Food Science 49: 127-131.

Irani, R. R., C. F. Callis, T. Liu (1959). "Flow Conditioning and Anticaking Agents." Industrial and Engineering Chemistry 51(10): 1285-1288.

Iyengar, J. R. and D. P. Sen (1970). "The Equilibrium Relative Humidity of Salted Fish (Barbus carnaticus and Rastrelliger carnagurta): The Effect of Calcium and Magnesium Impurities in Common Salt Used for Curing." Journal of Food Science and Technology 7(March): 17-19.

Kaufmann, D. W. (1960). Sodium Chloride. The Production and Properties of Salt and Brine.

Kuprianoff, J. (1958). 'Bound Water' in Foods. The Fundamental Aspects of the Drying of Foodstuffs. London, The Society of Chemical Industry: 14-23.

Laaksonen, T. J., Y. H. Roos, T. P. Labuza. (2001). "Comparisons of the Use of Desiccators With or Without Vacuum for Water Sorption and Glass Transition Studies." International Journal of Food Properties 4(3): 545-563.

Labuza, T. P. (1968). "Sorption Phenomena in Foods." Food Technology 22(March): 15-24.

Labuza, T. P. (1975). Interpretation of Sorption Data in Relation to the State of Constituent Water. Water Relations of Foods. R. B. Duckworth. London, Academic Press: 155-172.

Labuza, T. P., A. Kaanane, J. Y. Chen. (1985). "Effect of Temperature on the Moisture Sorption Isotherms and Water Activity Shift of Two Dehydrated Foods." Journal of Food Science 50: 385-391.

Lang, K. W., T. D. McCune, M. P. Steinberg. (1981). "A Proximity Equilibrium Cell for Rapid Determination of Sorption Isotherms." Journal of Food Science 46: 936-938.

Lang, K. W. and M. P. Steinberg (1981). "Linearization of the Water Sorption Isotherm for Homogeneous Ingredients over aw 0.3.-0.95." Journal of Food Science 46: 1450-1452.

Lowry, T. M. and F. C. Hemmings (1920). "The Properties of Powders. Part I.- The Caking of Salts." Society of the Chemical Industry 39(8): 101-110.

Mathlouthi, M. and B. Roge (2003). "Water Vapour Sorption Isotherms and the Caking of Food Powders." Food Chemistry 82: 61-71.

Moss, H. V., T. W. Schlib, W. G. Warning. (1933). "Tricalcium Phosphate as a Caking Inhibitor in Salt and Sugar." Industrial and Engineering Chemistry 25(2): 142-147.

Nelson, T. J. (1949). "Hygroscopicity of Sugar and Other Factors Affecting the Retention of Quality." Food Technology 3: 347-351.

O'Donnell, A. M., J. E. Bronlund, G. F. Brooks, A. H. J. Paterson (2002). "A Constant Humidity Air Supply System for Pilot Scale Applications." International Journal of Food Science and Technology 37: 369-374.

Paterson, A. H. J., J. E. Bronlund, G. F. Brooks (2001). The Blow Test for Measuring the Stickiness of Powders. Conference of Food Engineering 2001, AICHE Conference, Reno, Nevada, USA.

Peleg, M. (1993). "Assessment of a Semi-Empirical Four Parameter General Model for Sigmoid Moisture Sorption Isotherms." Journal of Food Process Engineering 16: 21-37.

Phoenix, L. (1966). "How Trace Additives Inhibit the Caking of Inorganic Salts." British Chemical Engineering 11(1): 34-38.

Plinke, M. A. E., D. Leith, F. Loffler (1994). "Cohesion in Granular Materials." Bulk Solids Handling 14(1): 101-106.

Schubert, H. (1984). "Capillary Forces - Modelling and Application in Particulate Technology." Powder Technology 37: 105-116.

Smith, D. S., C. H. Mannheim, S. G. Gilbert (1981). "Water Sorption Isotherms of Sucrose and Glucose by Inverse Gas Chromatography." Journal of Food Science 46: 1051-1053.

Stitt, F. (1958). Moisture Equilibrium and the Determination of Water Content of Dehydrated Foods. Fundamental Aspects of the Drying of Foodstuffs. London, The Society of Chemical Industry: 67-88.

Timmerman, E. O. (1989). "A B.E.T.-like Three Sorption Stage Isotherm." Journal of the Chemical Society, Faraday Transactions 1 85(7): 1631-1345.

Timmerman, E. O. and J. Chirife (1991). "The Physical State of Water Sorbed at High activities in Starch in Terms of the GAB Sorption Isotherm." Journal of Food Engineering 13: 171-179.

Weast, R. C. and M. J. Astle (1980). CRC Handbook of Chemistry and Physics. Boca Raton, Florida, CRC Press.

Whynes, A. L. and T. P. Dee (1957). "The Caking of Granular Fertilizers: An Investigation on a Laboratory Scale." Journal of Science and Food Agriculture 8: 577-591.

APPENDIX ONE NOMENCLATURE

a_w	Water activity	
A	Cross sectional area	m^2
A_s	Specific surface area	m^2/m^3
a	Quantity of moisture in the first adsorbed fraction	kg
b	Slope of the isotherm in multilayer fraction	
c	BET constant	
c_b	Surface concentration	kg/m^3
c_g	Constant	
c_p	Specific heat capacity	J/kg°C
c_{pa}	Specific heat capacity of air	J/kg°C
D	Moisture diffusivity	m^2/s
f	GAB constant	
F_H	Capillary binding force	N
F_P	Force due to pressure difference across liquid bridges	N
F_R	Surface tension force	N
g	Gravity	m/s^2
ΔG	Free energy	J
h	Enthalpy	J/kg
h	Third stage sorption isotherm constant	
H'	Third stage sorption isotherm intermediate	
H	Absolute humidity	$kg_{H2O}/kg_{dry\ air}$
h_c	Surface heat transfer coefficient	$W/m^2°C$
h_g	Enthalpy in the gas phase	J/kg
h_s	Enthalpy in the solid phase	J/kg
h_v	Enthalpy of water vapour	J/kg
ΔH_{vap}	Latent heat of vapourisation	J/kg
I	General node number	
I	Number of nodes	
k	Constant	
K	Avrami rate constant	s^{-3}
k_0	Boltzmann constant	erg/°C
k_g	Mass transfer coefficient	m/s
k_x	Liquid conductivity	kg/mh
L	Slab thickness	m
L	Length	m
m	Mass	kg
M	Moisture content	$kg_{H2O}/kg_{dry\ solid}$
M_0	BET monolayer moisture content	$kg_{H2O}/kg_{dry\ solid}$
n	Avrami coefficient	
N_{Ra}	Rayleigh number	
N_{Sh}	Sherwood number	
P	Vapour pressure	Pa
P_0	Vapour pressure of pure water	Pa
p_k	Capilary pressure	Pa
p_v	Vapour pressure	Pa
P_v	Partial pressure of water vapour	
p_w	Saturated vapour pressure	Pa

p_T	Total pressure	Pa
Q	Total enthalpy in porous matrix	J
Q_l	Heat absorbed in first layer	J
Q_s	Heat absorbed by homogenous surface	J
r	Radius	m
r_k	Capillary radius	mm
r_K	Kelvin radius	m
R	Universal gas constant	J/Kmol
R_1	Radii of curvature of liquid surface	nm
R_2	Radii of curvature of liquid surface	nm
RH	Relative Humidity	%
s	Slab thickness	m
S	Level of saturation	
ΔS	Entropy	J/mol
t	Time	s
T	Temperature	°C
T_a	Ambient temperature	°C
T_s	Surface temperature	°C
U	Circumference of pores	m
V	Volume	m^3
V	Volume of water adsorbed	kg/kgm^3
V_0	Molar volume	m^3/mol
V_m	Volume adsorbed in the monolayer	kg/kg
W	Total water in porous matrix	kg
W_w	Weight of water due to capillary movement	kg
x	Axial space dimension	m
Y	Fraction of unaccomplished temperature change	
Y_{av}	Average fraction of unaccomplished change	
z	Height	m

Greek letters

α	Thermal diffusivity	m^2/s
γ	Constant	
δ	Constrictivity in the porous matrix	
δ	Diffusion coefficient	m^2/s
Δ	Change	
ϵ	Porosity	
θ	Contact angle/Angle of wetting	rad
κ	Boltzmann constant	J/K
λ	Thermal conductivity	W/m°C
λ_g	Thermal conductivity of gas phase	W/m°C
λ_s	Thermal conductivity of solid phase	W/m°C
μ	Viscosity	Pa.s
μ	Intermediate in analytical solution	
ρ	Density	kg/m^3
ρ_a	Air density	kg/m^3
ρ_s	Solid phase particle density	kg/m^3
ρ_{bulk}	Bulk density	kg/m^3
$\rho_{particle}$	Particle density	kg/m^3
σ	Surface tension	N/m
τ	First order time constant	s
τ_z	Tortuosity of porous media	
Φ	Caking index	

APPENDIX TWO PSYCHOMETRIC PROPERTIES OF AIR

A2.1 Dry Air Enthalpy

(J/kg dry air)

$$h_a = c_{pa} \cdot T$$ **Equation A2. 1**

A2.2 Water Vapour Enthalpy

(J/kg water vapour)

$$h_v = c_{pv} \cdot T + h_{lv}$$ **Equation A2. 2**

A2.3 Dry Air Density

(kg dry air/m^3)

$$\rho_a = \frac{273.15}{224(273.15+T)\left(\frac{1}{29}+\frac{H}{18}\right)}$$ **Equation A2. 3**

A2.4 Vapour Pressure

(Pa)

$$\rho_v = \frac{29H \cdot p_T}{18+29H}$$ **Equation A2. 4**

A2.5 Saturated Water Vapour Pressure

(Pa)

$$p_w = e^{23.4795+\frac{3990.56}{T+233.833}}$$ **Equation A2. 5**

A2.6 Surface Vapour Pressure

(Pa)

$$p_s = a_w \cdot p_w$$ **Equation A2. 6**

A2.7 Relative Humidity

(%)

$$H_R = \frac{p_v}{p_w}$$ **Equation A2. 7**

A2.8 Absolute Humidity

(kg/kg dry air)

$$H = \frac{18p_v}{29(p_T - p_v)}$$ **Equation A2. 8**

APPENDIX THREE TRANSPORT MODEL FORMULATION

A3.1 ENTHALPY CONSERVATION EQUATIONS

A3.1.1 Enthalpy Balance in the Gas Phase

An enthalpy balance in the gas phase of the porous salt matrix can be written as;

$$\left[\begin{array}{l}\textit{Rate of accumulation}\\ \textit{of heat in the gas phase}\end{array}\right] = \left[\begin{array}{l}\textit{Rate of inflow of heat}\\ \textit{in diffused vapour}\end{array}\right] - \left[\begin{array}{l}\textit{Rate of outflow of heat}\\ \textit{in diffused vapour}\end{array}\right] + \left[\begin{array}{l}\textit{Rate of inflow of heat by}\\ \textit{conduction in gas phase}\end{array}\right]$$
$$- \left[\begin{array}{l}\textit{Rate of outflow of heat by}\\ \textit{conduction in gas phase}\end{array}\right] - \left[\begin{array}{l}\textit{Rate of outflow of heat}\\ \textit{in condensing vapour}\end{array}\right]$$

Equation A3. 1

When converted into equation form this gives;

$$\frac{\partial\left[h_g \cdot \varepsilon \cdot V \cdot \rho_a\right]}{\partial t} = \left[D \cdot \varepsilon \cdot A \cdot \frac{\partial\left[H \cdot \rho_a \cdot h_v\right]}{\partial x}\right]_{-ve} - \left[D \cdot \varepsilon \cdot A \cdot \frac{\partial\left[H \cdot \rho_a \cdot h_v\right]}{\partial x}\right]_{+ve} + \left[\lambda_g \cdot \varepsilon \cdot A \cdot \frac{\partial T}{\partial x}\right]_{-ve} - \left[\lambda_g \cdot \varepsilon \cdot A \cdot \frac{\partial T}{\partial x}\right]_{+ve} - j_{v\backslash l} \cdot h_{lv}$$

Equation A3. 2

A3.1.2 Enthalpy Balance in the Solid Phase

An enthalpy balance in the solid phase of the porous salt matrix can be written as;

$$\left[\begin{array}{l}\textit{Rate of accumulation}\\ \textit{of heat in solid phase}\end{array}\right] = \left[\begin{array}{l}\textit{Rate of inflow of heat}\\ \textit{by conduction}\end{array}\right] - \left[\begin{array}{l}\textit{Rate of outflow of heat}\\ \textit{by conduction}\end{array}\right] + \left[\begin{array}{l}\textit{Rate of inflow of heat}\\ \textit{in condensing vapour}\end{array}\right]$$

Equation A3. 3

When converted into equation form this gives;

$$\frac{\partial\left[h_s(1-\varepsilon) \cdot V \cdot \rho_s\right]}{\partial t} = \left[\lambda_s \cdot (1-\varepsilon) \cdot A \cdot \frac{\partial T}{\partial x}\right]_{-ve} - \left[\lambda_s \cdot (1-\varepsilon) \cdot A \cdot \frac{\partial T}{\partial x}\right]_{+ve} + j_{v\backslash l} \cdot h_{lv}$$

Equation A3. 4

A3.1.3 Total Enthalpy Balance

A total enthalpy balance for the porous salt matrix can be written as;

$$\left[\begin{array}{l}\textit{Total enthalpy}\\ \textbf{\textit{in bulk salt}}\end{array}\right] = \left[\begin{array}{l}\textit{Enthalpy of}\\ \textbf{\textit{gas phase}}\end{array}\right] + \left[\begin{array}{l}\textit{Enthalpy of}\\ \textbf{\textit{solid phase}}\end{array}\right]$$

Equation A3. 5

When written as an equation this gives;

$$Q = (h_g \cdot \varepsilon \cdot V \cdot \rho_a) + [h_s \cdot (1-\varepsilon) \cdot V \cdot \rho_s] \qquad \textbf{Equation A3. 6}$$

Differentiating with respect to time gives;

$$\frac{\partial Q}{\partial t} = \frac{\partial [h_g \cdot \varepsilon \cdot V \cdot \rho_a]}{\partial t} + \frac{\partial [h_s \cdot (1-\varepsilon) \cdot V \cdot \rho_s]}{\partial t} \qquad \textbf{Equation A3. 7}$$

The parallel model for effective thermal conductivity of porous materials is written as;

$$\lambda = \varepsilon \cdot \lambda_g + (1-\varepsilon) \cdot \lambda_s \qquad \textbf{Equation A3. 8}$$

When Equations A3.2, A3.4, A3.7 and A3.8 are combined this gives;

$$\frac{\partial Q}{\partial t} = D \cdot \varepsilon \cdot V \cdot \frac{\partial^2 [H \cdot \rho_a \cdot h_v]}{\partial x^2} + \lambda \cdot V \cdot \frac{\partial^2 T}{\partial x^2} \quad \textit{for } t<0 \textit{ and } 0<x<L \qquad \textbf{Equation A3. 9}$$

A3.2 MOISTURE CONSERVATION EQUATIONS

A3.2.1 Moisture Balance in the Gas Phase

A moisture balance for the gas phase of the porous salt matrix can be written as;

$$\left[\begin{array}{l}\textit{Rate of accumulation of}\\ \textit{moisture in gas phase}\end{array}\right] = \left[\begin{array}{l}\textit{Rate of inflow of}\\ \textit{moisture by diffusion}\end{array}\right] - \left[\begin{array}{l}\textit{Rate of outflow of}\\ \textit{moisture by diffusion}\end{array}\right] - \left[\begin{array}{l}\textit{Rate of outflow of}\\ \textit{moisture by condensation}\end{array}\right]$$

Equation A3. 10

When expressed as an equation this results in;

$$\frac{\partial [\varepsilon \cdot V \cdot H \cdot \rho_a]}{\partial t} = \left| D \cdot \varepsilon \cdot A \cdot \frac{\partial H \cdot \rho_a}{\partial x} \right|_{-ve} - \left| D \cdot \varepsilon \cdot A \cdot \frac{\partial H \cdot \rho_a}{\partial x} \right|_{+ve} - j_{v\backslash s} \qquad \textbf{Equation A3. 11}$$

A3.2.2 Moisture Balance in the Solid Phase

A moisture balance for the solid phase of the porous salt matrix can be written as;

$$\left[\begin{array}{l}\textit{Rate of accumulation of}\\ \textbf{\textit{moisture in the solid phase}}\end{array}\right] = \left[\begin{array}{l}\textit{Rate of inflow of}\\ \textbf{\textit{moisture by condensation}}\end{array}\right]$$

Equation A3. 12

When written in equation form this gives;

$$\frac{\partial [(1-\varepsilon) \cdot V \cdot M \cdot \rho_s]}{\partial t} = j_{v\backslash s} \qquad \textbf{Equation A3. 13}$$

A3.2.3 Total Moisture Balance

A total moisture balance for the combined porous salt matrix can be written as;

$$\left[\begin{array}{c}\textit{Total moisture}\\ \textit{in bulk lactose}\end{array}\right] = \left[\begin{array}{c}\textit{Moisture in}\\ \textit{gas phase}\end{array}\right] + \left[\begin{array}{c}\textit{Moisture in}\\ \textit{solid phase}\end{array}\right] \qquad \textbf{Equation A3. 14}$$

Expressed in equation form this gives;

$$W = [\varepsilon \cdot V \cdot H \cdot \rho_a] + [(1-\varepsilon) \cdot V \cdot M \cdot \rho_s] \qquad \textbf{Equation A3. 15}$$

Differentiating with respect to time gives;

$$\frac{\partial W}{\partial t} = \frac{\partial[\varepsilon \cdot V \cdot H \cdot \rho_a]}{\partial t} + \frac{\partial[(1-\varepsilon) \cdot V \cdot M \cdot \rho_s]}{\partial t} \qquad \textbf{Equation A3. 16}$$

Combining Equations A3.11, A3.13 and A3.16 gives;

$$\frac{\partial W}{\partial t} = D \cdot \varepsilon \cdot V \cdot \frac{\partial^2 H \cdot \rho_a}{\partial x^2} \qquad \textit{for } t<0 \textit{ and } 0<x<L \qquad \textbf{Equation A3. 17}$$

A3.3 INITIAL CONDITIONS

$$T = f(T_{initial}) \qquad \textit{for all } x \textit{ at } t=0 \qquad \textbf{Equation A3. 18}$$

$$W = f(RH_{initial}) \qquad \textit{for all } x \textit{ at } t=0 \qquad \textbf{Equation A3. 19}$$

From these initial conditions all other initial values in the model can be calculated. (T, RH, M, H, ρ_a)

A3.4 BOUNDARY CONDITIONS

A third kind of boundary condition (heat conduction) over both the top and bottom boundaries is used to describe heat transfer over the boundaries. This is more consistent with the experimental apparatus than assuming a constant boundary temperature (first kind of boundary condition) as the plates take some time to heat up after a step change has been applied.

$$h_c(T - T_a) = 0 \qquad \textit{for } t \geq 0 \textit{ at } x=0,L \qquad \textbf{Equation A3. 20}$$

No moisture diffusion occurs over the top and bottom boundaries so a symmetry (fifth kind of boundary condition) is used to describe the transport of moisture at the boundaries.

$$\frac{\partial(H\rho_a)}{\partial x} = 0 \qquad \textit{for } t \geq 0 \textit{ at } x=0,L \qquad \textbf{Equation A3. 21}$$

APPENDIX FOUR MATHEMATICAL CODE

A4.1 AIR PROPERTIES

```
//**********************************************************************
***
//
// ********************* AirProps.H
**********************************
//
// A class for characterisation of air properties at atmospheric pressure.
//
// This class defines the fundamental properties of air as Temperature,
// Pressure and Absolute humidity. All other properties are obtained
// through function calls.
//
//**********************************************************************
***

#ifndef AirProps_H_
#define AirProps_H_

class AirProps {

public:

double  Temperature;                        // °C
double  Humidity;                                   // kg/kg dry air

const   double  Pressure;                   // = 101300 Pa

const   double DryAirSpecHeat;      // = 1006 J/kg°C
const   double WaterVapSpecHeat; // = 1875 J/kg°C
const    double       GasConstant;          // = 8.413 Nm/mol°C
const    double       LatentHeat;             // = 2.5e6 J/kg

AirProps(char[],double,char[],double); // Class AirProps constructor
void SetAirProps(char ina[], double aa, char inb[], double bb);
                                                                    // Sets
the Temperature and Humidity
double AirTemperature(char INa[],double a,char INb[]="None",double b=42);

double AirHumidity(char INa[],double a,char INb[]="None",double b=42);

double AirDensity();                        // Dry air density kg/m3
double AirDensity(char INA[],double A,char INB[]="None",double B=42);
```

```
double VapPressure();                    // Vapour Pressure (Pa) from Humidity
double VapPressure(char INA[],double A,char INB[]="None",double B=42);

double SatVapPressure();                 // Saturated Vapour Pressure (Pa) from
AirTemp
double SatVapPressure(char INA[],double A,char INB[]="None",double B=42);

double RH();                                          // RH from Humidity and
AirTemp
double RH(char INA_RH[],double A_RH,char INB_RH[]="None",double
B_RH=42);

double AirEnthalpy();                    // Air Enthalpy J/kg dry air
double AirEnthalpy(char INA[],double A,char INB[]="None",double B=42);

};

#endif          //AirProps_H_



// ********************************************************
//
// ************************ AirProps.cpp ********************
//
// A class for characterisation of air properties at atmospheric pressure.
//
// This class defines the fundamental properties of air as Temperature,
// Pressure and Absolute humidity. All other properties are obtained
// through function calls.
// ********************************************************


#include <string.h>
#include <math.h>
#include "c:\SaltCake\AirProps.h"

// ********************************************************
//
//              AirProps Constructor
//
// ********************************************************


AirProps::AirProps(char INA[], double A, char INB[], double B) :
        Pressure(1013e2),               // Pa
        DryAirSpecHeat(1006),           // J/kg°C
        WaterVapSpecHeat(1875),                     // J/kg°C
        GasConstant(8.413),                     // Nm/mol°C
```

```
        LatentHeat(2.5e6) {                     // J/kg

        SetAirProps(INA,A,INB,B);

};

void AirProps::SetAirProps(char ina[], double aa, char inb[], double bb) {

        Temperature = AirTemperature(ina,aa,inb,bb);
        Humidity = AirHumidity(ina,aa,inb,bb);
};



// ***********************************************************
//
//              Air Humidity Functions
//
// ***********************************************************


double AirProps::AirHumidity(char INa[], double a, char INb[] ,double b) {

        double dummyH;

        //******************* Sorting code ***********************

        //. rearranges arguements so "Humidity" is last if it is present.
        if (stricmp(INa,"Temperature") == 0) {
                char * INc = INb;
                double c;
                c = b;
                INb = INa;
                b = a;
                INa = INc;
                a = c;
        }

        //. sets INb to "Temperature" if second arguement is not given
        if (stricmp(INb,"None") == 0) {
                INb = "Temperature";
                b = Temperature;
        }


        //. checks if INb = "Humidity" and changes it so INa = "Humidity
        if (stricmp(INb,"Humidity") == 0) {
                INa = INb;
```

```
            a = b;
        }

        //****************** Calculation code **********************

        //. Humidity
        if (stricmp(INa,"Humidity") == 0) {
            dummyH = a;
        }

        //. RH and Temperature
        if ((stricmp(INa,"RH") == 0) && (stricmp(INb,"Temperature") == 0)) {
            dummyH = 18.0*a*exp(23.4795-3990.56/(b+233.833))
                                    /(29.0*(Pressure-a*exp(23.4795-
3990.56/(b+233.833))));
        }

        //. AirDensity and Temperature
        if ((stricmp(INa,"AirDensity") == 0) && (stricmp(INb,"Temperature") == 0))
{
            dummyH = 18.0*(273.15/(22.4*(273.15+b)*a)-1/29.0);
        }

        //. Air Enthalpy and Temperature
        if ((stricmp(INa,"AirEnthalpy") == 0) && (stricmp(INb,"Temperature") ==
0)) {
            dummyH = (a-
DryAirSpecHeat*b)/(WaterVapSpecHeat*b+LatentHeat);
        }

        return dummyH;
};



// ********************************************************
//
//          Temperature Functions
//
// ********************************************************


double AirProps::AirTemperature(char INa[],double a,char INb[] , double b) {

        double dummyTemp;

        //****************** Sorting code **********************

        //. rearranges arguements so "Humidity" is last if it is present.
        if (stricmp(INa,"Humidity") ==0) {
```

```
            char * INc = INb;
            double c;
            c = b;
            INb = INa;
            b = a;
            INa = INc;
            a = c;
        }

        //. sets INb to "Humidity" if second arguement is not given
        if (stricmp(INb, "None") == 0) {
            INb = "Humidity";
            b = Humidity;
        }

        //. checks if INb = "Temperature" and changes it so INa = "Temperature"
        if (stricmp(INb,"Temperature") == 0) {
            INa = INb;
            a = b;
        }

        //******************** Calculation code ************************

        //. Temperature
        if (stricmp(INa,"Temperature") == 0)  {
            dummyTemp = a;
        }

        // .RH and Humidity inputed from user
        else if ((stricmp(INa,"RH") == 0) && (stricmp(INb,"Humidity") == 0)) {
            dummyTemp = 3990.56/(23.4795-log(29*b*Pressure/(18+29*b)/a))-
233.833;
        }

        //. AirEnthalpy and Humidity from user
        else if ((stricmp(INa,"AirEnthalpy") == 0) && (stricmp(INb,"Humidity") ==
0)) {
            dummyTemp = (a-
b*LatentHeat)/(DryAirSpecHeat+b*WaterVapSpecHeat);
        }

        //. AirDensity and Humidity from user
        else if ((stricmp(INa,"AirDensity") == 0) && (stricmp(INb,"Humidity") ==
0)) {
            dummyTemp = (273.15/(a*22.4*(1/29.0+b/18.0)))-273.15;
        }

        //. room for more functions here

        return dummyTemp;
```

```
};

// ********************************************************
//
//          AirDensity Functions
//
// ********************************************************

double AirProps::AirDensity() {
        return 1/(22.4*(273.15+Temperature)*(1/29.0+Humidity/18.0)/273.15);
};

double AirProps::AirDensity(char INA[],double A,char INB[],double B) {

        double Humidity_int = AirHumidity(INA,A,INB,B);
        double Temperature_int = AirTemperature(INA,A,INB,B);
        return
1/(22.4*(273.15+Temperature_int)*(1/29.0+Humidity_int/18.0)/273.15);
};


// ********************************************************
//
//          Vapour Pressure Functions
//
// ********************************************************

double AirProps::VapPressure() {
        return 29*Humidity*Pressure/(18+29*Humidity);
};


double AirProps::VapPressure(char INA[],double A,char INB[],double B) {
        double Humidity_int = AirHumidity(INA,A,INB,B);
        return 29*Humidity_int*Pressure/(18+29*Humidity_int);
};


// ********************************************************
//
//          Saturated Vapour Pressure Functions
//
// ********************************************************

double AirProps::SatVapPressure() {
        return exp(23.4795-3990.56/(Temperature+233.833));
};


double AirProps::SatVapPressure(char INA[],double A,char INB[],double B) {
```

```
        double Temperature_int = AirTemperature(INA,A,INB,B);
        return exp(23.4795-3990.56/(Temperature_int+233.833));
};


// ***********************************************************
//
//          Relative Humidity Functions
//
// ***********************************************************

double AirProps::RH() {
        return VapPressure()/SatVapPressure();
};

double AirProps::RH(char INA_RH[],double A_RH,char INB_RH[],double B_RH) {
        return VapPressure(INA_RH,A_RH,INB_RH,B_RH)

        /SatVapPressure(INA_RH,A_RH,INB_RH,B_RH);
};

// ***********************************************************
//
//          Air Enthalpy Functions
//
// ***********************************************************

double AirProps::AirEnthalpy() {
        return DryAirSpecHeat*Temperature+Humidity

        *(WaterVapSpecHeat*Temperature+LatentHeat);
};


double AirProps::AirEnthalpy(char INA[],double A,char INB[],double B) {

        double Temperature_int = AirTemperature(INA,A,INB,B);
        double Humidity_int = AirHumidity(INA,A,INB,B);

        return DryAirSpecHeat*Temperature_int+Humidity_int

        *(WaterVapSpecHeat*Temperature_int+LatentHeat);
};
```

A4.2 NODES

```
#ifndef Node_H_
#define Node_H_

#include <iostream.h>
#include <stdlib.h>
#include "c:\SaltCake\SaltProps.h"
#include "c:\SaltCake\AirProps.h"


enum Boolean {Yes, No};


class Ambient {
public:
char label[10];
Boolean ConstantTemperature;
double Temperature;
double TempArray[200];
double TimeInterval;
double htc;
friend iostream;
friend fstream;

Ambient(char* nm);
void SetAmbient(double temp,double h);
void GetAndSetValues();
void UpdateAmbient(double t);
};

class Node {

public:

Salt L;
static double Time;
static double dt;
static double dx;
double Heat;
double Water;
double Vol;
double Tempnew,EffMCnew;
Node();
void SetNode(char inA[],double ina,char inB[],double inb,char inC[],double inc,
        char inD[] = "None",double ind = 42,char inE[] = "None",double ine = 42);
void GetAndSetValues();
void UpdateAir();
```

```
};

class InternalNode : public Node {
public:
void Transport(Node L_Node, Node R_Node);

};

class LeftNode : public Node {
public:
void Transport(Ambient L_Node,Node R_Node);
};

class RightNode : public Node {
public:
void Transport(Node L_Node,Ambient R_Node);
};

#endif          //Node_H_
```

```
#include <string.h>
#include <math.h>
#include <iostream.h>
#include <fstream.h>
#include "c:\SaltCake\SaltProps.h"
#include "c:\SaltCake\AirProps.h"
#include "c:\SaltCake\Node.h"


double Node::dt=0;
double Node::dx=0;
double Node::Time=0;

Ambient::Ambient(char* nm) {
        strcpy(label,nm);
        SetAmbient(20,60);
        TimeInterval=600;
};

void Ambient::SetAmbient(double temp,double h) {
        int I=0;
        while(!(I>199)) {
                TempArray[I]=temp;
                I++;
```

```
        }
        htc = h;
};

void Ambient::GetAndSetValues() {
        double IntA,IntB;
        char answer;
        cout << "Use constant temperature for " << label << " (y/n)?" << '\t';
        cin >> answer;
        if (answer == 'n') {
                char filename[13];
                cout << "Enter temperature history filename ";
                cin >> filename;
                ifstream infile(filename);
                int I=0;
                while(!infile.eof()) {
                        infile >> TempArray[I];
                        I++;
                }
                infile.close();
                cout << "Enter time interval for file" << filename;
                cin >> TimeInterval;
                cout << "Enter heat transfer coefficient        ";
                cin >> htc;
        }
        else {
                cout << label << " Boundary Temperature (°C)   " << '\t';
                cin >> IntA;
                cout << label << " Boundary HTC              " << '\t';
                cin >> IntB;
                SetAmbient(IntA,IntB);
                }
};

void Ambient::UpdateAmbient(double t) {
          int I,j;
          I=(int) t/TimeInterval;
       I=abs(I);
          j = abs((int)t % (int)TimeInterval);
          Temperature = TempArray[I]+(TempArray[I+1]-
TempArray[I])*j/TimeInterval;
};




Node::Node() {
        Vol = 1e-5;
```

```
        Water = 0;
        Heat = 0;
};

void Node::GetAndSetValues() {
        double IntA,IntB;
        cout << "Initial Salt Temperature (°C)" << '\t';
        cin >> IntA;
        cout << "Initial Salt Water Activity  " << '\t';
        cin >> IntB;
        L.SetAirProps("Temperature",IntA,"RH",IntB);
        cout << "Initial Percent Amorphous              " << '\t';
        cin >> IntA;
        cout << "Initial Crystallinity of Amorphous" << '\t';
        cin >>IntB;
        if (IntB ==0) {L.SetAmorphous("PercentAmorph",IntA);}
        else {L.SetAmorphous("PercentAmorph",IntA,"Crystallinity",IntB);};
        cout << "Porosity                                                    "
<< '\t';
        cin >> IntB;
        if (IntB == 0) {L.SetPorosity();}
        else {L.SetPorosity(IntB);};
};

void Node::UpdateAir() {
        L.SetAirProps("Temperature",Tempnew,"RH",L.RH("EffectiveMC",EffMCne
w));
};



void InternalNode::Transport(Node L_Node, Node R_Node) {
double Tempmin = (L.Temperature+L_Node.L.Temperature)/2;
double Tempmax = (L.Temperature+R_Node.L.Temperature)/2;
Heat = Heat+dt*Vol/pow(dx,2)*L.TConduct*(L_Node.L.Temperature
                        -2*L.Temperature+R_Node.L.Temperature)

        +L.Diffusivity("Temperature",Tempmin)*(L.WaterVapSpecHeat*Tempmin
                        +L.LatentHeat)*(L_Node.L.Humidity*L_Node.L.AirDensity()
                        -L.Humidity*L.AirDensity())
                        -
L.Diffusivity("Temperature",Tempmax)*(L.WaterVapSpecHeat*Tempmax
                        +L.LatentHeat)*(L.Humidity*L.AirDensity()
                        -R_Node.L.Humidity*R_Node.L.AirDensity());
Water = Water+dt*Vol/pow(dx,2)*(L.Diffusivity("Temperature",Tempmin)
                        *(L_Node.L.Humidity*L_Node.L.AirDensity()-
L.Humidity*L.AirDensity())
                        -
L.Diffusivity("Temperature",Tempmax)*(L.Humidity*L.AirDensity()
                        -R_Node.L.Humidity*R_Node.L.AirDensity()));
```

```
L.NewAmorphState(dt);

double diffMC = L.MoistureContent();
double diffT = L.Temperature;
double EffMC = L.MoistureContent();
double Temp = L.Temperature;
while ((fabs(diffMC)>1e-50) && (fabs(diffT)>1e-2)) {
        Tempnew = (Heat-
Vol*L.Porosity*L.AirDensity("RH",L.RH("EffectiveMC",EffMC),"Temperature",Te
mp)*L.LatentHeat

        *L.AirHumidity("RH",L.RH("EffectiveMC",EffMC),"Temperature",Temp))

        /(Vol*L.Porosity*L.AirDensity("RH",L.RH("EffectiveMC",EffMC),"Temper
ature",Temp)*(L.DryAirSpecHeat

        +L.AirHumidity("RH",L.RH("EffectiveMC",EffMC),"Temperature",Temp)
                *L.WaterVapSpecHeat)+(1-L.Porosity)*Vol*L.ParticleDensity
                *(L.SaltSpecHeat+EffMC*L.WaterSpecHeat));
        EffMCnew = (Water-
L.Porosity*Vol*L.AirHumidity("RH",L.RH("EffectiveMC"

        ,EffMC),"Temperature",Temp)*L.AirDensity("RH",L.RH("EffectiveMC",Eff
MC),"Temperature",Temp))
                /((1-L.Porosity)*Vol*L.ParticleDensity);
        diffT = Temp-Tempnew;
        diffMC = EffMC-EffMCnew;
        Temp = Tempnew;
        EffMC = EffMCnew;
}
};


void LeftNode::Transport(Ambient L_Node, Node R_Node) {
double Tempmax = (L.Temperature+R_Node.L.Temperature)/2;
Heat = Heat+2*dt*Vol/dx*(L_Node.htc*(L_Node.Temperature
                        -L.Temperature)-L.TConduct/dx*(L.Temperature-
R_Node.L.Temperature)
                        -
L.Diffusivity("Temperature",Tempmax)/dx*(L.WaterVapSpecHeat*Tempmax
                        +L.LatentHeat)*(L.Humidity*L.AirDensity()
                        -R_Node.L.Humidity*R_Node.L.AirDensity()));
Water = Water+2*dt*Vol/pow(dx,2)*(-L.Diffusivity("Temperature",Tempmax)
                        *(L.Humidity*L.AirDensity()-
R_Node.L.Humidity*R_Node.L.AirDensity()));
L.NewAmorphState(dt);

double diffMC = L.MoistureContent();
double diffT = L.Temperature;
double EffMC = L.MoistureContent();
```

```
double Temp = L.Temperature;
while ((fabs(diffMC)>1e-50) && (fabs(diffT)>1e-2)) {
        Tempnew = (Heat-
Vol*L.Porosity*L.AirDensity("RH",L.RH("EffectiveMC",EffMC),"Temperature",Te
mp)*L.LatentHeat

        *L.AirHumidity("RH",L.RH("EffectiveMC",EffMC),"Temperature",Temp))

        /(Vol*L.Porosity*L.AirDensity("RH",L.RH("EffectiveMC",EffMC),"Temper
ature",Temp)*(L.DryAirSpecHeat

        +L.AirHumidity("RH",L.RH("EffectiveMC",EffMC),"Temperature",Temp)
                *L.WaterVapSpecHeat)+(1-L.Porosity)*Vol*L.ParticleDensity
                *(L.SaltSpecHeat+EffMC*L.WaterSpecHeat));
        EffMCnew = (Water-
L.Porosity*Vol*L.AirHumidity("RH",L.RH("EffectiveMC"

        ,EffMC),"Temperature",Temp)*L.AirDensity("RH",L.RH("EffectiveMC",Eff
MC),"Temperature",Temp))
                /((1-L.Porosity)*Vol*L.ParticleDensity);
        diffT = Temp-Tempnew;
        diffMC = EffMC-EffMCnew;
        Temp = Tempnew;
        EffMC = EffMCnew;
}
};

void RightNode::Transport(Node L_Node,Ambient R_Node) {
double Tempmin = (L.Temperature+L_Node.L.Temperature)/2;
Heat = Heat+2*dt*Vol/dx*(-R_Node.htc*(L.Temperature-R_Node.Temperature)
                        +L.TConduct/dx*(L_Node.L.Temperature-L.Temperature)

        +L.Diffusivity("Temperature",Tempmin)/dx*(L.WaterVapSpecHeat*Tempmi
n
                        +L.LatentHeat)*(L_Node.L.Humidity*L_Node.L.AirDensity()-
L.Humidity*L.AirDensity()));
Water = Water+2*dt*Vol/pow(dx,2)*(L.Diffusivity("Temperature",Tempmin)
                        *(L_Node.L.Humidity*L_Node.L.AirDensity()-
L.Humidity*L.AirDensity()));
L.NewAmorphState(dt);

double diffMC = L.MoistureContent();
double diffT = L.Temperature;
double EffMC = L.MoistureContent();
double Temp = L.Temperature;
while ((fabs(diffMC)>1e-50) && (fabs(diffT)>1e-2)) {
        Tempnew = (Heat-
Vol*L.Porosity*L.AirDensity("RH",L.RH("EffectiveMC",EffMC),"Temperature",Te
mp)*L.LatentHeat
```

```
        *L.AirHumidity("RH",L.RH("EffectiveMC",EffMC),"Temperature",Temp))

        /(Vol*L.Porosity*L.AirDensity("RH",L.RH("EffectiveMC",EffMC),"Temper
ature",Temp)*(L.DryAirSpecHeat

        +L.AirHumidity("RH",L.RH("EffectiveMC",EffMC),"Temperature",Temp)
                *L.WaterVapSpecHeat)+(1-L.Porosity)*Vol*L.ParticleDensity
                *(L.SaltSpecHeat+EffMC*L.WaterSpecHeat));
        EffMCnew = (Water-
L.Porosity*Vol*L.AirHumidity("RH",L.RH("EffectiveMC"

        ,EffMC),"Temperature",Temp)*L.AirDensity("RH",L.RH("EffectiveMC",Eff
MC),"Temperature",Temp))
                /((1-L.Porosity)*Vol*L.ParticleDensity);
        diffT = Temp-Tempnew;
        diffMC = EffMC-EffMCnew;
        Temp = Tempnew;
        EffMC = EffMCnew;
}
};
```

A4.3 SALT PROPERTIES

```
// ********************************************************
//
// ********************** SaltProps.h **********************
//
// A class for characterisation of salt in equilibrium with air.
//
// This class defines the fundamental properties of salt as
// amorphous content, water activity all other properties are obtained
// through function calls.
// ********************************************************

#ifndef SaltProps_H_
#define SaltProps_H_

#include "c:\SaltCake\AirProps.h"


class Salt : public AirProps {

        public:

        double Porosity;            // voidage fraction
        double PercentAmorph;       // amount of amorphous material
        double Crystallinity;       // crystallinity of amorphous portion

        double TConduct;                                // effective thermal conductivity

        const double ParticleDensity;  // salt particle density kg/m3
        const double SaltSpecHeat;  // salt specific heat capacity J/kg°C
        const double WaterSpecHeat;    // liquid water specific heat capacity J/kg°C


        //constructor
        Salt();                         // sets porosity, airspace,PercentAmorph and
 Crystallinity

        void SetAmorphous(char INa[],double a,char INb[]="Crystallinity",double b =
 1e-15);
        void SetPorosity(double epsilon = 0.4);

        void NewAmorphState(double timestep);
        double NewCrystallinity(double timestep);
        double RateConstant();
        double TGlass();
        double MoistureContent(char IN[]="None",double in=42,
                                char INb[]="None",double inb=42);
                                // effective moisture content f(RH) kg/kg dry salt
```

```
        double MC_Alpha(char IN[]="None",double in=42);
                                // moisture content of crystalline salt kg/kg dry salt
        double MC_Amorphous(char IN[]="None",double in=42);
                                // moisture content of amorphous salt kg/kg dry salt
        double Diffusivity(char IN[]="None",double in=42);
  double RH();
        double RH(char INa[],double a,char INb[]="None",double b = 42);



};


#endif          //SaltProps_H_




// ********************************************************
//
// ************************ SaltProps.cpp ************************
//
// A class for characterisation of salt in equilibrium with air.
//
// This class defines the fundamental properties of salt as
// amorphous content, water activity all other properties are obtained
// through function calls.
// ********************************************************

#include "c:\SaltCake\AirProps.h"
#include "c:\SaltCake\SaltProps.h"
#include <string.h>
#include <math.h>

Salt::Salt() :
        AirProps("Humidity",0.011,"Temperature",20),
        ParticleDensity(2161),
        SaltSpecHeat(850),
        WaterSpecHeat(4180) {
        SetPorosity();
        TConduct = 0.6983;
        SetAmorphous("PercentAmorph",0.05,"Crystallinity",1e-18);
};


void Salt::SetPorosity(double epsilon) {
        Porosity = epsilon;
};
```

```
void Salt::SetAmorphous(char INa[],double a,char INb[], double b) {
        if (stricmp(INa,"Crystallinity") == 0) {
                char * INc = INa;
                double c = a;
                INa = INb;
                a = b;
                INb = INc;
                b = c;
        }
        if (stricmp(INa,"PercentAmorph") == 0) {
                PercentAmorph = a;
        }
        if (stricmp(INb,"Crystallinity") == 0) {
                Crystallinity = b;
        }
};

void Salt::NewAmorphState(double timestep) {
        PercentAmorph = PercentAmorph/(1-Crystallinity)*(1-
NewCrystallinity(timestep));
        Crystallinity = NewCrystallinity(timestep);
        int j=42;
};

double Salt::NewCrystallinity(double timestep) {
        const double Avrami_m = 3;

        double dummy_Cry;
        if ((PercentAmorph > 0) && (RateConstant() > 0) && (Crystallinity < 1)) {
                dummy_Cry = Crystallinity+timestep*Avrami_m*(1-Crystallinity)*
                        pow((-log(1-Crystallinity)),(Avrami_m-1)/Avrami_m)*
                        pow(RateConstant(),(1/Avrami_m));
        }
        else {dummy_Cry = Crystallinity;}

        if (dummy_Cry > 1) { dummy_Cry = 1;}
        return dummy_Cry;
};

double Salt::RateConstant() {
        const double Avrami = 3;
        double thalf;
        if (Temperature > TGlass()) {
                thalf = pow10(11-17.44*(Temperature-TGlass())/
                                        (51.6+Temperature-TGlass()));
                return log(2)/pow(thalf,Avrami);
        }
        else {return 0;}
```

```
};

double Salt::TGlass() {
        const double Tg1 = 101;
        const double Tg2 = -135;
        const double K = 7.2;
        return ((1-MC_Amorphous())*Tg1+K*MC_Amorphous()*Tg2)/
                                ((1-MC_Amorphous())+K*MC_Amorphous());
};


double Salt::MoistureContent(char INa[],double ina,char INb[],double inb) {

        if (stricmp(INa,"None") == 0) {
                INa = "RH";
                ina = RH();
        }
        if (stricmp(INb,"None") == 0) {
                inb = PercentAmorph;
        }
        return MC_Alpha(INa,ina)+MC_Amorphous(INa,ina)*inb;
};
double Salt::MC_Alpha(char IN[],double in) {
        const double Aa = 0.001;
        const double Bb = 0.1;
        const double Cc = 1000;

        if (stricmp(IN,"None") == 0) {
                IN = "RH";
                in = RH();
        }

     return (Aa+Bb*in)/(Cc*(0.75305-in));
};


double Salt::MC_Amorphous(char IN[],double in) {
        const double VmGAB = 0.0491;
        const double cGAB = 4.33;
        const double kGAB = 1.18;

        if (stricmp(IN,"None") == 0) {
                IN = "RH";
                in = RH();
        }
        return VmGAB*cGAB*kGAB*in/((1-kGAB*in)*(1+(cGAB-1)*kGAB*in));
};

double Salt::Diffusivity(char IN[],double in) {
```

```
        if (stricmp(IN,"None") == 0) {
                IN = "Temperature";
                in = Temperature;
        }

        return Porosity*(0.0017255*(in+273.15)-0.2552)/10000;
};

double Salt::RH() {
        return AirProps::RH();
};

double Salt::RH(char INa[],double a,char INb[],double b){
        if ((stricmp(INa,"EffectiveMC") == 0) || (stricmp(INb,"EffectiveMC")==0)) {
                if ((stricmp(INb,"EffectiveMC") == 0)) {
                        char * INc = INb;
                        double c;
                        c = b;
                        INb = INa;
                        b = a;
                        INa = INc;
                        a = c;
                }
                if ((stricmp(INb,"None")==0)) {
                        INb = "PercentAmorph";
                        b = PercentAmorph;
                }
                if ((stricmp(INa,"EffectiveMC") == 0) &&
(stricmp(INb,"PercentAmorph")==0)) {
                        double Try1=0,Try2=1,MCalc=1,aw;
                        while (fabs(MCalc-a)>1e-15) {
                                aw=(Try1+Try2)/2;
                                MCalc = MoistureContent("RH",aw,INb,b);
                                if ((MCalc-a)<0) {Try1 = aw;}
                                else {Try2 = aw;}
                        }
                        return aw;
                }
        }
        else {return AirProps::RH(INa,a,INb,b);}
};
```

A4.4 SALT CAKING MODEL

```
//.
**********************************************************************
*******
//.                Program "SaltCake.cpp"
//.
**********************************************************************
*******

#include <iostream.h>
#include <fstream.h>
#include <string.h>
#include "c:\SaltCake\Node.h"
#include "c:\SaltCake\SaltProps.h"
#include "c:\SaltCake\AirProps.h"

enum {size = 15};
char filename[13];

ofstream outfile_RH;
ofstream outfile_Amorph;
ofstream outfile_Temp;
ofstream outfile_Tg;


InternalNode Inside[size];
LeftNode BottomNode;
RightNode TopNode;
Ambient BottomAmbient("Bottom"),TopAmbient("Top");

int NumberNodes;
double Tfinish,Tprint;
enum OutType {Temp,RH,Humidity,Hrhoa,Tg,Amorph};

void PrintOut(OutType x) {

        if (x==RH) {cout << Node::Time << "  ";}
        int i;
        switch(x) {
                case Temp:
                        //cout << BottomNode.L.Temperature << "  ";
                        outfile_Temp << Node::Time << "  ";
                        outfile_Temp << BottomNode.L.Temperature << "  ";
                        for (i=1;i<NumberNodes;i=i+1) {
                                //cout << Inside[i].L.Temperature << "  ";
                                outfile_Temp << Inside[i].L.Temperature << "  ";
                        };
                        //cout << TopNode.L.Temperature << endl;
```

```
                outfile_Temp << TopNode.L.Temperature << endl;
                break;
        case Amorph:
                //cout << BottomNode.L.PercentAmorph << "  ";
                outfile_Amorph << Node::Time << "  ";
                outfile_Amorph << BottomNode.L.PercentAmorph << "  ";
                for (i=1;i<NumberNodes;i=i+1) {
                        // cout << Inside[i].L.PercentAmorph << "  ";
                        outfile_Amorph << Inside[i].L.PercentAmorph << "  ";
                };
                cout << TopNode.L.PercentAmorph << endl;
                outfile_Amorph << TopNode.L.PercentAmorph << endl;
                break;
        case RH:
                outfile_RH << Node::Time << "  ";
                cout << BottomNode.L.RH() << "  ";
                outfile_RH << BottomNode.L.RH() << "  ";
                for (i=1;i<NumberNodes;i=i+1) {
                        cout << Inside[i].L.RH() << "  ";
                        outfile_RH << Inside[i].L.RH() << "  ";
                };
                cout << TopNode.L.RH() << endl;
                outfile_RH << TopNode.L.RH() << endl;
                break;
        case Tg:
                //cout << (BottomNode.L.Temperature-
BottomNode.L.TGlass()) << "  ";
                outfile_Tg << Node::Time << "  ";
                outfile_Tg << (BottomNode.L.Temperature-
BottomNode.L.TGlass()) << "  ";
                for (i=1;i<NumberNodes;i=i+1) {
                        //cout << (Inside[i].L.Temperature-Inside[i].L.TGlass())
<< "  ";
                        outfile_Tg << (Inside[i].L.Temperature-
Inside[i].L.TGlass()) << "  ";
                };
                //cout << (TopNode.L.Temperature-TopNode.L.TGlass()) <<
endl;
                outfile_Tg << (TopNode.L.Temperature-TopNode.L.TGlass())
<< endl;
        }


};


void main() {

OutType X1=RH;
OutType X2=Temp;
```

```
cin.width(sizeof(filename));
cout << "Results file name                " << '\t';
cin >> filename;
cout << endl;
char fname[13];
strncpy(fname,filename,13);

outfile_RH.open(strcat(filename,".RH"));
if(!outfile_RH) cerr<<"couldn't open RH outfile"<<endl;

outfile_Temp.open(strcat(fname,".tmp"));
if(!outfile_Temp) cerr<<"couldn't open amorphous outfile"<<endl;

Node::Time = 0;

cout << "Time step                    " << '\t';
cin >> Node::dt;
cout << "Print out interval              " << '\t';
cin >> Tprint;
cout << "Total Simulation time                  "        << '\t';
cin >> Tfinish;

//*************************************************************************
**********
// Setup Salt Conditions
//*************************************************************************
**********

cout << "Number of nodes                " << '\t';
cin >> NumberNodes;

double Thickness;
cout << "Slab thickness                          " << '\t';
cin >> Thickness;
Node::dx = (Thickness/NumberNodes);

char answer;
cout << "Initialise each node seperately?   " << '\t';
cin >> answer;
if (answer == 'n') {
        double IntA,IntB,IntC,IntD,IntE;
        cout << "Initial Salt Temperature (°C)" << '\t';
        cin >> IntA;
        cout << "Initial Salt Water Activity  " << '\t';
        cin >> IntB;
        cout << "Initial Percent Amorphous   " << '\t';
        cin >> IntC;
        cout << "Initial Crystallinity of Amorphous" << '\t';
        cin >> IntD;
        cout << "Porosity                        " << '\t';
```

```
        cin >> IntE;

        BottomNode.L.SetAirProps("Temperature",IntA,"RH",IntB);
        if (IntD == 0) {
                BottomNode.L.SetAmorphous("PercentAmorph",IntC);}
        else {

        BottomNode.L.SetAmorphous("PercentAmorph",IntC,"Crystallinity",IntD);};
        if (IntE == 0) {}
        else {BottomNode.L.SetPorosity(IntE);};
        BottomNode.Water =
BottomNode.L.Porosity*BottomNode.Vol*BottomNode.L.Humidity
                *BottomNode.L.AirDensity()+(1-
BottomNode.L.Porosity)*BottomNode.Vol
                *BottomNode.L.ParticleDensity*BottomNode.L.MoistureContent();
        BottomNode.Heat =
(BottomNode.L.DryAirSpecHeat*BottomNode.L.Temperature
                +BottomNode.L.Humidity*(BottomNode.L.WaterVapSpecHeat

        *BottomNode.L.Temperature+BottomNode.L.LatentHeat))*BottomNode.L.P
orosity

        *BottomNode.Vol*BottomNode.L.AirDensity()+(BottomNode.L.SaltSpecHea
t

        *BottomNode.L.Temperature+BottomNode.L.WaterSpecHeat*BottomNode.L
.Temperature
                *BottomNode.L.MoistureContent())*(1-
BottomNode.L.Porosity)*BottomNode.Vol
                *BottomNode.L.ParticleDensity;

        TopNode.L.SetAirProps("Temperature",IntA,"RH",IntB);
        if (IntD == 0) {
                TopNode.L.SetAmorphous("PercentAmorph",IntC);}
        else {

        TopNode.L.SetAmorphous("PercentAmorph",IntC,"Crystallinity",IntD);};
        if (IntE == 0) {}
        else {TopNode.L.SetPorosity(IntE);};
        TopNode.Water = TopNode.L.Porosity*TopNode.Vol*TopNode.L.Humidity
                *TopNode.L.AirDensity()+(1-TopNode.L.Porosity)*TopNode.Vol
                *TopNode.L.ParticleDensity*TopNode.L.MoistureContent();
        TopNode.Heat = (TopNode.L.DryAirSpecHeat*TopNode.L.Temperature
                +TopNode.L.Humidity*(TopNode.L.WaterVapSpecHeat

        *TopNode.L.Temperature+TopNode.L.LatentHeat))*TopNode.L.Porosity
                *TopNode.Vol*TopNode.L.AirDensity()+(TopNode.L.SaltSpecHeat

        *TopNode.L.Temperature+TopNode.L.WaterSpecHeat*TopNode.L.Temperat
ure
```

```
                *TopNode.L.MoistureContent())*(1-
TopNode.L.Porosity)*TopNode.Vol
                *TopNode.L.ParticleDensity;

        for (int i = 1;i < NumberNodes;i=i+1) {
                Inside[i].L.SetAirProps("Temperature",IntA,"RH",IntB);
                if (IntD == 0) {
                        Inside[i].L.SetAmorphous("PercentAmorph",IntC);}
                else {

        Inside[i].L.SetAmorphous("PercentAmorph",IntC,"Crystallinity",IntD);};
                if (IntE == 0) {}
                else {Inside[i].L.SetPorosity(IntE);};
                Inside[i].Water =
Inside[i].L.Porosity*Inside[i].Vol*Inside[i].L.Humidity
                        *Inside[i].L.AirDensity()+(1-
Inside[i].L.Porosity)*Inside[i].Vol
                        *Inside[i].L.ParticleDensity*Inside[i].L.MoistureContent();
                Inside[i].Heat = (Inside[i].L.DryAirSpecHeat*Inside[i].L.Temperature
                        +Inside[i].L.Humidity*(Inside[i].L.WaterVapSpecHeat

        *Inside[i].L.Temperature+Inside[i].L.LatentHeat))*Inside[i].L.Porosity

        *Inside[i].Vol*Inside[i].L.AirDensity()+(Inside[i].L.SaltSpecHeat

        *Inside[i].L.Temperature+Inside[i].L.WaterSpecHeat*Inside[i].L.Temperature
                        *Inside[i].L.MoistureContent())*(1-
Inside[i].L.Porosity)*Inside[i].Vol
                        *Inside[i].L.ParticleDensity;
        };
}
else {};


//*****************************************************************
**********
// Setup Ambient Conditions
//*****************************************************************
**********

BottomAmbient.GetAndSetValues();
TopAmbient.GetAndSetValues();
cout << endl;cout << endl;
PrintOut(X1);
PrintOut(X2);

//*****************************************************************
**********
// Start of program proper
```

```
//*****************************************************************************
**********
double Telapsed;

while (Node::Time <= Tfinish) {
        Node::Time = Node::Time + Node::dt;
        Telapsed = Telapsed + Node::dt;
        BottomAmbient.UpdateAmbient(Node::Time);
        TopAmbient.UpdateAmbient(Node::Time);

        BottomNode.Transport(BottomAmbient,Inside[1]);
        Inside[1].Transport(BottomNode,Inside[2]);
        for(int i=2;i < (NumberNodes-1);i=i+1) {
                Inside[i].Transport(Inside[i-1],Inside[i+1]);
        };
        Inside[NumberNodes-1].Transport(Inside[NumberNodes-2],TopNode);
        TopNode.Transport(Inside[NumberNodes-1],TopAmbient);

        BottomNode.UpdateAir();
        for (int i=1;i<NumberNodes;i=i+1) {
                Inside[i].UpdateAir();
        };
        TopNode.UpdateAir();

        if (Telapsed >= Tprint) {
                PrintOut(X1);
                PrintOut(X2);
                Telapsed = 0;
                };
};
PrintOut(X1);
PrintOut(X2);
};
```